Chapter 3: Reactor

Table of Contents

Chapter 3: Reactor

Table of Contents (continued)

Chapter 3: Reactor

Table of Contents (continued)

Chapter 3: Reactor

List of Tables

Chapter 3: Reactor

List of Figures

Intentionally Blank

Chapter 3
REACTOR

3.1 GENERAL

Note: As required by the Renewed Operating Licenses for Surry Units 1 and 2, issued March 20, 2003, various systems, structures, and components discussed within this chapter are subject to aging management. The programs and activities necessary to manage the aging of these systems, structures, and components are discussed in Chapter 18.

The reactor core is a multi-region cycled core. The fuel rods are coldworked, partially annealed zirconium alloy tubes containing slightly enriched uranium dioxide fuel. All fuel rods are pressurized with helium during fabrication to reduce stresses and strains and to increase fatigue life. Beginning in Cycle 21, some fuel rods contain fuel with a thin layer of boride coating on the outer surface to act as integral fuel burnable absorber (IFBA, References 1 & 2).

The fuel assembly is a canless type with the basic assembly consisting of the control rod guide thimbles joined to the grids and the top and bottom nozzles. The fuel rods are supported at several points along their length by the grids.

Control rod assemblies, flux suppression inserts (Unit 1 only, Cycles 13 through 20), and burnable poison rods are inserted into the guide thimbles of the fuel assemblies. Flux suppression inserts were removed after Cycle 20 of Unit 1. Beginning in Cycle 21, cores may use IFBA and/or discrete (fixed) burnable absorber rods. The absorber sections of the control rods are fabricated of silver-indium-cadmium alloy sealed in stainless steel tubes. The absorber material in the fixed burnable poison rods is in the form of either borosilicate glass sealed in stainless steel tubes, or Al_2O_3 - B_4C pellets in Zircaloy-4 tubes. The flux suppression inserts in Unit 1 consist of hafnium bar encapsulated in Zircaloy-4 tubing.

The control rod drive mechanisms are of the magnetic latch type. The latches are controlled by three magnetic coils. They are so designed that upon a loss of power to the coils, the control rod assembly is released and falls by gravity to shut down the reactor.

3.1 References

1. S. L. Davidson et al., *Reference Core Report, VANTAGE 5 Fuel Assembly,* WCAP-10444-P-A, September 1985.
2. S. L. Davidson et al., *VANTAGE+ Fuel Assembly Reference Core Report,* WCAP-12610-P-A, April 1995.

Intentionally Blank

3.2 DESIGN BASES

3.2.1 Performance Objectives

The reactor core average thermal power is 2546 MWt. The nuclear steam supply system power rating is 2558 MWt, which includes 12 MWt pump heat. This is the maximum thermal power rating for which the plant heat removal systems are designed.

The reactor core fuel loading and incore fuel management are designed to yield prespecified cycle average and core average burn-up values. Data for successive reload cycles can be found in the respective reload safety evaluations prepared by Vepco. Typical nuclear design data (representative of the initial core) can be found in Table 3.3-1.

The fuel rod cladding is designed to maintain its integrity for the anticipated rod life. The effects of fission gas release, fuel dimensional changes, and corrosion-induced and irradiation-induced changes in the mechanical properties of cladding are considered in the design of the fuel assemblies.

The control rods, being long and slender, are relatively free to conform to any small misalignments. Tests have shown that the rods are very easily inserted and not subject to binding even under conditions of severe misalignment.

The control rods provide sufficient reactivity control to terminate any credible power transient before reaching the departure from nucleate boiling ratio (DNBR) design limit (Section 3.2.3). This is accomplished by ensuring sufficient control rod worth to shut the reactor down by at least 1.77% in the hot condition with the most reactive control rod stuck in the fully withdrawn position. Redundant equipment is provided to add soluble poison to the reactor coolant to maintain shutdown margin when the reactor coolant is cooled to ambient temperatures.

During initial core design, experimental measurements from critical experiments or operating reactors, or both, were used to validate the methods employed in the design. Nuclear parameters were calculated for every critical phase of operation and, where applicable, were compared with design limits to show that an adequate margin of safety exists. This same general design procedure has been employed for all the subsequent reload cycles.

In the thermal/hydraulic design of reload cores, the maximum fuel and clad temperatures during normal reactor operation and at 118% thermal overpower are conservatively evaluated and verified to be consistent with safe operating limitations.

3.2.2 Design Criteria

3.2.2.1 Reactor Core Design

The reactor core, together with reliable process and decay heat removal systems and control and protection instrumentation, is designed to function throughout its design life without

exceeding the following limits, which preclude fuel damage with appropriate margins for transients:

1. Minimum DNBR equal to the DNBR design limit (Section 3.2.3).
2. Fuel centerline temperature below the melting point of UO_2.
3. The internal fission gas pressure of the lead rod in the core remains less than the value that would cause the diametral gap between the fuel and clad to increase due to outward cladding creep during steady state operation, and the DNB propagation criteria of WCAP-8963-P-A (Reference 1 & 2) is satisfied.
4. Clad stresses less than the cladding material yield strength.
5. Clad strain less than 1%.
6. Cumulative strain fatigue cycles less than 80% of design strain fatigue life.

Additional information on nuclear design can be found in Section 3.3.

3.2.2.2 **Suppression of Power Oscillations**

The design of the reactor core and related protection systems ensures that power oscillations that could cause fuel damage in excess of acceptable limits are not possible. Any tendency toward oscillation is readily suppressed.

The potential for possible spatial oscillations of power distribution for this core was reviewed as part of the core stability evaluation effort described in Section 1.6.1. Ex-core instrumentation is provided to obtain necessary information concerning axial and azimuthal power distributions. This instrumentation is adequate to enable the operator to monitor and control xenon-induced oscillations. Based on the deviations detected by the long ion chambers, provisions in the reactor control and reactor protection systems reduce trip setpoints and, if necessary, initiate load cutback to maintain DNBR margin as a result of these potential oscillations in power distribution. Incore instrumentation is used to periodically calibrate and verify the information provided by the ex-core instrumentation.

3.2.2.3 **Redundancy of Reactivity Control**

Control rods and soluble boron in the reactor coolant are the two independent reactivity control systems that are provided to ensure compliance with General Design Criterion 27, as discussed in Section 1.4.

3.2.2.4 **Reactivity Hot Shutdown Capability**

The control rods and soluble boron in the reactor coolant are designed so that the core can be made and held subcritical from any hot standby or operating condition, thus complying with General Design Criterion 28 as discussed in Section 1.4.

3.2.2.5 Reactivity Shutdown Capability

The worth of the control rods is designed to ensure a 1.77% delta k/k shutdown margin under any operating condition with the most reactive rod stuck in the fully withdrawn position. The control rods and dissolved boron from the safety injection system also ensures no DNB occurs for the most severe cooldown transient caused by a single active failure, as discussed in Section 1.4.

3.2.2.6 Reactivity Holddown Capability

The reactor is normally shut down within 2 seconds of a reactor trip signal with the control rods. Sufficient soluble boron is continually available for injection to maintain the core subcritical during approach to, and at, cold shutdown.

3.2.2.7 Reactivity Control Systems Malfunction

The reactor protection system is capable of protecting against any single malfunction of the reactivity control system, as discussed in response to General Design Criterion 31 in Section 1.4. Reactor shutdown with control rod assemblies is completely independent of normal control functions, as discussed in Chapter 7. The protection system limits reactivity transients so that the DNB ratio is not less than the DNBR design limit (Section 3.2.3) for any single malfunction in either the reactor coolant system or in the de-boration control system.

3.2.2.8 Maximum Reactivity Worth of Control Rods

Limits that include considerable margin are placed on the rates at which reactivity can be increased to ensure that the potential effects of a sudden or large change of reactivity cannot rupture the reactor coolant boundary or disrupt the core, its support structures, or other vessel internals so as to lose the capability to cool the core.

3.2.3 Safety Limits

The reactor is capable of meeting the performance objectives described in Section 3.2.1 throughout the core life under both steady-state and transient conditions without compromising the integrity of the fuel elements. Thus, the release of unacceptable amounts of fission products to the coolant is prevented.

Design parameters pertaining to safety limits are given below for the nuclear, thermal/hydraulic, and mechanical aspects of the design. This information can be considered as the basis for the identification of Technical Specification limits and setpoints. These limits and setpoints are subject to change after each reload, or if the operating strategy during a given cycle is altered for some reason.

3.2.3.1 Nuclear Limits

As required by Technical Specifications, the nuclear heat flux hot channel factors, $F_q(Z)$, do not exceed the limits assumed in the safety analysis.

The nuclear axial peaking factor, F_Z^N, and the nuclear enthalpy rise hot channel factor, $F_{\Delta H}^N$, are limited in their combined relationship so as not to exceed the F_q^N or DNBR limits.

The limiting nuclear hot-channel factors are higher than those calculated at full power for the range from all control rod assemblies fully withdrawn to maximum allowable control rod assembly insertion. Control rod assembly insertion limits as a function of power are delineated in the Technical Specifications to ensure that somewhat worse hot-channel factors do not occur at lower power levels due to control rod insertion, and that the DNBR is always greater at partial power than at full power.

The reactor protection system ensures that the reactor core nuclear limits are not exceeded.

3.2.3.2 **Reactivity Control Limits**

The control system and operating procedures provide adequate control of core reactivity and power distribution. The following control limits are met:

1. Sufficient control is available to produce a minimum hot shutdown margin of 1.77% delta k/k.
2. The shutdown margin is maintained with the most reactive control rod assembly stuck in the fully withdrawn position.
3. The shutdown margin is maintained at ambient temperature by the use of soluble poison.
4. There will be no DNB following a trip as a result of any single active failure in the steam system (e.g., safety valve, relief valve, or bypass valve sticking open), even if the most reactive control rod remains fully withdrawn.

3.2.3.3 **Thermal/Hydraulic Limits**

The reactor core is designed to meet the following limiting thermal/ hydraulic criteria:

1. The design DNBR limit during normal operation, including anticipated transients, is 1.30 for 15 x 15 LOPAR assemblies (all fuel Regions before Region 12 for each unit). For 15 x 15 SIF assemblies (Region 12 and subsequent Regions for each unit), the design DNBR limit is 1.46.
2. No fuel melts during any anticipated operating condition.

To maintain fuel rod integrity and prevent fission product release, it is necessary to prevent clad overheating under all anticipated operating conditions. This is accomplished by preventing departure from nucleate boiling, which, if it were to occur, would cause a large decrease in the heat transfer coefficient between the fuel rods and the reactor coolant, resulting in high clad temperatures.

The core thermal and hydraulic design basis requires that departure from nucleate boiling (DNB) be avoided with a 95% probability at a 95% confidence level during normal operation and

operational transients. This is one of the key analysis criteria in many of the Chapter 14 safety analyses. Historically, demonstration of compliance with this design basis has been accomplished by (1) deterministic application of key DNBR analysis uncertainties in transient analysis and (2) comparing the resultant departure from nucleate boiling ratio (DNBR) to the applicable DNBR correlation limit. The correlation DNBR limit is established to ensure that there is a 95% probability with 95% confidence that DNB will not occur when the calculated DNBR is at the DNBR limit. For normal operation, operational transients, and during transients which experience minor variations in power, temperature, and pressure near hot-full-power (HFP) conditions, a statistical application of key DNBR analysis uncertainties to the correlation DNBR limit may be employed as described below and in Section 3.4.3.2.

The DNB design basis for the 15 x 15 LOPAR fuel product is met by using a deterministic treatment of key analysis uncertainties for modeling initial transient analysis conditions. (See Section 3.4.3.2.) The W-3 correlation is used to predict the DNB heat flux for the 15 x 15 fuel. The DNBR limit described above is applicable for use in the Westinghouse THINC (Reference 3) code and the Virginia Power COBRA code with the W-3 correlation for the 15 x 15 LOPAR fuel product (Reference 4).

The DNB design basis for the 15 x 15 SIF fuel product is met by using either the deterministic methodology or the Virginia Power “Statistical DNBR Evaluation Methodology” (References 5 & 6). (See Section 3.4.3.2.) The DNBR limit described above is applicable for use in the Virginia Power COBRA code with the WRB-1 correlation (Reference 7) for the 15 x 15 SIF fuel product with either methodology.

The Statistical DNBR Evaluation Methodology is employed to determine a revised DNBR limit. This new limit combines the correlation uncertainty with the uncertainties of key DNBR analysis input parameters. Transient analysis with the revised methodology does not require that the uncertainties be applied in the initial conditions. Instead, nominal values may be used.

The Statistical DNBR Limit is developed by means of a Monte Carlo process. The variation of actual operating conditions about nominal statepoints due to parameter measurement and other key DNB uncertainties is modeled with a random number generator-based algorithm. This algorithm produces thousands of statepoints at each nominal statepoint. The random statepoints are then supplied to Virginia Power’s core thermal-hydraulic code, COBRA, which calculates the minimum DNBR. Each DNBR is randomized by a correlation factor as described in the topical report (Reference 5). The standard deviation of the resultant DNBR distribution is increased by a small sample correction factor to obtain its 95% upper confidence limit, thereafter being combined Root-Sum-Square with code and model uncertainties to obtain the total DNBR standard deviation, σ_{total}. The Statistical DNBR Limit (SDL) is then:

$$SDL = 1 + 1.645 \times \sigma_{total}$$

in which the 1.645 multiplier is the z-value for one-sided 95% probability of a normal distribution. Thus, this SDL is consistent with the design basis that departure from nucleate boiling (DNB) will not occur on at least 95% of the limiting fuel rods during normal operation and operational transients, and any transient conditions arising from faults of moderate frequency (Conditions I and II events) at a 95% confidence level. As an additional criterion, the SDL for the 15 x 15 SIF fuel with the Statistical DNBR Evaluation Methodology ensures that at least 99.9% of the core avoids DNB for these conditions.

The Statistical DNBR Evaluation Methodology is employed on a transient specific basis (Reference 6) as indicated in the transient analysis summary in Chapter 14.

Additional information on thermal/hydraulic design can be found in Section 3.4.

3.2.3.4 **Mechanical Limits**

3.2.3.4.1 Reactor Internals

The reactor internal components are designed to withstand the stresses resulting from start-up, steady-state operation with any number of pumps running, and shutdown conditions. No damage to the reactor internals occurs as a result of loss of pumping power.

Lateral deflection and torsional rotation of the lower end of the core barrel are limited to prevent excessive movements resulting from seismic disturbances, thus preventing interference with control rod assemblies. Core drop in the event of failure of the normal supports is limited so that the control rod assemblies do not disengage from the fuel assembly guide thimbles.

The structural components are designed to maintain their functional integrity in the event of a major loss-of-coolant accident (LOCA). The dynamic loading resulting from the pressure oscillations because of a LOCA does not prevent insertion of the control rod assemblies.

Seismic design criteria for the reactor internals are discussed in Appendix 15A. Additional information on mechanical design can be found in Section 3.5.

3.2.3.4.2 Fuel Assemblies

The fuel assemblies are designed to perform satisfactorily throughout their required lifetime. The loads, stresses, and strains resulting from the combined effects of flow-induced vibrations, earthquakes, reactor pressure, fission gas pressure, fuel growth, thermal strain, and differential expansion during both steady-state and transient reactor operating conditions have been considered in the design of the fuel rods and fuel assembly. The assembly is also structurally designed to withstand handling and shipping loads prior to irradiation, and to maintain sufficient integrity at the completion of design burnup to permit safe removal from the core, handling, shipment, and fuel reprocessing.

The fuel rods are supported at several locations along their length within the fuel assemblies by brazed or welded grid assemblies, which are designed to maintain control of the lateral spacing

between the rods throughout the design life of the assemblies. The magnitude of the support loads provided by the grids is established to minimize possible fretting without overstressing the cladding at the points of contact between the grids and fuel rods, and without imposing restraints of sufficient magnitude to result in buckling or distortion of the rods.

The fuel rod cladding is designed to withstand operating pressure loads without rupture, and to maintain encapsulation of the fuel throughout its design life.

3.2.3.4.3 Control Rod Assemblies

The criteria used for the design of the cladding on the individual control rods in the control rod assemblies are similar to those used for the fuel rod cladding. The cladding is designed to be free-standing under all operating conditions and to maintain encapsulation of the absorber material throughout the control rod design life. Allowance for wear during operation is included for the control rod cladding thickness.

Adequate clearance is provided between the control rods and the guide thimbles that position the rods within the fuel assemblies so that coolant flow along the length of the control rods is sufficient to remove the heat generated without overheating of the absorber cladding. The clearance is also sufficient to compensate for any misalignment between the control rods and guide thimbles and to prevent mechanical interference between the rods and guide thimbles under any operating condition.

3.2.3.4.4 Control Rod Drive Mechanisms

Each control rod drive mechanism is designed as a hermetically sealed unit to prevent leakage of reactor coolant water. All pressure-containing components are designed to meet the requirements of ASME Code Section III for Class A vessels.

The control rod drive mechanisms for the control rod assemblies provide control rod assembly insertion and withdrawal rates consistent with the required reactivity changes for reactor operational load changes. This rate is based on the worths of the various rod groups, which are established to limit power-peaking flux patterns. The maximum reactivity addition rate is specified to limit the magnitude of a possible nuclear excursion resulting from a control system or operator malfunction. Also, the control rod drive mechanisms provide a fast insertion rate during a trip of the control rod assemblies, which results in a rapid shutdown of the reactor for conditions that cannot be handled by the reactor control system.

3.2 REFERENCES

1. D. H. Risher et al, *Safety Analysis for the Revised Fuel Rod Internal Pressure Design Basis*, WCAP-8963-P-A, August 1978.

2. Letter from C. M. Stallings (VEPCO) to E. G. Case (NRC), *Amendment to Operating Licenses DPR-32 and DPR-37, Technical Specifications Change No. 65, Surry Power Station - Unit Nos. 1 and 2,* Serial No. 108, March 15, 1978.

3. L. E. Hochreiter and H. Chelemer, *Application of the THINC-IV Program to PWR Design*, WCAP-8054-P-A, February 1989.

4. F. W. Sliz and K. L. Basehore, *Vepco Reactor Core Thermal-Hydraulic Analysis Using the COBRA-IIIC/MIT Computer Code*, VEP-FRD-33-A, October 1983.

5. R. C. Anderson, *Statistical DNBR Evaluation Methodology*, VEP-NE-2-A, June 1987.

6. Letter from B. C. Buckley (NRC) to W. L. Stewart (Virginia Electric and Power Company), *Surry Units 1 and 2 - Issuance of Amendments Re: F Delta H Limit and Statistical DNBR Methodology*, Serial No. 92-405, June 1, 1992.

7. R. C. Anderson and N. P. Wolfhope, *Qualification of the WRB-1 CHF Correlation in the Virginia Power Cobra Code,* VEP-NE-3-A, July 1990.

3.3 NUCLEAR DESIGN

This section discusses the nuclear characteristics of the core, and evaluates the characteristics and design parameters that are significant with respect to the design objectives (Section 3.2.1). These evaluations demonstrate the capability of the reactor to achieve these objectives while performing safely under all steady-state and transient operational modes.

3.3.1 Reactivity Control Aspects

Reactivity control is provided by boron dissolved in the reactor coolant, movable neutron-absorbing control rod assemblies, fixed burnable poison rods, and/or integral fuel burnable absorber (IFBA).

The concentration of soluble boron is varied as necessary during the life of the core to compensate for changes in reactivity that occur with changes in temperature of the reactor coolant from cold shutdown to hot operating conditions, changes in reactivity associated with inventory changes in the fission product poisons xenon and samarium, reactivity losses associated with the depletion of fissile inventory and buildup of long-lived fission product poisons, and changes in reactivity due to burnable poison burnup.

The control rod assemblies provide reactivity control for: fast shutdown, reactivity changes associated with changes in the average coolant temperature above hot-zero-power temperature (since core average coolant temperature is increased with power level), reactivity associated with any void formation, and reactivity changes associated with the power coefficient of reactivity.

The control rod assemblies are divided into two categories according to their function. Thirty-two control rod assemblies compensate for changes in reactivity due to variations in operating conditions of the reactor, such as power or temperature. They are divided into four control groups or banks, each consisting of eight assemblies. Sixteen control rod assemblies provide additional shutdown reactivity, and are termed shutdown assemblies. The total shutdown worth of all the control rod assemblies is specified to provide adequate shutdown with the most reactive assembly stuck out of the core.

Burnable poison (fixed burnable poison rods and/or IFBA) provides control of part of the excess reactivity available during the core cycle. The primary function of burnable poison is to prevent the moderator temperature coefficient from being positive, under normal operating conditions, by reducing the soluble boron content of the reactor coolant at the beginning of life, as described in WCAP-7113 (Reference 1). The number and location of fixed burnable poison rods for the first core cycle is shown in Figure 3.3-1. The use of burnable poison in subsequent cycles is discussed in Section 3.3.3.2.2.

Since the presence of control rod assemblies and burnable poison influences flux shape in the core, it is pertinent to summarize some typical fission power density distributions. Figures 3.3-2 and 3.3-3 illustrate X-Y power density distributions for rodded and unrodded

conditions. The value of F_{xy} shown on each figure indicates the ratio of maximum power density to average power density.

3.3.2 Nuclear Design Data

The values of design parameters cited in this section and in Tables 3.3-1 through 3.3-3 generally pertain to the first Surry core cycle. The pertinent nuclear design data for each subsequent cycle of operation are contained in a reload safety evaluation prepared by Vepco prior to cycle start-up. The reload safety evaluation process involves an evaluation of the reload core during which the values of kinetics parameters, fuel temperatures, peaking factors, and core limits used in the currently applicable safety analysis are compared with corresponding values for the planned reload cycle. Where the evaluation shows parametric values for the planned cycle that are outside the bounds of the previous safety analysis, the specific accident analyses sensitive to these parameters are reevaluated or reanalyzed. If a reanalysis leads to Technical Specification changes, these are obtained from the NRC, also prior to cycle start-up.

3.3.2.1 Core Reactivity Characteristics

A summary of nuclear design data for the first cycle only, including core reactivity characteristics, is presented in Table 3.3-1. Discussion of the table is facilitated by use of line numbers. A summary of reactivity requirements and control rod worth is given in Tables 3.3-2 and 3.3-3, which may be used in conjunction with Table 3.3-1.

General structural characteristics are given in lines 1 through 10 of Table 3.3-1, while performance characteristics are listed in lines 11 through 22. Typical values of effective neutron multiplication constants and estimated critical boron (chemical shim) concentrations are listed for specified conditions in lines 23 through 41. Several of these items, such as soluble boron control, are discussed in greater detail below.

Adequate control to render the reactor subcritical at temperatures below the operating range is provided by the soluble boron concentration. The boron concentration during refueling, reported in line 32 of Table 3.3-1, based on all the control rod assemblies being inserted, provides approximately 10% delta k/k shutdown margin.[1] This concentration is also sufficient to maintain the core subcritical with no control rod assemblies inserted in the core. This is consistent with General Design Criteria No. 26 (GDC-26), which states that one of two independent reactivity control systems “shall be capable of holding the reactor core subcritical under cold conditions.” For cold shutdown at the beginning of core life, the concentration shown in Table 3.3-1, line 40, is sufficient for 1% delta k/k shutdown with all but the maximum-worth control rod assembly inserted.

The boron concentration for refueling is equivalent to less than 2% by weight boric acid (H_3BO_3), and is well within solubility limits at ambient temperature. This concentration is also

1. The text applies to the initial core cycle; see Technical Specifications for current shutdown requirements.

maintained in the spent-fuel pool, since it is directly connected with the refueling canal during refueling operations.

The initial full-power boron concentration without equilibrium xenon and samarium is shown in line 37 of Table 3.3-1. As these fission product poisons are built up, the boron concentration is reduced. This initial boron concentration assumes no full-length rod insertion. The xenon-free, zero-power shutdown, k = 0.99[1] or less, with all but the maximum-worth control rod assembly inserted, is maintained with the boron concentrations shown in lines 40 and 41, for the cold and hot conditions, respectively.

The boron concentrations given above are representative of those during the first operating cycle where burnable poison rods and the associated worth listed in lines 42, 43, and 44 were present. Core kinetic characteristics are dependent on boron concentrations, and the presence of burnable poison rods and control rods. A discussion of these factors follows.

3.3.2.2 **Kinetic Characteristics**

The response of the reactor core to unit conditions or operator adjustments during normal operation, as well as the response during abnormal or accidental transients, is determined by means of a detailed simulation. In these calculations, reactivity coefficients are required to couple the response of the core neutron multiplication to the variables that are set by conditions external to the core. Since the reactivity coefficients change during the life of the core, a range of coefficients is established to determine the response of the unit throughout life and to establish the design of the reactor control and protection system.

3.3.2.3 **Moderator Temperature Coefficient**

The moderator temperature coefficient in a core controlled by soluble boron is less negative than the coefficient in an equivalent rodded core. One reason is that control rods contribute a negative increment to the coefficient, and in a core using soluble boron, the control rods are only partially inserted. Also, the boron concentration is decreased with the decrease in water density upon an increase in temperature. This gives rise to a positive component of the moderator temperature coefficient due to the removal of boron from the core. This effect is directly proportional to the amount of reactivity controlled by the dissolved boron.

To reduce the soluble boron requirement for control of excess reactivity, burnable poison rods and/or IFBA rods are incorporated in the core design. The effect of reducing the soluble boron concentration is to make the moderator temperature coefficient more negative. This is caused by a reduction of the effect that coolant temperature and density changes have on the boron number density in the core.

The burnable poison rods for the initial core were borated glass tubes clad in stainless steel. Clusters of these rods were distributed throughout the core in vacant control rod guide thimbles.

1. The text applies to the initial core cycle; see Technical Specifications for current shutdown requirements.

The initial core pattern is shown in Figures 3.3-1 and 3.3-4 on a gross core and an assembly-wise basis, respectively. Information regarding research, development, and nuclear evaluation results of the burnable poison rods can be found in WCAP-7113 (Reference 1) and WCAP-9000 (Reference 2). The number of rods and the corresponding reactivity worth at beginning of life of the initial cycle are indicated in lines 42, 43, and 44 of Table 3.3-1.

Typically, the moderator temperature coefficient is negative at operating temperatures. The coefficient becomes more negative with increasing burnup, as a result of build-up of plutonium and fission products and reduction of the boron concentration. The reactivity loss due to equilibrium xenon is controlled by reduction of boron concentration. As xenon builds up, the boron concentration is reduced. The calculated range of the moderator temperature coefficient from beginning of life to end of life of the initial cycle is shown in line 45.

The control rods provide a negative contribution to the moderator coefficient. This is indicated in Figure 3.3-5, which shows a typical relationship between moderator temperature and moderator temperature coefficient, both with and without rods.

Design calculations for Surry reload cycles subsequent to cycle 1 have shown that the moderator temperature coefficient may be positive at the beginning of a cycle, with hot zero-power conditions and all rods out. Although control rod insertion can be used to bring the coefficient negative, this would lengthen the plant start-up after a refueling and would make the start-up more complex by requiring restrictions on boron concentration and control rod movement. Therefore, to facilitate start-up, it is desirable to allow a slightly positive moderator temperature coefficient at lower power levels. As the power level is raised, the average core water temperature becomes higher, as allowed by the programmed average temperature for the plant, tending to bring the moderator coefficient more negative. Also, the boron concentration can be reduced as xenon builds into the core. Thus, there is less need to allow a positive coefficient as full power is approached. As fuel burnup is achieved, boron is further reduced and the moderator coefficient becomes negative over the entire operating power range.

The impact of a positive moderator temperature coefficient on the accident analyses presented in Chapter 14 has been assessed. Any incident which was found to be sensitive to minimum or near-zero moderator coefficients was reanalyzed. In general, reanalysis was based on the assumptions and methods employed in the original accident analysis, with exceptions noted in the discussion of each incident in Chapter 14. Accidents not reanalyzed included those resulting in excessive heat removal from the reactor coolant system for which a large negative moderator coefficient is conservative, and those for which the moderator coefficient is assumed to be negative due to control rod insertion resulting from reactor trip.

The Technical Specifications allow a constant positive moderator temperature coefficient below 50% of rated power, decreasing linearly to zero at 100% of rated power. This provides ample operating flexibility and allows a reasonable degree of flexibility in core design and plant operation for future cycles.

A requirement that the reactor is not to be made critical with a reactor coolant temperature below 522°F is imposed to provide added assurance that the assumptions made in the safety analysis remain bounding by maintaining the moderator temperature within the range of those analyses.

The positive moderator temperature coefficient will exist for only a short time at beginning of cycle, and the Technical Specifications require the coefficient to be zero at full power. Because measurements are made in the start-up tests for each cycle to verify that the coefficient will meet the Technical Specifications, and because the accident analysis shows acceptable results, the NRC has found the operation of Surry Units 1 and 2 with a positive moderator temperature coefficient to be acceptable.

3.3.2.4 **Moderator Pressure Coefficient**

The moderator pressure coefficient has a sign opposite to the moderator temperature coefficient. The net effect of the moderator pressure coefficient on the total coefficient is small because of the small magnitude of the pressure coefficient, since a change of 50 psi in pressure has no more effect on reactivity than a half-degree change in moderator temperature. The calculated initial-core beginning-of-life and end-of-life pressure coefficients are shown in Table 3.3-1, line 46.

3.3.2.5 **Moderator Density Coefficient**

A uniform moderator density coefficient is defined as a change in the neutron multiplication per unit change in moderator density. The range of the moderator density coefficient from beginning to end of life of the initial core is specified in Table 3.3-1, line 47.

3.3.2.6 **Doppler and Power Coefficients**

The calculation of power coefficients in a large, slightly enriched core is complex. As fuel pellet temperature increases with power density, the resonance absorption in U-238 increases as a result of Doppler broadening of the resonances. The relationship between effective fuel temperature and resonance absorption in a fuel rod is sufficiently complex in itself. An additional degree of complexity is introduced in relating these resonance-broadening effects to actual operation of the core, in which non-uniform power and fuel temperature distributions are subject to continual change with control rod movements, fuel burnup, and varying heat transfer characteristics of the fuel rods.

The Doppler reactivity coefficient is defined as the change in neutron multiplication per degree change in the effective fuel temperature, delta k/k/°F. The variation in this quantity with effective fuel temperature is shown in Figure 3.3-6, as computed by the LEOPARD code (Reference 3). It may be observed that the Doppler coefficient is non-linear and becomes less negative as temperature increases. The integral under the curve between the effective fuel temperature associated with the hot-zero-power condition and that associated with full power represents the Doppler reactivity defect.

To obtain the integral or differential change in core reactivity with power, it is necessary to know the change in effective fuel temperature with power, delta T/delta P, as well as the Doppler coefficient, delta k/k/°F. An empirical approach is taken to calculate the behavior of delta T/delta P with power, based on operating experience of Westinghouse cores. Results obtained with this approach are illustrated in Figure 3.3-7, which shows reactivity effects associated with Doppler broadening only. (The results presented do not include any moderator coefficient, even though the moderator temperature changes with core power level.)

In the empirical model used above, a large temperature drop is assumed to occur across the fuel pellet-clad gap. Under conditions where this gap may be essentially "closed," the fuel temperature for a given power level, and the quantity delta T/delta P, may be significantly reduced. At a lower effective fuel temperature, the Doppler reactivity defect is reduced; however, the Doppler coefficient is more negative. The net effect of using a closed-gap model is a power coefficient that shows much less variation with power than that shown with a gap model. Results obtained using this model are shown in Figure 3.3-8, where it may be observed that the power coefficient at full power is similar to that obtained with the gap model.

The above discussion relates primarily to reactivity characteristics on a core basis. A similar situation exists with regard to local Doppler reactivity feedback characteristics, which are important in determination of the stability of the reactor to xenon oscillations. Calculations indicate that local reactivity feedback in the range of interest for stability (50% to 150% of core average power density) is relatively insensitive to the thermal model.

3.3.2.7 **Summary of Control Rod Requirements**

Figure 3.3-9 depicts the functional grouping and designation of the control rod assemblies.

Reactivity requirements of control rods at beginning and end of life are summarized in Table 3.3-2. The requirements, discussed below, include those that are associated with shutdown conditions.

3.3.2.8 **Total Power Defect**

Control rods must be available to compensate for the reactivity change incurred with a change in power level due to the Doppler effect. The magnitude of this change has been established by correlating the experimental results of numerous operating cores.

The average temperature of the reactor coolant increases with power level in the reactor. Since this increase in coolant temperature is actually a part of the power-dependent reactivity change, along with the Doppler effect and void formation, the associated reactivity change must be controlled by rods. The largest amount of reactivity that must be controlled is at the end of life, when the moderator temperature coefficient has its most negative value. The moderator temperature coefficient range for the initial cycle is given in Table 3.3-1, line 45, while the cumulative reactivity change is shown in the first line of Table 3.3-2. By the end of each fuel

cycle, the non-uniform axial depletion causes a severe power peak at lower power. The reactivity associated with this peak is part of the power defect.

3.3.2.9 **Operational Maneuvering Band**

Each control rod assembly control group is operated at power within a prescribed band of travel in the core to compensate for periodic changes in boron concentration, temperature, and pressure. The band has been defined as the operational maneuvering band. When the control rod assemblies reach either limit of the band, a change in boron concentration must be made to compensate for any additional change in reactivity.

3.3.2.10 **Control Rod Bite**

For good response to rapid changes in load, the control groups of control rod assemblies were originally positioned at a location that maintained a design minimum reactivity insertion rate. The partial control group insertion that was specified to provide the specified reactivity insertion rate is called control rod bite. The current analyses and design basis are met even when the unit is operated with all rods out of the core.

3.3.2.11 **Excess Reactivity Insertion Upon Reactor Trip**

Current control requirements are nominally based on providing 1.77% delta k/k shutdown at hot zero-power conditions, with the highest-worth control rod assembly assumed to be stuck in its fully withdrawn position.

3.3.2.12 **Calculated Rod Worths**

The control rod assemblies are arranged in a symmetric pattern as shown in Figure 3.3-9. Calculations are made to verify that the control rod worths are sufficient to meet the shutdown requirements. These worths are established assuming that the highest-worth control rod assembly is stuck in the fully withdrawn position. Table 3.3-3 lists the calculated worths for the beginning and end of the first cycle.

To be sure of maintaining a margin between calculated and required control rod worths, the calculated reactivity worths are decreased by 10% to account for any errors or uncertainties in the calculation.

A comparison between calculated and measured control rod worth shows the calculations to be well within the allowed uncertainty of 10%.

3.3.2.13 **Reactor Core Power Distribution**

In order to meet the performance objectives without violating safety limits, the peak to average power density must be within the limits set by the nuclear hot-channel factors. For the peak power point in the core at rated power, the nuclear heat flux hot-channel factor, F_q^N was established as specified in Table 3.3-1, line 21. For the hottest channel at rated power, the nuclear

enthalpy rise hot-channel factors, $F^{N}_{\Delta H}$ was established as specified in Table 3.3-1, line 22. These values are specific to the initial cycle.

Power capability of a PWR core is determined largely by consideration of the power distribution and its interrelationship to limiting conditions involving:

1. The linear power density.
2. The fuel cladding integrity.
3. The enthalpy rise of the coolant.

To determine the core power capability, local as well as gross core neutron flux distributions have been determined for various operating conditions at different times in core life.

The presence of control rods, burnable poison, flux suppression inserts (Unit 1 only, Cycles 13 through 20) and chemical shim concentration all play significant roles in establishing the fission power distribution, in addition to the influence of thermal/hydraulic and temperature feedback considerations. The computer programs used to determine neutron flux distributions include a model to simulate non-uniform water (and chemical shim) density distributions.

Thermal/hydraulic feedback considerations are especially important late in cycle life, when the magnitude of the flux redistribution and reactivity change with change in core power or control rod assembly movement are strongly influenced by enthalpy rise up the core and by the fuel burnup distribution. Consequently, extensive X-Y and Z power distribution analyses are performed to evaluate fission power distributions. Typical X-Y power distributions are presented in Figures 3.3-2 and 3.3-3 to illustrate the combined effect of a control rod assembly group upon assembly average power density. Incore instrumentation is employed to evaluate the core power distributions throughout core lifetime to ensure that the thermal design criteria are met.

The Ex-Core Nuclear Instrumentation System supplies the necessary information for the operator to control the core power distribution within the limits established for the protection system design. This information consists of a multipen recorder, which displays the upper and lower ion chamber signals, and an indicator that gives the difference in these two signals for each long ion chamber. These ion chamber signals to the recorders and indicators are calibrated against incore power distribution obtained from the movable detector system generated in the adjacent section of the core. This essentially divides the core into eight sections, four in the upper half and four in the lower half.

The relationship between core power distribution and ex-core nuclear instrumentation readings was established during the start-up testing program (Chapter 13). Incore flux measurements were made for reactor power in the range of 25 to 100%. These measurements, together with long ion chamber currents, were processed to yield the relationships between core average axial power generation, axial peaking factor, and axial offset as indicated by the ex-core

nuclear instrumentation. These relationships can be checked during operation to assess the effect of core burnup on the sensitivity between incore power distribution and ex-core readings.

The reactor core may be subject to axial xenon oscillations at the end of a fuel cycle life. The axial instability is due principally to the negative moderator temperature coefficient of reactivity that exists at end of life. Since the moderator coefficient at beginning of life is small, stability against axial oscillations is greatly increased at beginning of life. Consequently, stability margin experiments would not be informative at beginning of life.

A more detailed discussion of the background, analytical, and experimental data which form the basis for this approach is given in WCAP-7208 (Reference 4).

Ex-core neutron flux detectors were added to meet Regulatory Guide 1.97 and Appendix R requirements. These are discussed in Section 7.11.

3.3.3 Analytic Methods and Supporting Experimental Data

3.3.3.1 Introduction

The confidence in procedures and design methods for the initial core cycles was based on comparison of these methods with experimental results. The experiments included critical experiments performed at the Westinghouse Reactor Evaluation Center and other facilities, and also measured data from operating power reactors. Extensive descriptions of these analytic methods and the supporting experiment theory correlations are given in References 5 through 16. Discussion of these items may be found in other safety analysis reports on similar stations (e.g., the FSAR for Carolina Power and Light Company's H. B. Robinson Unit No. 2, Docket No. 50-261).

The current core analysis methodology is described in the following section.

3.3.3.2 Reload Methodology

3.3.3.2.1 Introduction

Each reload core is evaluated to demonstrate that it will not adversely affect the safety of the plant. The evaluation is accomplished utilizing the methodology described in VEP-FRD-42 Revision 2.1-A (Reference 17).

3.3.3.2.2 Core Description

The Surry cores consist of 157 fuel assemblies surrounded by a core baffle, barrel, and thermal shield, and enclosed in a steel pressure vessel. The pressure inside the vessel is maintained at a nominal 2250 psia. The coolant (and moderator) is pressurized water, which enters the bottom of the core at a nominal 540°F and undergoes a nominal average rise in temperature of 65°F before exiting the core. The average coolant temperature is 573.0°F and the average linear power density of the core is 6.5 kW/ft.

Each of the 157 fuel assemblies consists of 204 fuel rods (except fuel assemblies which have been reconstituted, see Section 3.5.2.1) arranged in a 15 x 15 square array. The fuel used in the Surry cores consists of slightly enriched uranium dioxide fuel pellets contained within a Zircaloy-4 or ZIRLO clad. A small gap containing pressurized helium exists between the pellets and the inner diameter of the clad. For the positions in the 15 x 15 array not occupied by fuel rods, there are 20 guide tube locations for fixed burnable poison rods, flux suppression inserts (Unit 1 only, Cycles 13 through 20), or control rods and one centrally located instrumentation tube. The fuel rods in each fuel assembly are supported by seven grids located along the length of the assembly. In the original Surry fuel design, all of these grids were fabricated from Inconel-718. In the Surry Improved Fuel (SIF) design, which was introduced in Cycle 10 (Batch 12) at each unit, the five middle grids on the assembly are made from zirconium-based alloy (Zircaloy-4 or ZIRLO). Inconel continues to be used for the top and bottom grids on the SIF fuel assemblies. These grids are mechanically attached to the guide tubes, which are, in turn, fastened to the upper and lower nozzles, and thus provide for assembly structural support. Beginning with the feed for Cycle 13 (Region 15), the Surry fuel assemblies also include an additional protective bottom Inconel grid, located directly above the bottom nozzle. This protective grid is a debris resistance feature, and is not considered an assembly structural component. Beginning in Cycle 21, each fuel assembly may contain from 0 to 148 integral fuel burnable absorber (IFBA) rods. The IFBA fuel rod design includes a thin layer of boride coating on the outer surface of the majority of the fuel pellets in the fuel rod, as well as axial blankets. The axial blanket is a six-inch (approximate) stack of slightly enriched annular fuel pellets without boride coating located at the top and bottom of the fuel stack in each IFBA rod. Cores may continue to use discrete (fixed) burnable poison rod assemblies in conjunction with IFBA fuel assemblies.

There are 48 rod cluster control assemblies (referred to as control rods) used to control core reactivity. The absorber material of the control rods is an alloy consisting of 80% silver, 15% indium, and 5% cadmium. The various control rods are arranged in and move in symmetrically located groups, or banks. Banks A, B, C, and D are denoted as the control banks and are moved in a fixed sequential pattern to control the reactor over the power range of operation. The remaining rods are denoted as shutdown banks and are used to provide shutdown margin.

In addition to the control rods, a chemical (boric acid) shim is used to control excess core reactivity and to facilitate operational flexibility. Above certain concentrations of chemical shim, burnable poison rods and/or integral fuel burnable absorber rods are also used to control excess reactivity. Burnable poison can also be used to shape (i.e., improve) the core power distribution. The burnable poison rods contain borosilicate in the form of Pyrex glass clad in a stainless steel tube, or Al_2O_3 pellets in Zircaloy-4 tubes. Burnable poison rod assemblies, which may be used in any fuel assembly not under a control rod bank location, typically consist of clusters of either 8, 12, 16, or 20 rods that are inserted into the Zirconium-based alloy control rod guide tubes. IFBA fuel assemblies typically contain up to 148 IFBA rods symmetrically distributed throughout each assembly.

Flux suppression insert (FSI) assemblies were used in peripheral core locations in Unit 1 from Cycle 13 to Cycle 20 to suppress the neutron leakage flux in the radial and axial vicinity of reactor vessel weld locations. Each FSI contained twenty neutron absorber rods which were inserted into the fuel assembly guide thimble tubes. Each neutron absorber rod contained a hafnium stack encapsulated in thick walled Zircaloy cladding. The fast and thermal neutron flux in each fuel assembly with an FSI was reduced by reducing power through the insertion of negative reactivity. The active absorber region of the FSI assemblies was preferentially loaded toward the bottom of the active fuel region. By itself, this tended to skew the core average axial power distribution. To minimize this impact, some burnable poison rods with absorber removed from the bottom of the rodlets were used in Surry 1 cores with FSIs. Removal of the absorber had the effect of a positive reactivity insertion, which offset some of the axial impact of the FSIs. Other than the use of less absorber material and biasing the location of the poison stack toward the top of the fuel stack, these short burnable poison assemblies were mechanically identical to other current burnable poison assemblies.

Flux suppression inserts were removed from the Unit 1 core following operation of Cycle 20 and after approval of a revised methodology to assess the impact of fluence on vessel welds. When the FSIs were removed from the core, the use of shorter burnable poison assemblies was eliminated.

3.3.3.2.3 Conclusions

The effect of a given reload on previously acceptable safety limits is documented in a reload safety evaluation report. The report addresses the mechanical, nuclear, and thermal/hydraulic design of the reload core, and provides references wherein more detailed supporting information can be found.

3.3 REFERENCES

1. P. M. Wood, E. A. Bassler, P. E. MacDonald, and D. F. Paddleford, *Use of Burnable Poison Rods in Westinghouse Pressurized Water Reactors*, WCAP-7113, 1969.

2. Westinghouse Proprietary, *Nuclear Design of Pressurized Water Reactors with Burnable Poison Rods*, WCAP-9000, Revision 1, 1969.

3. R. F. Barry, *The Revised LEOPARD Code - A Spectrum Dependent Nonspatial Depletion Program*, WCAP-2759, March 1965.

4. Westinghouse Proprietary, *Power Distribution Control of Westinghouse Pressurized Water Reactors*, WCAP-7208, 1968.

5. L. W. Strawbridge, *Calculations of Lattice Parameters and Criticality for Uniform Water Moderated Lattices*, WCAP-3269-25, 1964.

6. W. J. Eich and W. P. Kovacik, *Reactivity and Neutron Flux Studies in Multiregion Loaded Cores*, WCAP-1433, 1961.

7. J. D. McGaugh and R. H. Chastain, *Power Density vs. Burnup Distribution in Yankee Core I*, WCAP-6051, 1963.

8. W. T. Sha, *An Analysis of Reactivity Worth of the Rod Cluster Control (RCC) Elements and Local Water Hole Power Density Peaking*, WCAP-3269-47, 1965.

9. C. G. Poncelet, *Effects of Fuel Burnup on Reactivity and Reactivity Coefficients in Yankee Core I*, WCAP-6055, 1963.

10. *Yankee Core Evaluation Program Quarterly Progress Report for the Period Ending June 30, 1963*, WCAP-6055, 1963.

11. E. Hellstrand and G. Lundgren, "The Resonance Integral for Uranium Metal and Oxide," *Nuclear Science and Engineering*, Vol. 12, No. 435, 1962.

12. E. Hellstrand, *Journal of Applied Physics*, Vol. 28, No. 1493, 1957.

13. E. Hellstrand, P. Blomberg, and S. Horner, "The Temperature Coefficient of the Resonance Integral for Uranium Metal and Oxide," *Nuclear Science and Engineering*, Vol. 8, No. 497, 1960.

14. A. Sauer, "Approximate Escape Probabilities," *Nuclear Science and Engineering*, Vol. 16, No. 329, 1963.

15. K. M. Case, F. de Hoffman, and G. Plascek, *Introduction to the Theory of Neutron Diffusion*, 1953.

16. W. T. Sha, *An Experimental Evaluation of the Power Coefficient in Slightly Enriched PWR Cores*, WCAP-3269-40, 1965.

17. Nuclear Engineering Staff, *Reload Nuclear Design Methodology*, VEP-FRD-42 Rev. 2.1-A, August 2003.

The following information is HISTORICAL and is not intended or expected to be updated for the life of the plant.

Table 3.3-1
TYPICAL NUCLEAR DESIGN DATA (INITIAL CORE)

Structural Characteristics	
1. Fuel weight (UO_2)	175,600 lb
2. Zircaloy weight	36,300 lb
3. Core diameter	119.7 in.
4. Core height	144 in.
Reflector Thickness and Composition	
5. Top - water plus steel	approximately 10 in.
6. Bottom - water plus steel	approximately 10 in.
7. Side - water plus steel	approximately 15 in.
8. H_2O/U volume ratio (cold)	4.18
9. Number of fuel assemblies	157
10. UO_2 rods per assembly	204
Performance Characteristics	
11. Heat output (initial rating)	2441 MWt
12. NSSS heat output (initial rating)	2449 MWt
13. NSSS heat output (corresponding to maximum calculated turbine rating)	2554 MWt
Fuel Burnup	
14. First cycle (average)	12,600 MWd/MTU
15. First core (average)	22,300 MWd/MTU
16. Design equilibrium batch average	31,500 MWd/MTU
Fuel Enrichment	
17. Weight percent (region 1)	1.85
18. Weight percent (region 2)	2.55
19. Weight percent (region 3)	3.10
20. Weight percent (equilibrium)	3.20

The following information is HISTORICAL and is not intended or expected to be updated for the life of the plant.

Table 3.3-1 (continued)
TYPICAL NUCLEAR DESIGN DATA (INITIAL CORE)

Hot-Channel Factors	
21. Nuclear heat flux hot-channel factor, F_q^N	2.72
22. Nuclear enthalpy rise hot-channel factor, $F_{\Delta H}^N$	1.58
Control Characteristics	
Effective Multiplication (Beginning of Life) with Burnable Poison Rods	
23. Cold, no power, clean	1.176
24. Hot, no power, clean	1.145
25. Hot, full power, clean	1.124
26. Hot, full power, Xe and Sm equilibrium	1.090
Control Rod Assemblies	
27. Material	5% Cd - 15% In - 80% Ag
28. Full length	48
29. Partial length (removed from core)	5
30. Number of absorber rods per control rod assembly	20
31. Total rod worth, BOL	See Table 3.3-3
Boron Concentration	
32. Refueling shutdown, rods in (k=0.90)	2000 ppm
33. Shutdown (k=0.99) with rods inserted, clean, cold	780 ppm
34. Shutdown (k=0.99) with all rods inserted, clean, hot	370 ppm
35. Shutdown (k=0.99) with no rods inserted, clean, cold	1250 ppm
36. Shutdown (k=0.99) with no rods inserted, clean, hot	1240 ppm
37. Clean	1005 ppm[a]

The following information is HISTORICAL and is not intended or expected to be updated for the life of the plant.

Table 3.3-1 (continued)
TYPICAL NUCLEAR DESIGN DATA (INITIAL CORE)

Boron Concentration (continued)	
38. Xenon equilibrium	740 ppm[a]
39. Xenon and samarium equilibrium	705 ppm[a]
40. Shutdown (k=0.99) all but one rod inserted, cold, clean	909 ppm
41. Shutdown (k=0.99) all but one rod inserted, hot, clean	509 ppm
Burnable Poison Rods	
42. Number and material of burnable poison rods	816 borated pyrex glass
43. BP worth, hot, delta k/k	6.9%
44. BP worth, cold, delta k/k	5.3%
Range of Kinetic Characteristics	
45. Moderator temperature coefficient (delta k/k)	$+0.3 \times 10^{-4}$ [b] to -3.5×10^{-4} per °F
46. Moderator pressure coefficient (delta k/k)	-0.3×10^{-6} to $+3.5 \times 10^{-6}$ per psi
47. Moderator density coefficient (delta k/k)	-0.1 to +0.3 per gm/cm^3
48. Doppler coefficient (delta k/k)	-0.1×10^{-5} to -1.6×10^{-5} per °F
49. Delayed neutron fraction	0.50 to 0.72%
50. Prompt neutron lifetime	2.5×10^{-5} sec
51. Moderator void coefficient (delta k/k)	$+0.5 \times 10^{-3}$ to -2.5×10^{-3} per % void

a. To control at hot full power, full length rods not inserted, k=1.0 (with burnable poison and part length rods in).
b. The positive coefficient does not occur at operating conditions (see Figure 3.3-5).

Table 3.3-2
TYPICAL REACTIVITY REQUIREMENTS FOR CONTROL RODS

	Percent delta k/k	
Requirements	Beginning of Life	End of Life
Control		
Power defect (combined Doppler, T_{avg}, and void effects)	1.75	3.28
Operation maneuvering band	0.70	0.70
Control rod bite	0.10	0.10
Total Control	2.55	4.08

Note: Specific numerical values for a given fuel cycles are updated as necessary in the associated reload safety evaluation report.

Table 3.3-3
TYPICAL CONTROL ROD WORTHS (DELTA k/k)

Core Conditions[a]	Rod Configurations	Percent Worth	Less 10%[b]	Design Reactivity Requirements	Shutdown Margin
BOL, HFP	48 rods in	10.05			
	47 rods in; highest-worth rod stuck out	8.85	7.96	2.55	5.41
EOL, HFP (1st cycle)	48 rods in	9.83			
	47 rods in; highest-worth rod stuck out	8.11	7.30	4.08	3.22
EOL, HFP (3rd cycle)	48 rods in	8.57			
	47 rods in; highest-worth rod stuck out	6.52	5.87	4.08	1.79

Note: Specific numerical values for a given fuel cycle are updated as necessary in the associated reload safety evaluation report.

a. BOL = beginning of life.
EOL = end of life.
HFP = hot full power.
b. Calculated rod worth is reduced by 10% to allow for uncertainties.

The following information is HISTORICAL and is not intended or expected to be updated for the life of the plant.

Figure 3.3-1
CYCLE 1 BURNABLE POISON CLUSTER LOCATIONS

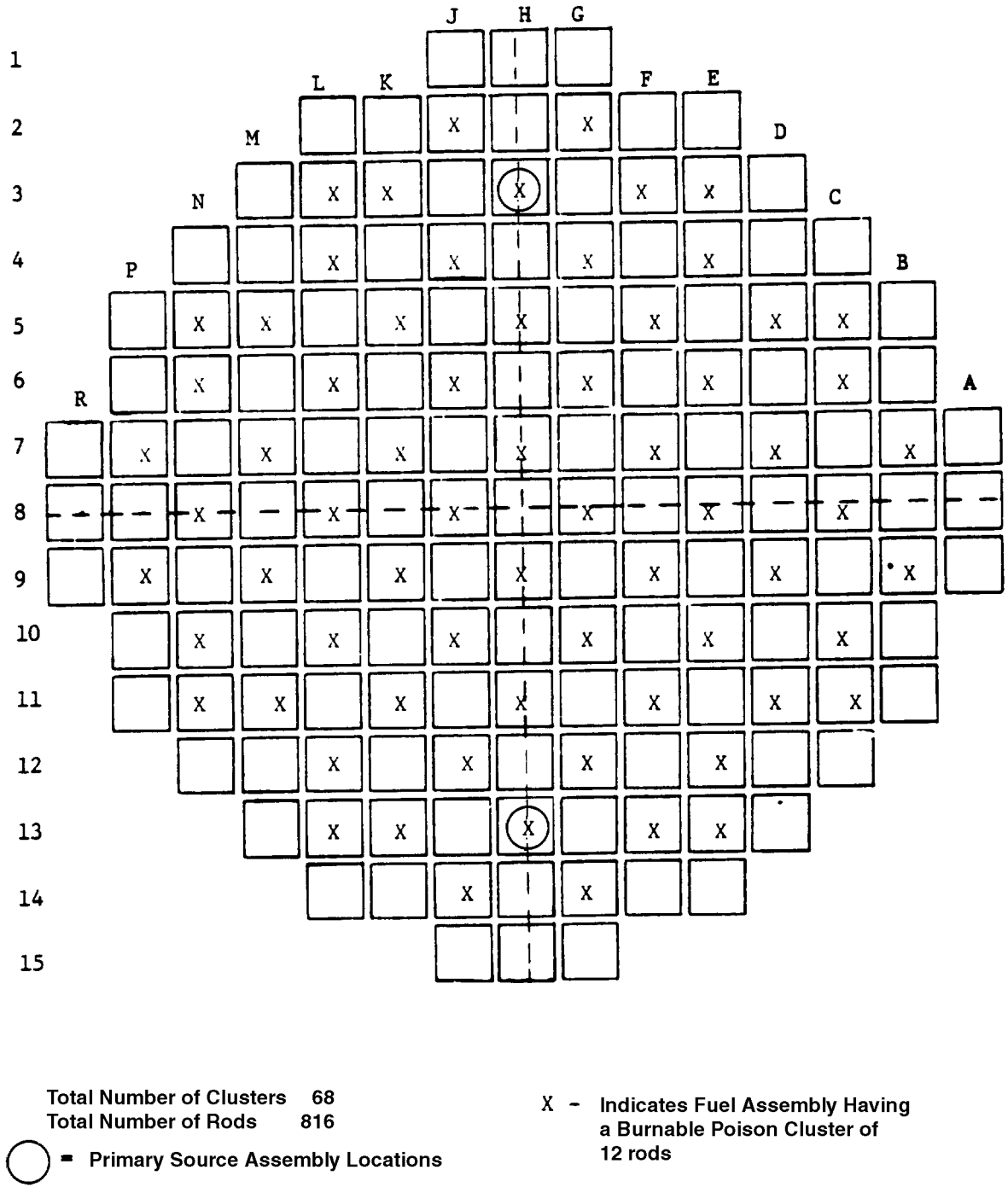

Figure 3.3-2
NORMALIZED POWER DENSITY DISTRIBUTION AT BEGINNING OF LIFE,
GROUP D INSERTED, HOT FULL POWER, NO XENON

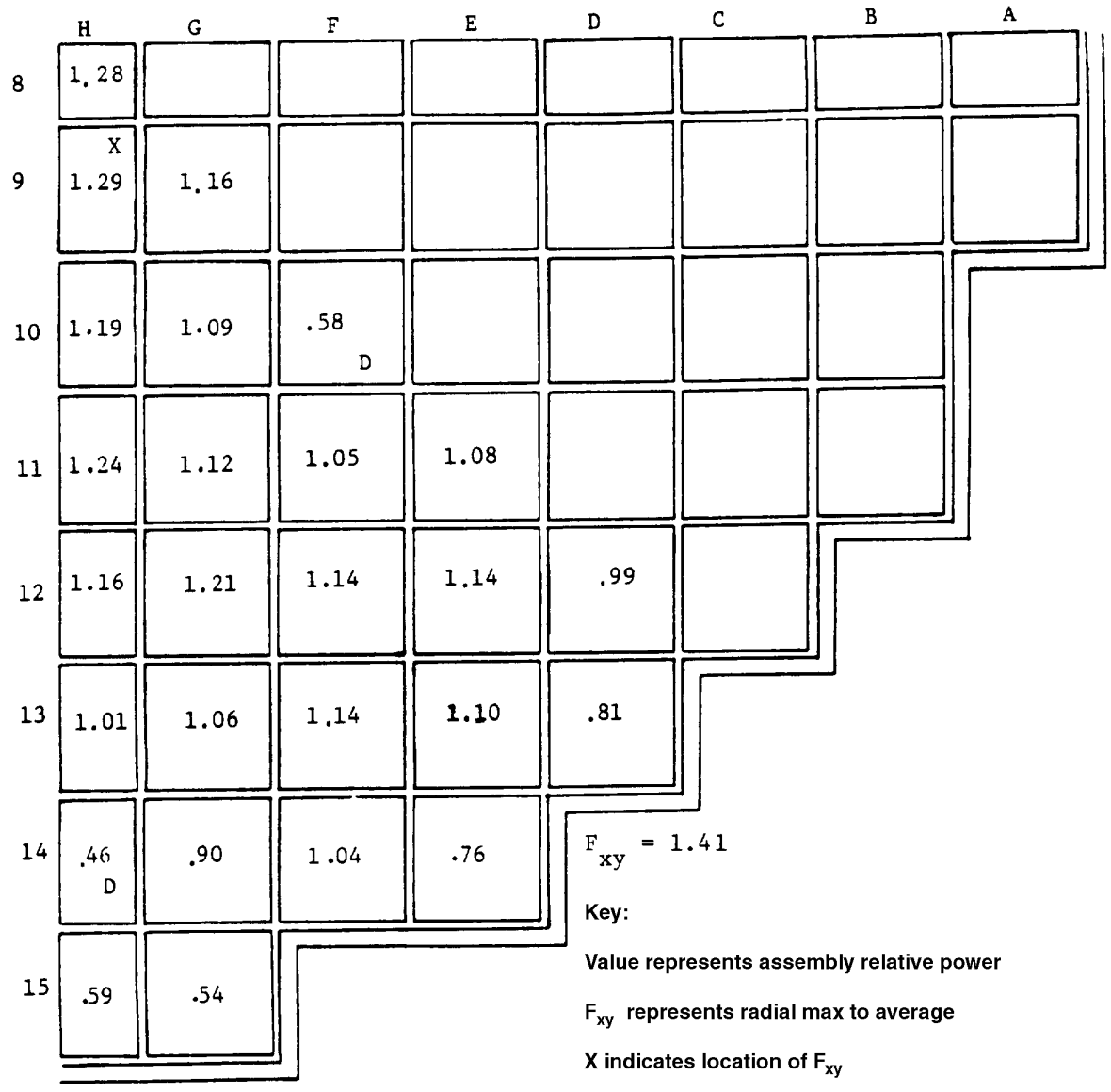

S0303002

Figure 3.3-3
NORMALIZED POWER DENSITY DISTRIBUTION AT BEGINNING OF LIFE,
UNRODDED CORE, HOT FULL POWER, NO XENON

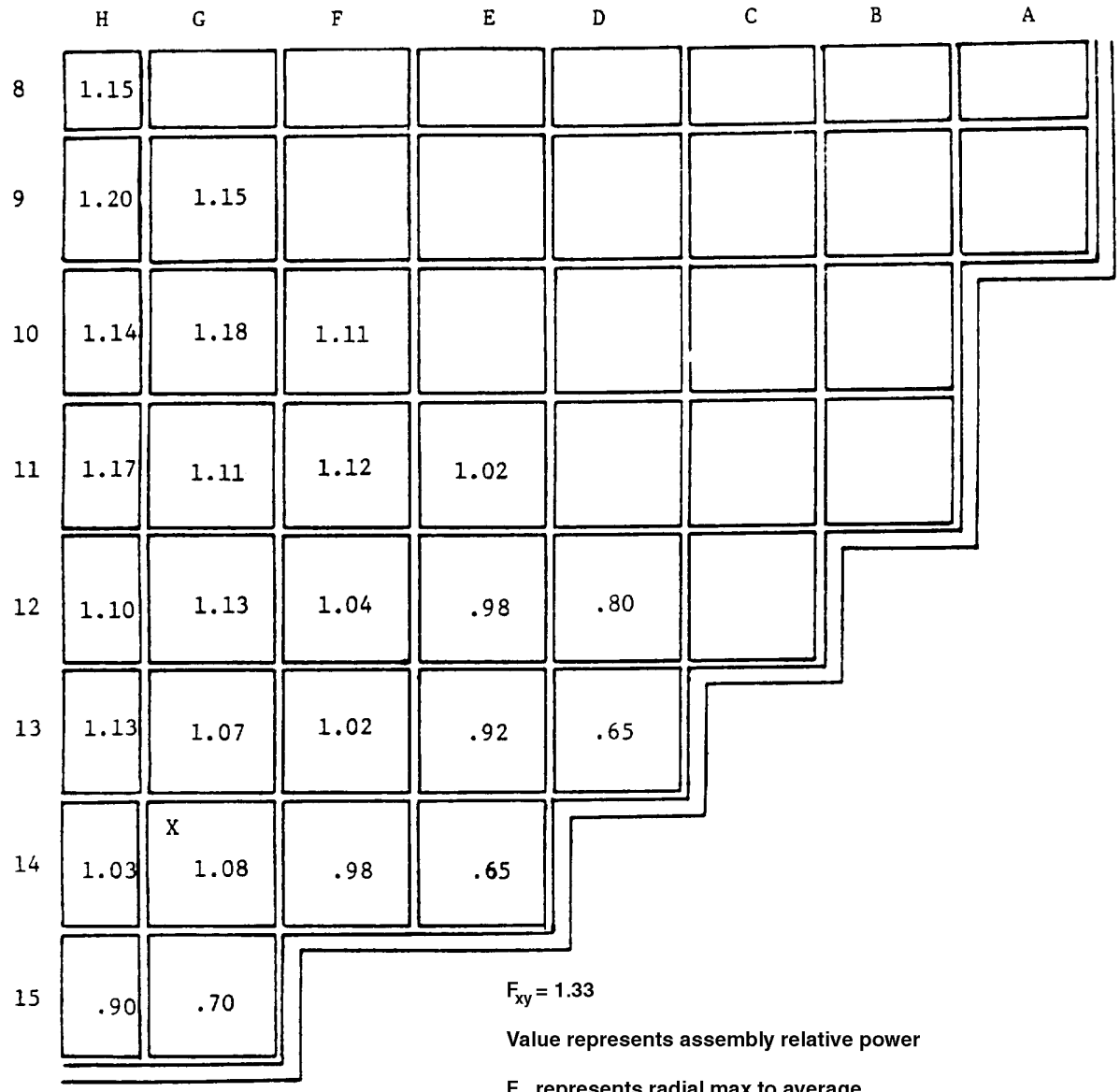

S0303003

Figure 3.3-4
ARRANGEMENT OF BURNABLE POISON RODS WITHIN AN ASSEMBLY

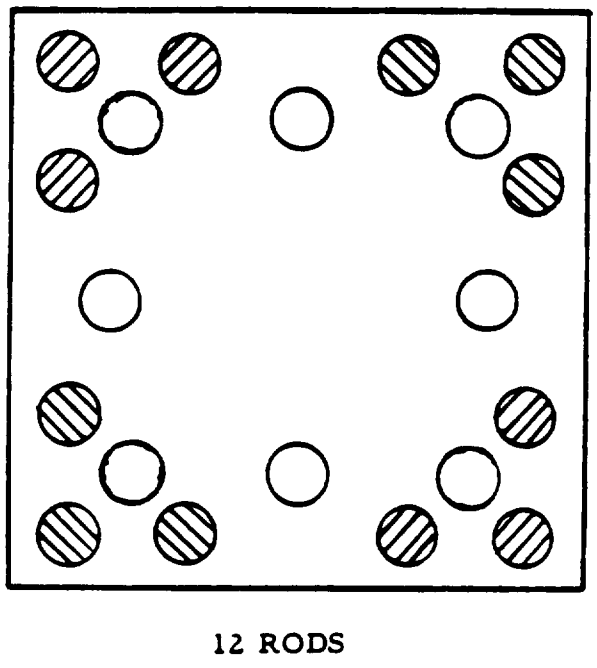

Figure 3.3-5
MODERATOR TEMPERATURE COEFFICIENT VS. MODERATOR TEMPERATURE

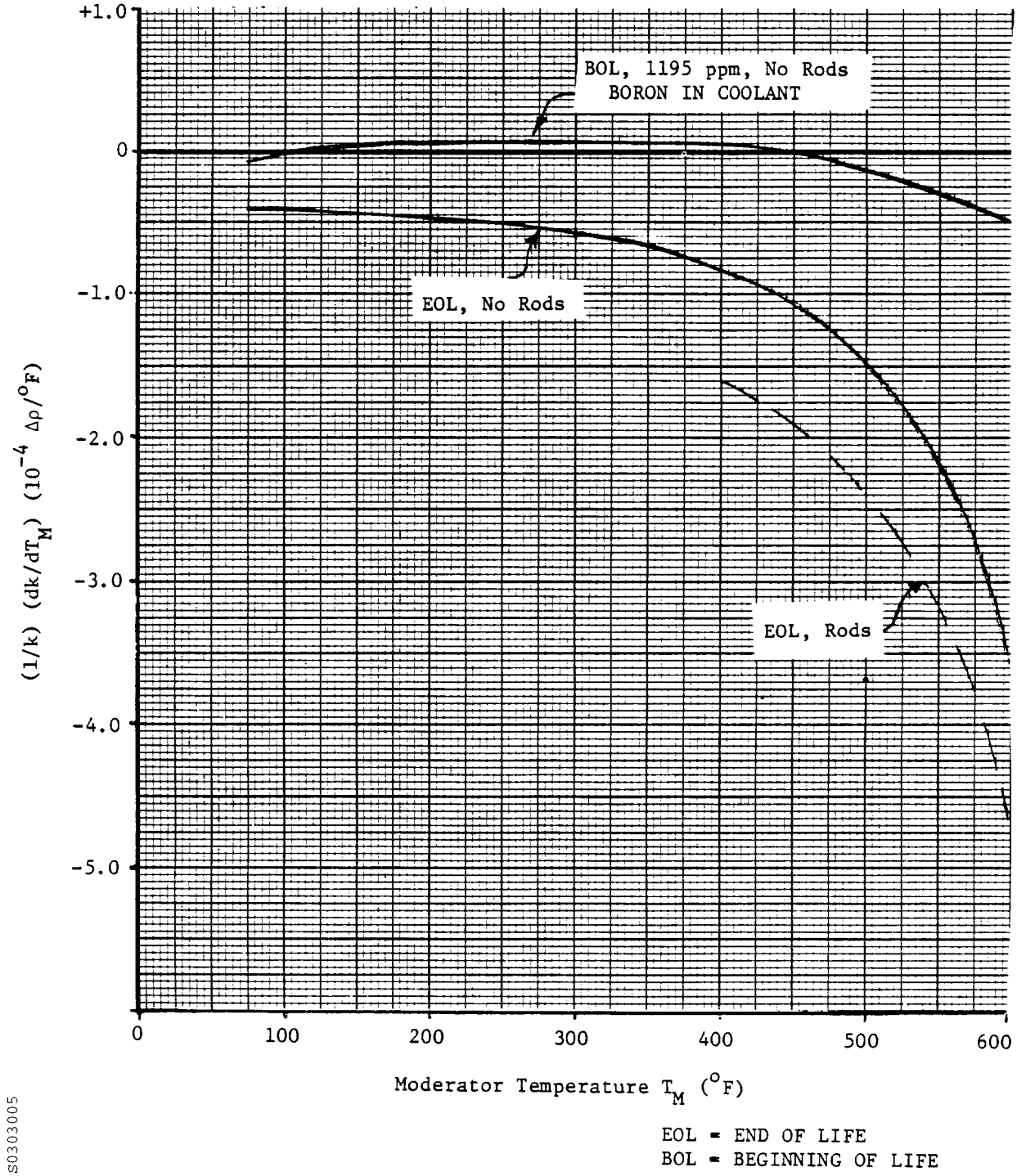

Figure 3.3-6
DOPPLER COEFFICIENT VS. EFFECTIVE FUEL TEMPERATURE (BOL)

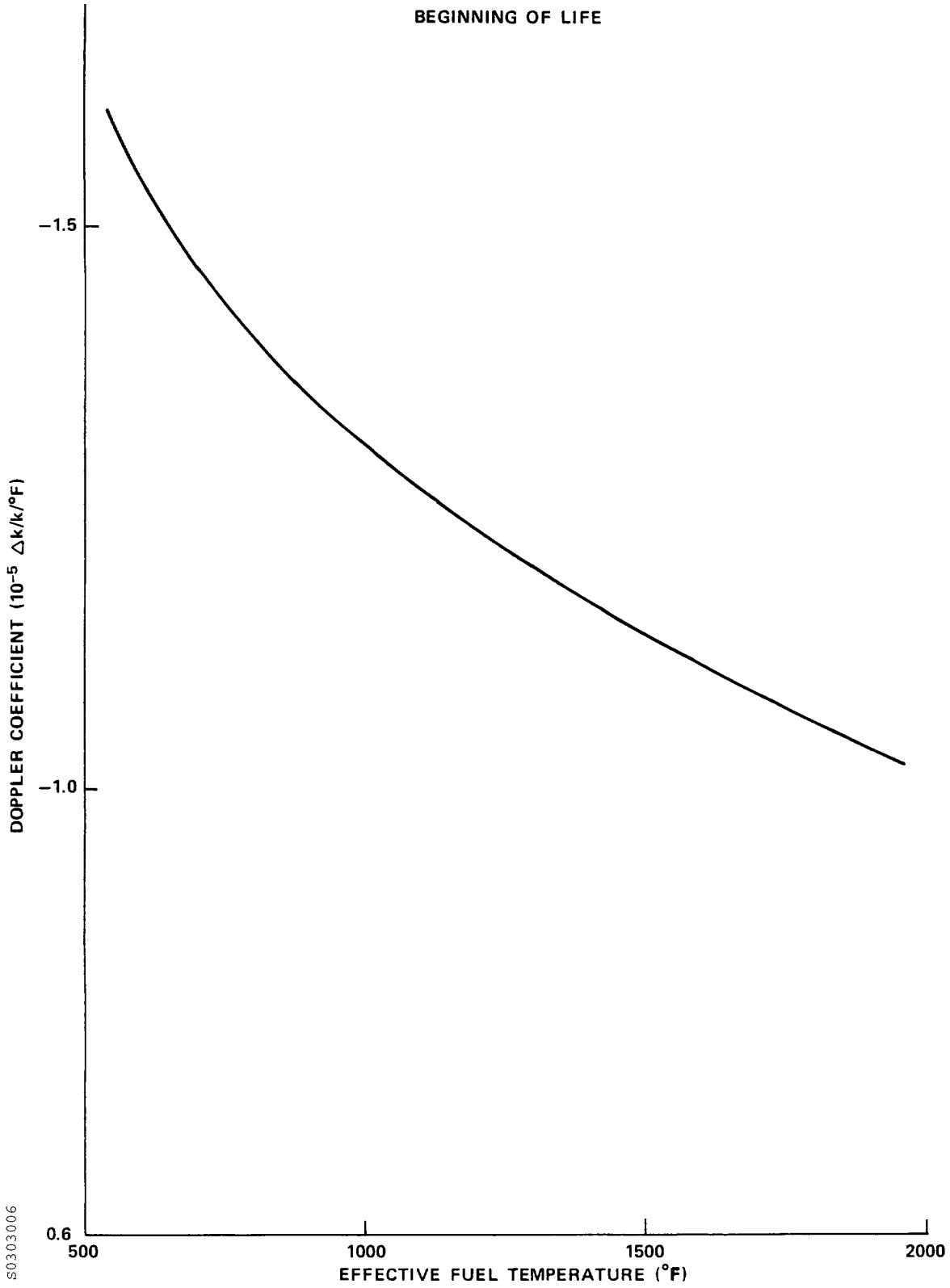

Figure 3.3-7
POWER COEFFICIENT (AIR GAP MODEL)

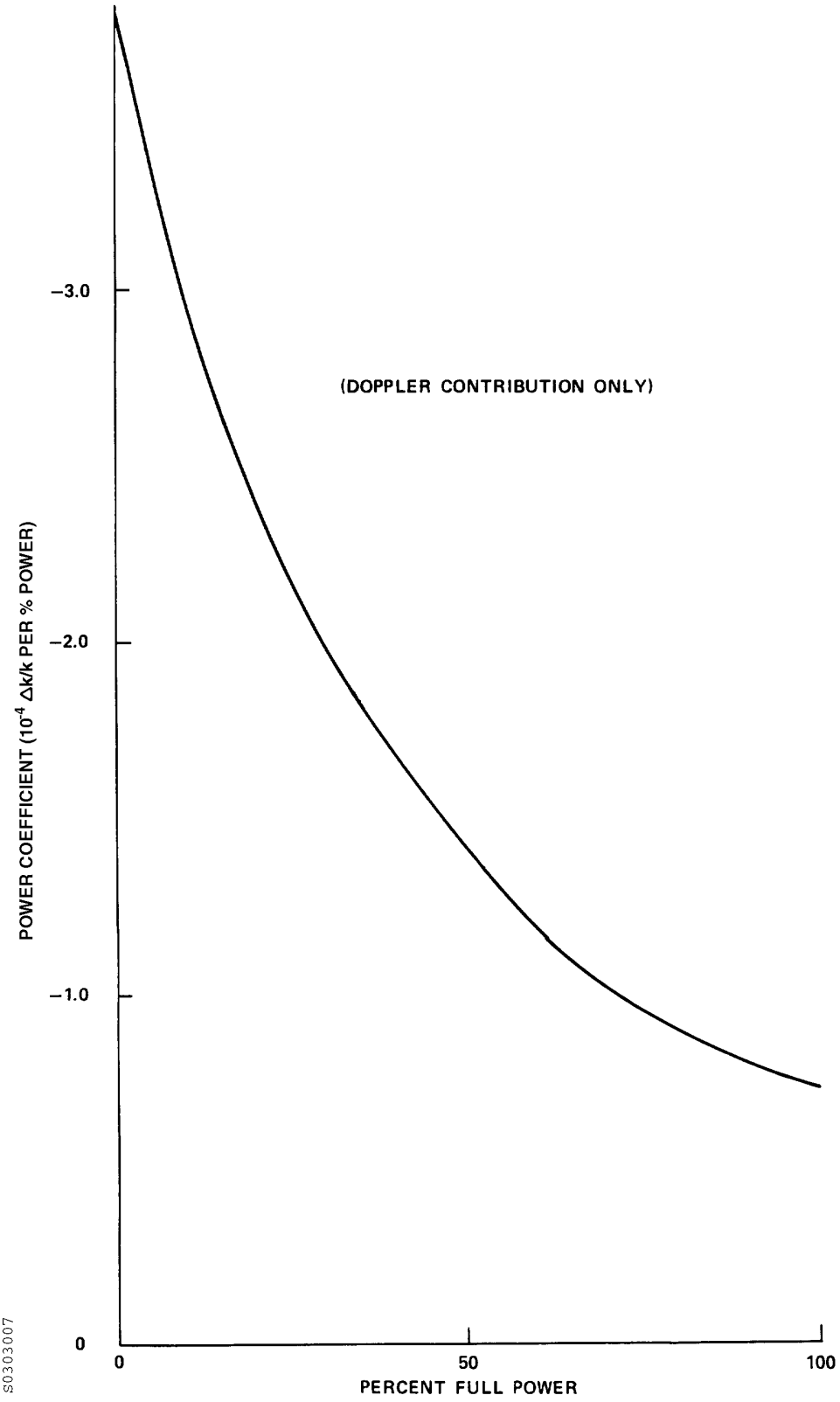

Figure 3.3-8
POWER COEFFICIENT (CLOSED GAP MODEL)

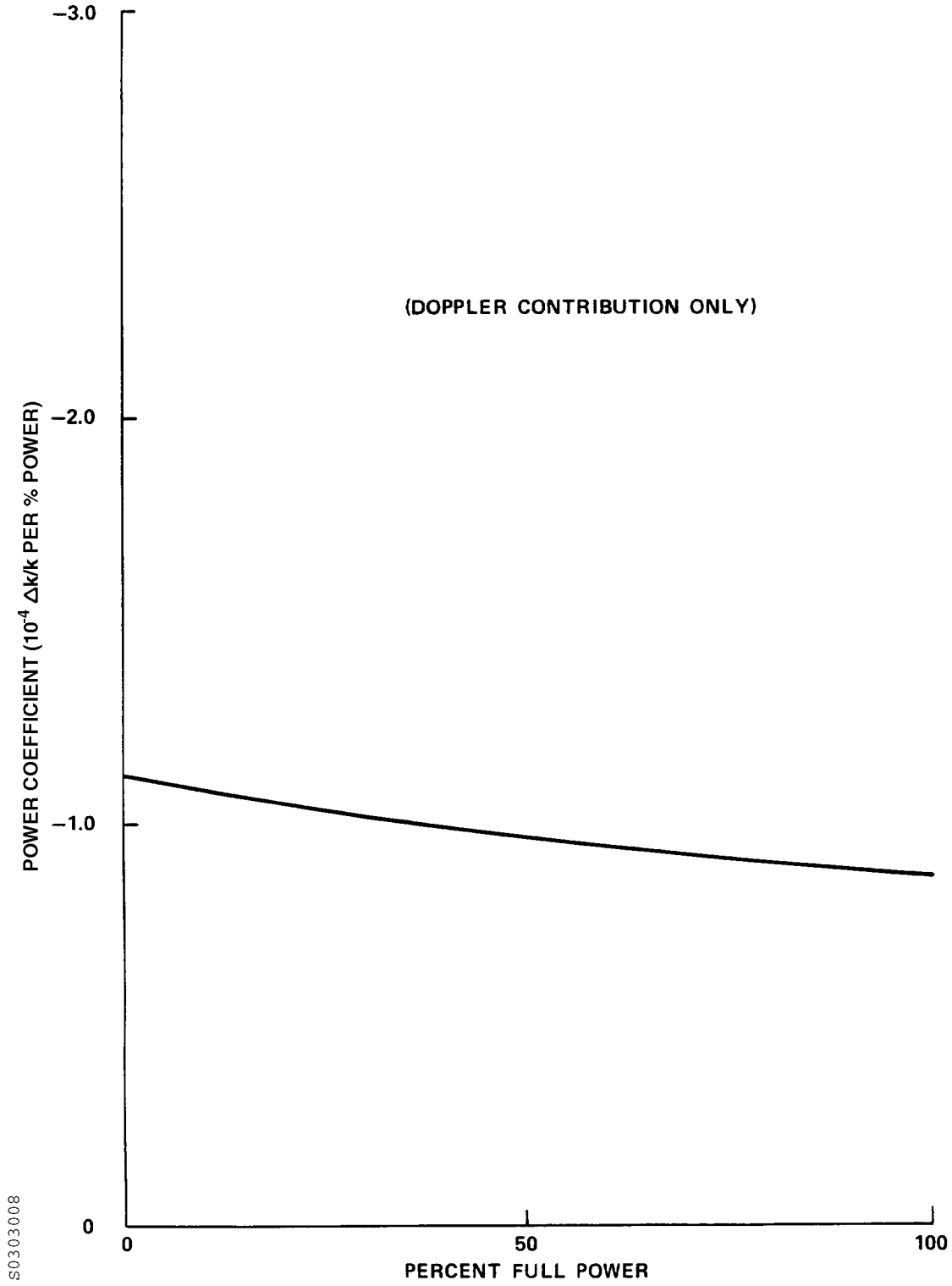

Figure 3.3-9
CONTROL ROD BANK LOCATIONS

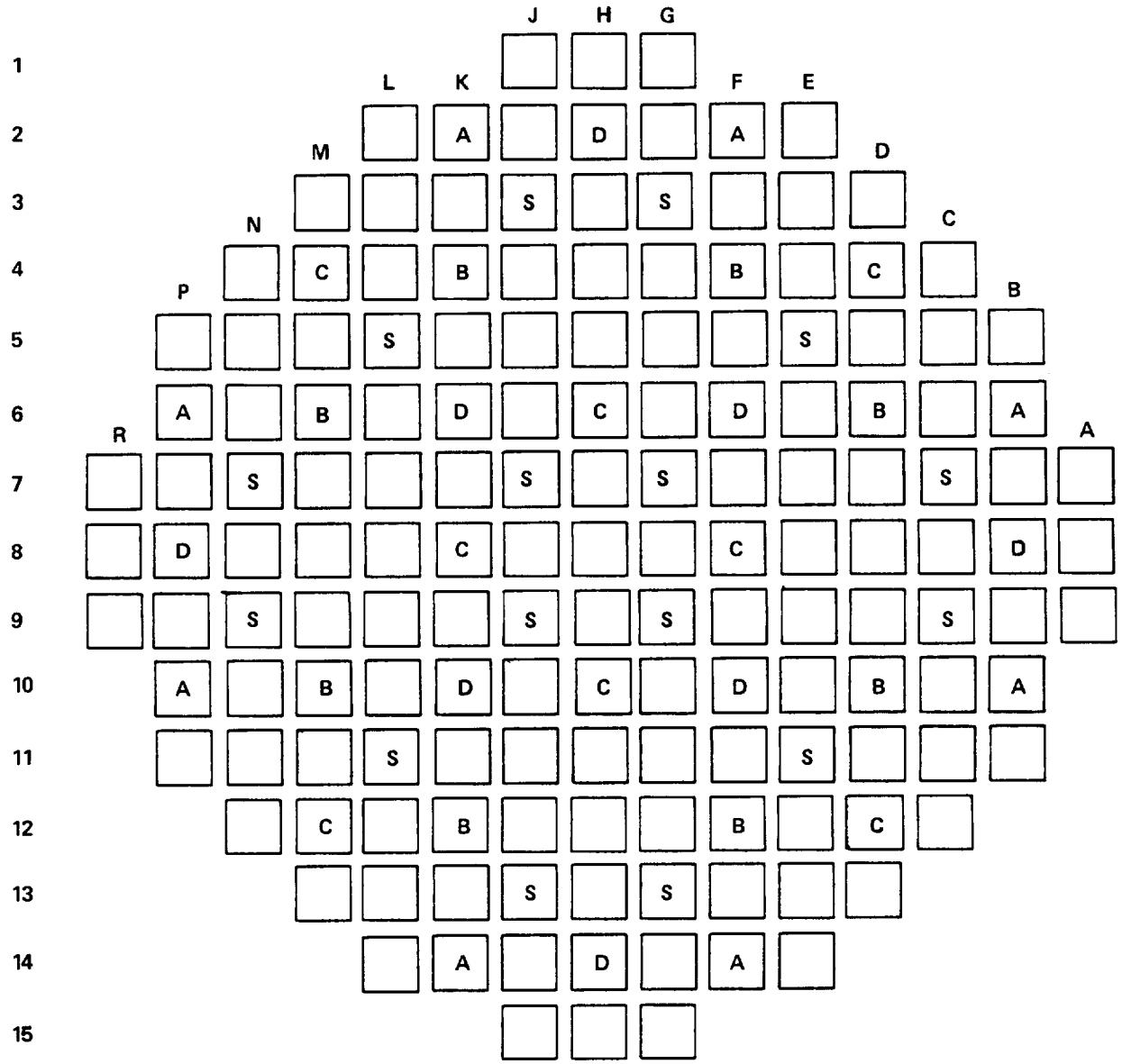

CONTROL ROD ASSEMBLY BANKS

FUNCTION	NUMBER OF ASSEMBLIES
CONTROL BANK D	8
CONTROL BANK C	8
CONTROL BANK B	8
CONTROL BANK A	8
SHUTDOWN (S)	16
	48

S0303009

3.4 THERMAL/HYDRAULIC DESIGN AND EVALUATION

3.4.1 Thermal/Hydraulic Characteristics of the Design

3.4.1.1 Fuel and Cladding Temperatures

Consistent with the thermal-hydraulic design bases, the following discussion pertains mainly to fuel pellet temperature evaluation. The thermal-hydraulic design assures that the maximum fuel temperature is below the melting point of UO_2 (melting point of 5080°F (Reference 6) unirradiated and decreasing by 58°F per 10,000 MWD/MTU). To preclude center melting and as a basis for overpower protection system setpoints, a calculated centerline fuel temperature of 4700°F has been selected as the overpower limit. This provides sufficient margin for uncertainties in the thermal evaluations. The temperature distribution within the fuel pellet is predominantly a function of the local power density and the UO_2 thermal conductivity. However, the computation of radial fuel temperature distributions combines crud, oxide, cladding gap and pellet conductances. The factors which influence these conductances, such as gap size (or contact pressure), internal gas pressure, gas composition, pellet density, and radial power distribution within the pellet, etc., have been combined into a semi-empirical thermal model with the model modifications for time dependent fuel densification given in References 1 and 50. This thermal model enables the determination of these factors and their net effects on temperature profiles. The temperature predictions have been compared to inpile fuel temperature measurements and melt radius data with good results.

As described in References 1 and 50 fuel rod thermal evaluations (fuel centerline, average and surface temperatures) are determined throughout the fuel rod lifetime with consideration of time dependent densification. To determine the maximum fuel temperatures, various burnup rods, including the highest burnup rod, are analyzed over the rod linear power range of interest.

The principle factors which are employed in the determination of the fuel temperature are discussed below.

3.4.1.1.1 UO_2 Thermal Conductivity

At the higher temperatures, thermal conductivity is best obtained by utilizing the integral conductivity to melt which can be determined with more certainty.

From an examination of the data, it has been concluded that the best estimate for the value of $\int_0^{2800°C} K dt$ is 93 watts/cm. The design curve for the thermal conductivity is shown in Figure 3.4-1. Thermal conductivity for UO_2 at 95% theoretical density can be represented best by the following equation:

$$K = \frac{1}{(11.8 + 0.0238T)} + 8.775 \times 10^{-13} T^3$$

where:

K= watts/cm-°C

T = °C

3.4.1.1.2 Radial Power Distribution in UO_2 Fuel Rods

An accurate description of the radial power distribution as a function of burnup is needed for determining the power level for incipient fuel melting and other important performance parameters such as pellet thermal expansion, fuel swelling and fission gas release rates.

This information on radial power distribution in UO_2 fuel rods is determined with the neutron transport theory code, LASER. The LASER Code has been validated by comparing the code predictions on radial burnup and isotopic distributions with measured radial microdrill data. A "radial power depression factor," f, is determined using radial power distributions predicted by LASER. The factor f enters into the determination of the pellet centerline temperature, T_C, relative to the pellet surface temperature, T_s, through the expression:

$$\int_{T_S}^{T_C} K(T)dt = \frac{q'f}{4\pi}$$

where:

K(T) = the thermal conductivity for UO_2 with a uniform density distribution

q' = the linear power generation rate

f = radial power depression factor

3.4.1.1.3 Gap Conductance

The temperature drop across the pellet-clad gap is a function of the gap size and the thermal conductivity of the gas in the gap. The gap conductance model is selected such that when combined with the UO_2 thermal conductivity model, the calculated fuel centerline temperatures reflect the inpile temperature measurements.

The temperature drop across the gap is calculated by assuming an annular gap conductance model of the following form:

$$h = \frac{K_{gas}}{\frac{\delta}{2}(GMF) + \delta_r}$$

where:

h = contact conductance, Btu/hr-ft^2-°F

K_{gas} = thermal conductivity of the gas mixture including a correction factor for the accommodation coefficient for light gases (e.g. helium), Btu/hr-ft-°F

δ = diametral gap size, ft

δ_r = effective gap spacing due to surface roughness, ft

GMF = a gap multiplication factor to eliminate bias between predicted and measured values or an empirical correlation derived from the thermocouple and melt radius data.

The larger gap conductance value from these two equations is used to calculate the temperature drop across the gap for finite gaps.

For evaluations in which the pellet-clad gap is closed, a contact conductance is calculated. The contact conductance between UO_2 and zirconium alloy cladding has been measured and found to be dependent on the contact pressure, composition of the gas at the interface and the surface roughness. This information together with the surface roughness found in Westinghouse reactors leads to the following correlation:

$$h = 0.6P + \frac{K_{gas}}{\delta_r}$$

where: P = contact pressure, psi

3.4.1.1.4 Surface Heat Transfer Coefficients

Forced convection heat transfer coefficients are obtained from the familiar Dittus-Boelter correlation (Reference 5), with the properties evaluated at bulk fluid conditions:

$$\frac{hD_e}{K} = 0.023\left(\frac{D_eG}{\mu}\right)^{0.8}\left(\frac{C_p\mu}{K}\right)^{0.4}$$

where:

h = heat transfer coefficient, Btu/hr-ft^2-°F

D_e = equivalent diameter, ft

K = thermal conductivity, Btu/hr-ft-°F

G = mass velocity, lb_m/hr-ft^2

H = dynamic viscosity, lb_m/ft-hr

C_p = heat capacity, Btu/lb_m-°F

This correlation has been shown to be conservative for rod bundle geometries with pitch to diameter ratios in the range used by PWRs.

The onset of nucleate boiling occurs when the clad wall temperature reaches the amount of superheat predicted by Thom's (Reference 39) correlation. After this occurrence, the outer clad wall temperature is determined by the Thom's correlation in the fuel rod thermal evaluations (References 1, 40, & 50):

$$\Delta T_{sat} = \left[0.072^{(-P/1260)}\right](q'')^{0.5}$$

where:

ΔT_{sat} = wall superheat, $T_W - T_{sat}$, °F

q" = wall heat flux, Btu/hr-ft^2

P = pressure, psia

T_W = outer cladding wall temperature, °F

T_{sat} = saturation temperature of coolant at P, °F

In sub-channel analysis, THINC-IV (References 41 & 42) uses the Thom's correlation to predict the inception of nucleate boiling and to select the void fraction correlation. The COBRA IIIC/MIT computer code (Reference 30), however, uses the Jens and Lottes correlation (Reference 43) to predict the inception of nucleate boiling.

3.4.1.1.5 Fuel Clad Temperatures

The outer surface of the fuel rod at the hot spot operates at a temperature of approximately 660°F for steady state operation at rated power throughout core life due to the onset of nucleate boiling. Initially (beginning-of-life), this temperature is that of the clad metal outer surface.

During operation over the life of the core, the buildup of oxides and crud on the fuel rod surface causes the temperature of the outer surface of the clad metal to increase. Allowance is made in the fuel center melt evaluation for this temperature rise. Since the thermal-hydraulic design basis limits DNB, adequate heat transfer is provided between the fuel clad and the reactor coolant so that the core thermal output is not limited by considerations of clad temperature.

3.4.1.2 **Westinghouse Experience with High-Power Fuel Rods**

Westinghouse experience (through 1969) with non-pressurized fuel rods operating at high power ratings has been summarized in the Indian Point Unit 2 Preliminary Safety Analysis Report (Docket 50-247) and in the Preliminary Safeguards Report for the Saxton Reactor operating at 35 MWt (Docket 50-146). These reports present considerable statistical evidence of successful operation of 1368 high-performance Zircaloy-clad fuel rods in the Carolina-Virginia Test Reactor (CVTR) and 94,920 rods in the Shippingport Core I Blanket. After the date of these reports, a significant amount of additional information was developed relating to the integrity of free-standing Zircaloy-clad oxide fuel rods at high power ratings. In addition, a comprehensive

experimental program was performed to extend the operating experience to higher power and to higher exposures. This information is summarized in Figure 3.4-2.

Figure 3.4-2 shows that 30 Saxton Plutonium Project non-pressurized fuel rods operated at a design peak power level of up to 18.5 kW/ft to a peak exposure of approximately 30,000 MWD/MTU (megawatt days per metric ton of metal (U + Pu)). No failures occurred with this fuel. In the Saxton overpower test, two selected fuel rods from the Saxton Plutonium Project assemblies were removed after peak exposure of 18,000 MWD and inserted in a subassembly for short-time irradiation at a design rating of 25 kW/ft. Results of this program indicated satisfactory performance of the fuel in every respect. The Saxton Plutonium Project was extended by irradiating approximately 250 rods to peak burnups of about 50,000 MWD/MTU at design linear power levels ranging from 9.5 to 23.6 kW/ft.

In the above tests (performed on non-pressurized rods), the strain fatigue experienced by the cladding was more severe than that expected to occur for pressurized rods, which would be placed under identical operating conditions.

Internally pressurized fuel rods have been investigated at Westinghouse. These investigations included ex-core and incore experimental programs and analytical studies. Fuel rods internally pressurized with various gases were irradiated in the Saxton reactor. Test results showed that initial pressurization was effective in substantially reducing the rate of cladding-creep onto the UO_2 fuel. The Saxton test results confirmed the results of analyses that predict fuel-cladding mechanical interaction early in life for non-pressurized fuel rods, and delayed interaction for initially pressurized fuel rods.

To verify the substantial design margin that exists with regard to excessive internal pressures in a fuel rod, several highly pressurized Zircaloy-clad fuel rods were irradiated for several months in the Saxton reactor, then removed for examination. At an internal pressure of approximately 3500 psia (as compared to the design value of 2250 psia), the fuel rods operated satisfactorily for the period of the test without any indication of failure. Two fuel rods, deliberately tested at unrealistically high internal pressures, experienced clad cracking but operated satisfactorily for the period of the test.

Westinghouse irradiated many internally pressurized fuel rods in Saxton and also at the Jose Cabrera plant in Spain. Approximately 150 fuel rods were subjected to long-term irradiation testing. These tests provided additional confirmation of the suitability of internally pressurized fuel rods. This long-term testing program was continued at Saxton until 1971 and at Jose Cabrera until 1972, and provided verification of core life performance data with the fuel rod design bases.

The initial Surry fuel was intended to operate to a peak fuel exposure of 49,000 MWD/MTU. The change in fuel characteristics as a function of exposure had been investigated in certain cases, but the exact nature and extent of such changes to the planned exposures had not been investigated in great detail. However, based upon work at lower exposures (References 6 & 8-10), such property changes were not considered of major significance and

tended to saturate at relatively low exposures. The models used to predict the thermal performance of the fuel in the initial Surry cores were combined in an integrated computer program to enable consideration of the several effects arising due to irradiation. These thermal models were compared to data in the literature, with generally good correlation. The thermal performance of current fuel is similarly evaluated using an overall fuel design code that has been shown to provide good agreement with a variety of published and proprietary data (References 1 & 50).

More recent experience with ZIRLO- and Zircaloy-clad fuel is described in WCAP-8183 (Reference 11), *Operational Experience with Westinghouse Cores*, which is updated periodically.

3.4.1.3 **Pressure Drop and Hydraulic Forces**

The total pressure loss across the reactor vessel, including the inlet and outlet nozzles, and the pressure drop across the core are listed in Table 3.4-1. The values for the original design include a 10% uncertainty factor, whereas the current design values are presented as nominal values.

The thermal/hydraulic design parameters are given in Table 3.4-1.

3.4.2 Heat Flux Ratio and DNB Correlation

Departure from nucleate boiling is predicted by analysis of hydrodynamic and heat transfer phenomena and is affected by the local and upstream conditions, including the flux distribution.

In reactor design, the heat flux associated with departure from nucleate boiling and the location of departure from nucleate boiling are both important. The magnitude of the local fuel rod temperature after departure from nucleate boiling occurs depends upon the axial location of the occurrence. The W-3 DNB correlation and its modification for the “L”-grid (References 12 & 44), which have been utilized in the analysis of 15 x 15 LOPAR assemblies (all assemblies prior to Region 12 on both units), incorporate both local and system parameters in predicting the local DNB heat flux. These correlations include the non-uniform flux effect and the upstream effect, which includes inlet enthalpy and distance. The local DNB heat flux ratio, defined as the ratio of the DNB heat flux to the local heat flux, is indicative of the margin available in the local heat flux to the onset of departure from nucleate boiling. The WRB-1 DNB correlation, which is used in the analysis of 15 x 15 Surry Improved Fuel (SIF) assemblies (Region 12 of both units and subsequent regions), is based on local fluid conditions and represents the rod bundle data with better accuracy over a wide range of variables than previous correlations (W-3 based) used in design.

3.4.2.1 **W-3 Correlation**

The W-3 DNB correlation was developed to predict the DNB flux and the location of departure from nucleate boiling equally well for uniform and axially non-uniform heat flux distributions. This correlation replaced the preceding WAPD W-2 correlations (published in

Nucleonics (Reference 13), May 1963), in order to eliminate the discontinuity of the latter at the saturation temperature, and to provide a single unambiguous criterion of the design margin.

The sources of the data used in developing this correlation were:

WAPD-188 (1958)	CU-TR-No. 1 (NW-208) (1964)
ASME Paper 62-WA-297 (1962)	CISE-R-90 (1964)
CISE-R-63 (1962)	DP-895 (1964)
ANL-6675 (1962)	AEEW-R-356 (1964)
GEAP-3766 (1962)	BAW-3238-7 (1965)
AEEW-R-213 and 309 (1963)	AE-RTL-778 (1965)
CISE-R-74 (1963)	AEEW-355 (1965)
CU-MPR-XIII (1963)	EUR-2490.e (1965)

The comparison of the measured to predicted DNB flux of this correlation is given in Figure 3.4-3. The local flux DNBR versus the probability of not reaching departure from nucleate boiling is plotted in Figure 3.4-4. This plot indicates that with a DNBR equal to the design DNBR limit (Section 3.2.3), the probability of not reaching departure from nucleate boiling is 95% at a 95% confidence level.

Rod bundle data without mixing vanes agree very well with the predicted DNB flux, as shown in Figure 3.4-5. The rod bundle data with mixing vanes, shown in Figure 3.4-6, show on the average an 8% higher value of DNB heat flux than predicted by the W-3 DNB correlation.

It should be emphasized that the inlet subcooling effect of the W-3 correlation was obtained from both uniform and non-uniform data. The existence of an inlet subcooling effect has been demonstrated to be real, and hence the actual subcooling was used in the calculations. The W-3 correlation was developed from tests with flow in tubes and rectangular channels. Good agreement was obtained when the correlation was applied to test data for rod bundles.

The form of the W-3 correlation was presented by Tong in Reference 45. The W-3 predicted heat flux at DNB is calculated as follows:

$$q'' = \frac{q''_{DNB,\,EU,\,Dh}}{F}(CWF)(F'_s)$$

where:

$q''_{DNB,EU,Dh}$ = W-3 Equivalent Uniform Heat Flux with all flow cell walls heated

F = Nonuniform Heat Flux Factor (F-factor)

CWF = W-3 Cold Wall Factor

F'_s = W-3 Modified Spacing Factor

Subsequent to Reference 45, an extensive experimental program was performed to investigate the behavior of DNB due to non-uniform axial heat flux distribution, heater rod lengths, axial grid spacing, and grids with and without mixing vanes. The results of these tests are documented in References 44, 46, 47, and 48.

3.4.2.1.1 W-3 Equivalent Uniform Flux DNB Correlation

The equivalent uniform DNB flux $q'_{DNB,EU}$ is calculated from the W-3 equivalent uniform flux DNB correlation as follows:

$$\frac{q'_{DNB,EU}}{10^6} = [(2.022 - 0.0004302p) + (0.1722 - 0.0000984p)e^{(18.177 - 0.004129p)X}] \times \left[1.037 + \frac{G}{10^6}(0.1484 - 1.596X + 0.1729X|X|)\right] \times [1.157 - 0.869X] \times [0.2664 + 0.8357e^{-3.151D_e}] \times [0.8258 + 0.000794(H_{sat} - H_{in})]$$

The ranges of the parameters in the data used to develop the correlation are:

System pressure	p = 1000 to 2300 psia
Mass velocity	$G = 1.0 \times 10^6$ to 5.0×10^6 lb/hr-ft^2
Equivalent diameter	D_e = 0.2 to 0.7 in.
Quality	X = -0.25 to +0.15
Inlet enthalpy	H_{in}, no limit, Btu/lb
Length	L = 10 to 144 in.
Heated perimeter/Wetted perimeter	D_h/D_e = 0.88 to 1.00

Geometries - circular tube, rectangular channel, and rod bundles

Flux - uniform and equivalent uniform flux converted from non-uniform data by using the F-factor of Reference 12.

3.4.2.1.2 Nonuniform Heat Flux Factor (F-factor)

The F-factor relates DNB data for axially non-uniform power distributions to DNB data for axially uniform power distributions (Reference 45). Reference 46 documented the experimental

program to investigate the effects on DNB due to non-uniform axial heat flux distributions. It was concluded therein that the use of the F-factor was an acceptable means of accounting for axially non-uniform power distributions.

The local non-uniform $q''_{DNB,N}$ is calculated as follows:

$$q''_{DNB,N} = \frac{q''_{DNB,EU}}{F}$$

where:

$$F = \frac{C}{q''_{local\ at\ l_{DNB}}(1 - e^{-Cl_{DNB}})} \int_0^{l_{DNB}} q''(z) e^{-C(l_{DNB} - z)} dz$$

l_{DNB} = distance from the inception of local boiling to the point of DNB

z = distance from the inception of local boiling, measured in the direction of the flow

The empirical constant, C, as presented in Reference 12, was revised in Reference 45 through the use of more recent non-uniform DNB data. However, the revised expression (showing less than 1% deviation from that of Reference 12) does not significantly influence the value of the F-factor and the DNBR. It does provide a better prediction of the location of departure from nucleate boiling.

The new expression is:

$$C = 0.15 \frac{(1 - \chi_{DNB})^{4.31}}{(G/10^6)^{0.478}} in^{-1}$$

where:

G = mass velocity lb/hr-ft^2

χ_{DNB} = quality of the coolant at the location where DNB flux is calculated

In determining the F-factor, the value of q''_{local} at l_{DNB} was measured at $z = l_{DNB}$, the location where the DNB flux is calculated. For a uniform flux, F becomes unity, so that $q''_{DNB,N}$ reduces to $q''_{DNB,EU}$. The comparisons of predictions by using W-3 correlations and the non-uniform DNB data obtained by B&W (Reference 15), Lee (References 16 & 17), and Obertelli (Reference 16) are given in Figures 3.4-8 and 3.4-9. To determine the predicted location of departure from nucleate boiling, the ratio of the predicted DNB flux to the local heat flux along the length of the channel must be evaluated. The location of the minimum DNBR is considered to be the location of departure from nucleate boiling.

3.4.2.1.3 W-3 Cold Wall Factor

The W-3 equivalent uniform flux DNB correlation is used for predicting DNB in channels which are entirely, or almost entirely, surrounded by heated walls (i.e., typical cells). The W-3 Cold Water Factor (CWF) accounts for the presence of unheated surfaces due to thimble or instrument tubes (i.e., thimble cells) (Reference 45). References 47 and 48 documented the experimental program to investigate the effect on DNB due to thimble cold wall cells. It was concluded that the cold wall factor is appropriate for rod bundles with mixing vane grids.

The W-3 Cold Wall Factor from Reference 45 is:

$$CWF = 1.0 - R_u[13.76 - 1.372e^{(1.78X)} - 4.732(G/10^6)^{-0.0535} - 0.0619(P/10^3)^{0.14} - 8.509(D_h)^{0.107}]$$

where:

$R_u = 1 - (D_e/D_h)$

X = local quality, fraction

G = local mass velocity, lb/hr-ft^2

P = primary system pressure, psia

D_h = equivalent diameter based on heated perimeter, inches

3.4.2.1.4 Modified Spacer Factor, R-Grid and L-Grid Correlations

To account for mixing between subchannels due to spacer grids, Tong (Reference 45) developed a spacer grid factor for use with the W-3 equivalent uniform flux correlation. However, the use of the W-3 equivalent uniform flux correlation with this spacer factor yielded conservative predictions, particularly in rod bundles with mixing vane grid spacers. Hence, a correlation factor was developed to adapt the W-3 correlation (which was developed based on single-channel data) to rod bundles with mixing vane spacer grids. This correction factor, termed the “Modified Spacer Factor,” was developed as a multiplier on the W-3 correlation.

The Modified Spacer Factor (F'_s) was developed from rod bundle DNB test results conducted in the Westinghouse high-pressure water loop at Columbia University. These tests were conducted on non-uniform axial heat flux test sections to determine the DNB performance of a low parasitic, top-split mixing-vane grid design, referred to as the “R” grid. A description of this test program and a summary of the results are given in References 48 and 49. This Modified Spacer Factor for the “R” grid is:

$$F'_{S,R} = (1.445 - 0.0371L)(P/225.896)^{0.5}(e^{(X+0.2)^2} - 0.73) + K_S(G/10^6)(TDC/0.019)^{0.35}$$

where:

L = total heated core length, ft

P = primary system pressure, psia

X = local quality, fraction

K_S = axial grid spacing coefficient

G = local mass velocity, lb/hr-ft^2

TDC = thermal diffusion coefficient

Additional DNB testing was conducted with an "L" type grid. A description of this test program and a summary of the results are given in Reference 48. The Modified Spacer Factor for the "L" grid is simply:

$$F'_{S,L} = F'_{S,R} \times 0.986$$

3.4.2.2 **WRB-1 Correlation**

The details of the proprietary WRB-1 correlation are provided in Reference 35. The WRB-1 correlation was developed exclusively from Westinghouse rod mixing vane grid bundle data (over 1100 points) based on local fluid conditions. This correlation accounts directly for cold wall effects, and variations in rod heated length and grid spacing. The F-factor (Section 3.4.2.1.2) is employed for axially non-uniform heat flux profiles.

The applicable range of variables is:

Pressure	$1440 \le P \le 2490$ psia
Local Mass Velocity	$0.9 \le G_{loc} / 10^6 \le 3.7$ lb/ft^2-hr
Local Quality	$-0.2 \le X_{loc} \le 0.3$
Heated Length, Inlet to CHF Location	$L_h \le 14$ ft
Grid Spacing	$13 \le g_{sp} \le 32$ in.
Equivalent Hydraulic Diameter	$0.37 \le d_e \le 0.60$ in.
Equivalent Heated Hydraulic Diameter	$0.46 \le d_h \le 0.59$ in.

Figure 3.4-7 shows measured critical heat flux plotted against predicted critical heat flux using the WRB-1 correlation (Reference 36).

3.4.2.3 Procedure for Using W-3 and WRB-1 Correlation

In predicting the local DNB flux in a non-uniform heat flux channel, the following two steps are required:

1. The uniform DNB heat flux, $q''_{DNB, EU}$, is computed with the W-3 or WRB-1 correlation using the specified local reactor conditions.
2. This equivalent uniform heat flux is converted into corresponding non-uniform DNB heat flux, $q''_{DNB,N}$, for the non-uniform flux distribution in the reactor. The non-uniform DNB heat flux, $q''_{DNB,N}$, is given by:

$$q''_{DNB, N} = \frac{q''_{DNB, EU}}{F}$$

The DNB heat flux ratio is defined as:

$$DNBR = \frac{q''_{DNB, N}}{q''_{loc}}$$

where q''_{loc} is the actual local heat flux.

To calculate the minimum DNBR of a reactor coolant flow channel, the values of $(q''_{DNB,N})/(q''_{loc})$ along the channel are evaluated and the minimum value is selected as the minimum DNBR in that channel.

The W-3 and WRB-1 correlations depend on both local conditions and inlet enthalpies of the actual system fluid. Thus, the minimum DNBRs calculated with the correlations provide a measure of the margin on heat flux when compared to the DNBR design limits.

3.4.3 Thermal/Hydraulic Evaluation

3.4.3.1 Core Analysis

The basic objective of core thermal-hydraulic analysis is to verify that safety limits established by departure from nucleate boiling (DNB) concerns are met. Thermal-hydraulic design parameters are presented in Table 3.4-1. DNB, which could occur on the heating surface of the fuel rod, is characterized by sudden decrease in the heat transfer coefficient with corresponding increase in the surface temperature. DNB is of concern in reactor design because of the possibility of fuel cladding rod failure resulting from the increased temperature.

In order to preclude potential DNB related fuel damage, a design basis is established and is expressed in terms of a minimum departure from nucleate boiling ratio (MDNBR). DNBR is the ratio of the predicted heat flux at which DNB occurs (i.e., the critical heat flux, CHF) and the local heat flux of the fuel rod. By imposing a design DNBR limit, adequate heat transfer between the fuel cladding and the reactor coolant is assured. DNBRs greater than the design limit indicate the existence of thermal margin within the nuclear core. Thus, the purpose of core

thermal-hydraulic analysis, or DNB analysis, is the accurate calculation of DNBRs in order to assess and quantify core thermal margin.

In performing DNB analysis, a subchannel approach is commonly used wherein a section of the core is modeled as an array of adjoining subchannels. Each subchannel is defined as the flow channel formed by four fuel rods, or by three fuel rods and a guide thimble tube. When the fuel rods are given design radial and axial power distributions, the array represents the region of maximum design power generation. Within this array, the hottest subchannel (hot channel) is identified with the fuel rod which has the highest integrated power (hot fuel rod). Engineering uncertainties are applied to the hot channel and the hot fuel rod in order to conservatively account for manufacturing tolerances. A detailed thermal analysis of the core is then performed to determine the flows and enthalpies at each axial position within the hot channel.

When performing the thermal analysis, it is necessary to consider the effect that the surrounding core region has on the subchannel flows. The problem is basically one of integrating the relatively small subchannel geometry into a larger geometry which is representative of the entire core. Traditionally, the problem has been solved by using a multistage method involving at least two analyses. A core analysis is first performed to provide crossflow boundary conditions which are used in the subsequent subchannel analysis. In the core analysis, each fuel assembly is modeled as a single, lumped flow channel. In the subchannel analysis, the hot assembly is modeled separately as an array of subchannels. Hot assembly crossflows determined in the first analysis are used as boundary conditions in the second analysis in order to simulate the effects of the core on the subchannel flows. The original Surry thermal-hydraulics design code, THINC (Reference 14), is a multistage code.

An alternate, more direct approach for performing the thermal analysis is a single stage method. Using this method, a single analysis is performed in which an array of subchannels representing the hot assembly is combined with an array of lumped channels which represent the remaining assemblies within a core segment. Using this single geometry, boundary conditions are not required since the effect of the core is inherently included when computing the subchannel flows. Although single stage analyses have been performed previously, the thermal-hydraulic codes then in existence were capable of handling only a limited number of channels. This necessitated coarse simulations of the core consisting of only a few subchannels together with very large lumped channels representing many assemblies. However, the development of the COBRA IIC/MIT computer code (Reference 30) has provided the capability to analyze geometries consisting of up to 200 channels. Thus, it is now possible to perform single stage thermal analyses using the same radial nodalization as used in the traditional multistage analyses.

This concept has been applied by Virginia Electric and Power Company (Vepco) in the development of a core thermal-hydraulics analysis capability. This capability is based upon a single stage analysis which incorporates the geometries and methodologies used in multistage analyses. The accuracy of this approach has been verified through comparisons with analyses which were used in the design and licensing of the Surry Nuclear Power Station.

The COBRA IIIC/MIT computer code calculates the flow and enthalpy within interconnected flow channels by solving finite difference equations of continuity, energy, and momentum. The mathematical model is applicable to both steady state and transient conditions, and the model considers both turbulent mixing and diversion crossflow. In formulating the mathematical model, one-dimensional, two-phase, separated slip-flow was assumed to exist during boiling. The two-phase flow structure was assumed to be fine enough to allow specification of void fraction as a function of enthalpy, flow rate, heat flux, pressure, position and time. Sonic velocity propagation effects were not included. Within a channel, the diversion crossflow velocity was assumed to be small compared to the axial velocity. This assumption allowed the use of a simplified equation for the conservation of transverse momentum.

The equations are solved as a boundary value problem by using a semi-explicit finite difference scheme. The boundary conditions for the problem are in the inlet enthalpy, inlet mass velocity and exit pressure. The boundary value solution is obtained by assuming a uniform exit pressure distribution. (The equations do not require actual pressures since only pressure differences are used.) When performing a computation, the code iterates over the length of the core until convergence of the flow solution is obtained. Convergence is achieved when the change in any channel flow is less than a user specified fraction of the flow from the previous iteration.

The same finite difference equations are used for both steady state and transient computations. For steady state calculations, the time step, Δt, is set equal to an arbitrarily large value thereby negating the time dependent terms. For transient calculations, the time step is set equal to a user specified value. When performing a transient calculation, a steady state calculation is first performed to obtain initial conditions. Time dependent forcing functions consisting of inlet temperature, inlet flow, system pressure, and core average heat flux are used to establish boundary conditions at succeeding times. The calculation iterates over the first time step until the flow solution converges. The converged solution is then used as the initial conditions for the new time, and the procedure continues for all of the subsequent time steps.

Although the equations of continuity, energy and momentum form the basic structure of the mathematical model, their solution is still dependent upon the use of empirical correlations. Of major importance are the correlations used in calculating the pressure gradient and those used in calculating turbulent mixing. Once the flow solution is obtained, additional correlations are used in calculating the DNBR distribution. The COBRA IIIC/MIT computer code allows user specification of the appropriate correlations.

The NRC has approved the use of the Vepco version of the COBRA-IIIC/MIT code as an alternative approach for performing reactor core thermal-hydraulic analysis. The NRC staff found Reference 30 “to be acceptable for referencing by Vepco in future reload licensing submittals for North Anna, Surry and future plants of the same design.”

3.4.3.2 Application of the W-3 and WRB-1 Correlation in Design

During steady-state operation at the nominal design conditions, the values of the DNBR are determined. Under adverse operating conditions, particularly overpower transients, more limiting conditions develop than those existing during steady-state operation.

For transients which are analyzed with a deterministic treatment of key DNBR analysis uncertainties, initial conditions are obtained by combining maximum steady-state errors with nominal values. The following steady-state errors are considered:

1. Core Power +2 percent calorimetric error allowance
2. Average RCS temperature +4°F controller deadband and measurement error allowance
3. Pressurizer pressure ±30 psi steady-state fluctuations and measurement error allowance
4. Reactor flow Thermal design flow

Initial values for core power, average reactor coolant system temperature, and pressurizer pressure are selected to minimize the initial DNBR unless otherwise stated in the sections describing specific accidents (See Chapter 14).

The ranges of permissible initial reactor operating conditions of core flow rate, system temperatures and system pressure are stated in the Technical Specifications for Surry Power Station.

For transients which are analyzed under the Virginia Power *Statistical DNBR Evaluation Methodology* (Reference 36), nominal values are used for the initial conditions in the transient analysis. The use of the Statistical DNBR Evaluation Methodology does not require that the uncertainties be applied in the initial conditions since these uncertainties are statistically incorporated in the design DNBR limit (see Section 3.2.3.3). The Statistical DNBR Evaluation Methodology is employed on a transient specific basis (Reference 37) as indicated in the transient analysis summary in Chapter 14.

3.4.3.3 Effects of Departure From Nucleate Boiling on Neighboring Rods

Westinghouse has never observed departure from nucleate boiling to occur in a group of neighboring rods in a rod bundle as a result of departure from nucleate boiling in one rod in the bundle.

3.4.3.3.1 Departure From Nucleate Boiling With Physical Burnout

Westinghouse (Reference 18) has conducted DNB tests in a 25-rod bundle where physical burnout occurred with one rod. After this occurrence, the 25-rod test section was used for several days to obtain more DNB data from the other rods in the bundle. The burnout and deformation of the rod did not affect the performance of neighboring rods in the test section during the burnout, or the validity of the subsequent DNB data points as predicted by the W-3 correlation. No occurrences of flow instability or other abnormal operation were observed.

3.4.3.3.2 Departure From Nucleate Boiling With Return to Nucleate Boiling

Additional DNB tests were conducted by Westinghouse (Reference 19) in 19-rod and 21-rod bundles. In these tests, departure from nucleate boiling without physical burnout was experienced more than once on single rods in the bundles for short periods of time. Each time, a reduction in power of approximately 10% was sufficient to reestablish nucleate boiling on the surface of the rod. During these and subsequent tests, no adverse effects were observed on this rod or any other rod in the bundle as a consequence of operating in departure from nucleate boiling.

3.4.3.4 **Hydrodynamic and Flow Power Coupled Instability**

The interaction of hydrodynamic and spatial effects has been considered, and it is concluded that a large margin exists between the design conditions and those for which an instability is possible.

It has been known for some time that heated channels in parallel can lead to flow instability. If substantial boiling takes place, periodic flow instabilities have been observed. As long ago as 1938, Ledinegg (Reference 20) proposed a stability criterion, on the basis of which the concept of inlet orificing has been developed to stabilize flow. Later work (References 21, 22 & 23) demonstrated that periodic instabilities are possible that violate the Ledinegg criterion.

In normal flow channels with little or no boiling, the type of instability proposed by Ledinegg is not possible, since it results primarily from the large changes in water density along the channel flow path due to boiling. Moreover, the periodic instabilities examined by Quandt (References 21 & 22) and Meyer (Reference 23) are not exhibited in non-boiling channels of the type found in PWR cores (Reference 24).

3.4.3.5 **Fuel Rod Bow**

Rod bowing in excess of that originally expected was observed in Westinghouse 15 x 15 low parasitic (LOPAR) fuel assemblies. Based on these observations, Westinghouse developed an empirical model to conservatively predict rod bow. Westinghouse used the model to analyze the impact of increased rod bow on the DNBR. The conclusion was that the impact of rod bow could be accommodated by existing design margins, and reactor safety was not affected. This information was formally submitted for NRC generic review in January 1976 (Reference 25).

Several inherent design margins were generically associated with Westinghouse DNBR analyses of LOPAR fuel, and were used to accommodate the increased rod bowing as discussed in Reference 25. The LOPAR conservatisms include:

1. Axial heat flux spikes.
2. Better data correlation resulting in a 95 x 95 confidence level DNBR limit of 1.24 versus the original limit of 1.30.

3. Pitch reduction modeling.

4. Assumed thermal diffusion coefficient (TDC) values.

Further testing by Westinghouse of selected rods (for a thimble cell) bowed into contact indicated that the inherent design margins identified above could not offset the DNBR reduction being seen. As a result, penalties on FΔH were required by the NRC (Reference 26).

Based on more recent test data obtained and evaluated by Westinghouse, the appropriate reductions in FΔH (or DNBR) resulting from fuel rod bow during irradiation were determined to be significantly less than those accommodated in the Technical Specifications as a result of Reference 26. The more recent tests were concerned with the determination of the DNBR reduction due to rod bow when selected rods (forming a thimble cell) were bowed to 85% channel closure. As documented in References 25, 26, and 27, the 85% channel closure would not be exceeded, on a 95 x 95 basis, for a region of fuel up to 33,000 MWD/MTU (the nominal region average discharge burnup). The DNBR reduction associated with the 85% channel closure tests was found to be 11.7% for 15 x 15 LOPAR fuel (Reference 27). The 11.7% DNBR reduction was more than completely offset by existing thermal margins in the core design. The inherent thermal margins previously delineated for the 15 x 15 LOPAR fuel provided thermal margins in excess of 18%. Therefore, the appropriate reduction in FΔH due to rod bow was determined to be zero at all operating conditions for the Surry Power Stations (Reference 28). The NRC subsequently approved this position (Reference 29).

More recently, Westinghouse employed a revised rod bow evaluation methodology (Reference 31) to significantly reduce the required rod bow penalty. NRC approval (Reference 32) of Reference 31 permitted Virginia Electric and Power Company to apply the reduced penalty in DNBR evaluation, thus freeing most of the available retained DNBR margin for other uses. No Technical Specification changes were required, but the NRC was notified (Reference 33) in an information letter of Virginia Power's use of the reduced penalty. The NRC, subsequently, approved a further reduction in the maximum applicable burnup from 33,000 to 24,000 MWD/MTU (Reference 34).

The rod bow behavior of the SIF assemblies is predicted to be within the bounds of existing 15 x 15 LOPAR assembly rod bow data (Reference 49). The most probable causes of significant rod bow are rod-grid and pellet-clad interaction forces and wall thickness variation (WTV). The SIF assembly will have reduced grid forces (due to the greater irradiation-induced relaxation of the zirconium alloy grids) and the same fuel tube thickness-to-diameter ration (t/d) as the LOPAR assembly, which should tend to decrease SIF rod bow compared to LOPAR fuel. For a given burn-up, the magnitude of rod bow gap closure for the SIF assembly is conservatively taken to be the same as that applied to the 15 x 15 LOPAR fuel assembly.

The design margin for 15 x 15 SIF assemblies consists of the percentage difference between either the DNBR design limit (Section 3.2.3.3) and the COBRA/WRB-1 (Reference 38) code/correlation DNBR limit of 1.17 for the deterministic DNB methodology or the statistical

DNBR limit (SDL) of 1.27 for the Statistical DNBR Evaluation Methodology. (References 36 & 37). (See Section 3.2.3.3 for additional discussion on DNBR limits.) These percentage differences between the design DNBR limit and the code/correlation limit, or the statistical DNBR limit, represents generic retained margin, against which penalties may be assessed to account for the DNB effect of changes in the fuel product, plant operating conditions, or analysis methodology (e.g., fuel rod bowing).

3.4 REFERENCES

1. R. A. Weiner et al., *Improved Fuel Performance Models for Westinghouse Fuel Rod Design and Safety Evaluations,* WCAP-10851-P-A (Proprietary), August 1988.
2. A. M. Ross and R. D. Stoute, *Heat Transfer Coefficient Between UO_2 and Zircaloy-2,* AECL-1552, June 1962.
3. T. G. Godfrey et al., *Thermal Conductivity of Uranium Dioxide and Armco Iron by an Improved Radial Heat Flow Technique*, ORNL-3556, June 1964.
4. J. A. L. Robertson et al., "Temperature Distribution of UO_2 Fuel Elements, "*Journal of Nuclear Materials*, Vol. 7, No. 3, pp. 255-262, 1962.
5. F. W. Dittus and L. M. K. Boetler, *Heat Transfer in Automobile Radiators of the Tubular Type,* California University Publication in Engineering, Vol. 2 no. 13 pp. 443-461, 1930.
6. J. A. Christensen, R. J. Allio, and A. Biancheria, *Melting Point of Irradiated Uranium Dioxide*, WCAP-6065, February 1965.
7. WCAP-3385 (Series), Saxton Plutonium Program, Quarterly Progress Reports.
8. D. J. Clough and J. B. Sayers, *The Measurement of the Thermal Conductivity of UO_2 Under Irradiation in the Temperature Range 150°-1600°C*, Report AERE-R4690, U.K.A.E.A. Research Group, Harwell G. B., December 1964.
9. I. Devold, *A Study of the Temperature Distribution in UO_2 Reactor Fuel Elements*, Report AE-318, Aktiebolaget Atomenergi, Stockholm, Sweden, 1968.
10. J. P. Stora, D. de B. Desirgorzes, R. Deimas, P. Daschamps, B. Travard, and C. Rionigot, *Conductilite Thermique de l'Oxyde d'Uranium Fritte dans les Conditions d'Utilisation en Pile*, CEA-R-2586, 1964 (also EURAEC 1095).
11. WCAP-8183, *Operational Experience with Westinghouse Cores*, (latest revision).
12. L. S. Tong, "Prediction of Departure from Nucleate Boiling for an Axially Non-Uniform Heat Flux Distribution," *Journal of Nuclear Energy*, Vol. 21, pp. 241-248, 1967.
13. L. S. Tong, H. B. Currin, and A. G. Thorp II, "New Correlations Predict DNB Conditions," *Nucleonics*, May 1963. Also WCAP-1997, 1963.

14. H. Chelemer, J. Weisman, and L. S. Tong, *Subchannel Thermal Analysis of Rod Bundle Cores*, WCAP-7015, January 1967.

15. D. F. Judd et al., *Non-Uniform Heat Generation Experimental Program*, BAW-3238-7, 1965.

16. D. H. Lee and J. D. Obertelli, *An Experimental Investigation of Forced Convection Burnout in High Pressure Water, Part II, Preliminary Results for Round Tubes with Non-Uniform Axial Heat Flux Distribution*, AEEW-R-309, Winfrith, England, 1963.

17. D. H. Lee, *An Experimental Investigation of Forced Convection Burnout in High Pressure Water, Part IV, Large Diameter Tubes at About 1600 psi,* AEEW-R-479, Winfrith, England, 1966.

18. J. Weisman, A. H. Wenzel, L. S. Tong, D. Fitzsimmons, W. Thorne, and J. Batch, "Experimental Determination of the Departure from Nucleate Boiling in Large Rod Bundles at High Pressure," AIChE, Preprint 29, Ninth National Heat Transfer Conference, Seattle, Washington, 1967.

19. L. S. Tong, H. Chelemer, J. E. Casterline, and B. Matzner, "Critical Heat Flux (DNB) in Square and Triangular Array Rod Bundles," *JSME Semi-International Symposium, Paper #256*, Tokyo, Japan, 1967.

20. M. Ledinegg, *Die Warme*, 61 (48), pp. 891-8, 1938.

21. E. R. Quandt, *Analysis of Parallel Channel Transient Response and Flow Oscillations*, WAPD-AD-TH-489, 1959.

22. E. R. Quandt, "Analysis and Measurement of Flow Oscillations," *Chemical Engineering Progress Symposium Series*, Vol. 57, No 32, p. 111, 1961.

23. J. E. Meyer and R. P. Rose, *Journal of Heat Transfer*, Vol. 85, No. 1, p. 1, 1963.

24. L. S. Tong et al., "HYDNA Digital Computer Program for Hydrodynamic Transient," CVNA-77, 1961.

25. Westinghouse Electric Corporation, *Fuel Rod Bowing*, WCAP-8692, December 1975.

26. U.S. Nuclear Regulatory Commission, *Interim Safety Evaluation Report on Effects of Fuel Rod Bowing on Thermal Margin Calculations for Light Water Reactors (Revision 1)*, February 16, 1977.

27. Westinghouse Electric Corporation, letter NS-CE-1580 to NRC, October 24, 1977.

28. Virginia Electric Power Company, letter from C. M. Stallings (Vepco) to E. G. Case (NRC), Serial No. 095, February 21, 1978.

29. U.S. Nuclear Regulatory Commission, letter from A. Schwencer (NRC) to W. L. Proffitt (Vepco), July 27, 1979.

30. F. W. Sliz & K. L. Basehore, *Vepco Reactor Core Thermal-Hydraulic Analysis Using the COBRA-IIIC/MIT Computer Code*, VEP-FRD-33-A, October 1983.

31. Skarita, J., et al., *Fuel Rod Bow Evaluation*, WCAP-8691 Rev. 1 (July 1979)

32. Letter from C. O. Thomas (NRC) to E. P. Rahe, Jr. (W), *Acceptance for Referencing of Licensing Topical Report WCAP-8691 (P) /WCAP-8692 (NP)*, dated December 29, 1982.

33. Letter from W. L. Stewart (Virginia Electric and Power Company) to H. R. Denton (NRC), *Virginia Power Reduction in Rod Bow DNBP Penalty for Surry Power Station Unit Nos. 1 & 2*, Serial No. 85-064, dated March 21, 1985.

34. Letter from C. Berlinger (NRC) to E. P. Rahe, Jr. (Westinghouse), *Request for Reduction in Fuel Assembly Burnup Limit for Calculation of Maximum Rod Bow Penalty*, June 18, 1986.

35. Motley, F. E., et al., *New Westinghouse Correlation WRB-1 for Predicting Critical Heat Flux in Rod Bundles with Mixing Vane Grids*, WCAP-8763-NP-A (July 1984).

36. R. C. Anderson, *Statistical DNBR Evaluation Methodology*, VEP-NE-2-A, June 1987.

37. Letter from B. C. Buckley (NRC) to W. L. Stewart (Virginia Electric and Power Company), *Surry Units 1 and 2—Issuance of Amendments Re: F Delta H Limit and Statistical DNBR Methodology*, Serial No. 92-405, June 1, 1992.

38. R. C. Anderson and N. P. Wolfhope, *Qualification of the WRB-1 CHF Correlation in the Virginia Power COBRA Code*, VEP-NE-3-A, July 1990.

39. J. R. S. Thom, W. M. Walker, T. A. Fallon, and G. F. S. Reising, *Boiling in Sub-cooled Water During Flowup Heated Tubes or Annuli,* Proceedings of the Institute of Mechanical Engineers, Vol. 180, Pt. C, 1955-1966, pp. 226-46.

40. W. J. Leech, D. D. Davis, and M. S. Benzvi, *Revised PAD Code Thermal Safety Model,* WCAP-8720-A2 (Proprietary), October 1982.

41. L. E. Hochreiter, H. Chelemer, and P. T. Chu, *THINC-IV, An Improved Program for Thermal-Hydraulic Analysis of Rod Bundle Cores,* WCAP-7956-A, February 1989.

42. L. E. Hochreiter, *Application of the THINC IV Program to PWR Design,* WCAP-8054-P-A (proprietary), 1973, and WCAP-8195-A (nonproprietary), February 1989.

43. W. H. Jens and P. A. Lottes, *Analyses of Heat Transfer, Burnout, Pressure Drop, and Density Data for High Pressure Water,* USAEC Report ANL-4627, Argonne National Laboratory (1951).

44. F. F. Cadek and F. E. Motley, *Application of Modified Spacer Factor to L Grid Typical & Cold Wall Cell DNB,* WCAP-7988-P-A (Proprietary) and WCAP-8030-A (Non-proprietary), January 1975.

45. L. S. Tong, *Boiling Crisis and Critical Heat Flux,* AEC Critical Review Series, TID-25887, 1972.

46. Westinghouse Electric Corporation reports WCAP-7411, Revision 1-P-A (Proprietary) and WCAP-7813-A (Non-proprietary) entitled *Rod Bundle Axial Non-Uniform Heat Flux DNB Tests and Data,* January 1975.

47. Westinghouse Electric Corporation reports WCAP-7695, Add. 1-P-A (Proprietary) and WCAP-7958, Add. 1-A (Non-proprietary) entitled *DNB Test Results for R Grid Thimble Cold Wall Cells,* January 1975.

48. Westinghouse Electric Corporation reports WCAP-7695-P-A (Proprietary) and WCAP-7958-A (Non-proprietary) entitled *DNB Test Results for New Mixing Vane Grids (R),* January 1975.

49. W. L. Stewart (Virginia Power) to U. S. Nuclear Regulatory Commission, *Proposed Technical Specifications Change Surry Improved Fuel Assembly,* Serial No. 87-188, May 26, 1987.

50. J. P. Foster et al., *Westinghouse Improved Performance Analysis and Design Model (PAD 4.0),* WCAP-15063-P-A, Revision 1, with Errata (Proprietary), July 2000.

Table 3.4-1
THERMAL/HYDRAULIC DESIGN PARAMETERS

	Original Design	Current Operation
Total core heat output	2441 MWt	2546 MWt
Total core heat output	8331×10^6 Btu/hr	8687×10^6 Btu/hr
Heat generated in fuel	97.4%	97.4%
Maximum thermal overpower	112%	118%
Nominal system pressure	2250 psia	2250 psia
Coolant flow		
Total flow rate	100.7×10^6 lb/hr	101.1×10^6 lb/hr
Average velocity along fuel rods	14.2 ft/sec	14.0 ft/sec (1)
Average mass velocity	2.31×10^6 lb/hr-ft^2	2.27×10^6 lb/hr-ft^2
Coolant temperature		
Nominal inlet, °F	543	540.4
Average rise in vessel	62.2	65.2
Average rise in core	65.3	68.9
Average in core	577	576.5
Average in vessel	574.3	573.0
Average core discharge	608.3	609.3
Average vessel discharge	605.6	605.6
Heat transfer		
Active heat transfer surface area	42,460 ft^2	42,460 ft^2
Average heat flux	191,100 Btu/hr-ft^2	199,300 Btu/hr-ft^2
Average linear power	6.18 kW/ft	6.45 kW/ft
Peak linear power for normal operation	14.4 kW/ft	15.0 kW/ft (2)
Temperature at peak linear power for prevention of fuel centerline melt	<4700°F	<4700°F
Pressure drop		
Across core	26.5 psi	22.6 psi
Across vessel, including nozzles	47.0 psi	47.0 psi
DNBR Correlation	W-3, L-grid (Std)	WRB -1 (SIF)

1) Based on core flow rate and vessel T_{avg}

2) Based on 2.32 F_Q

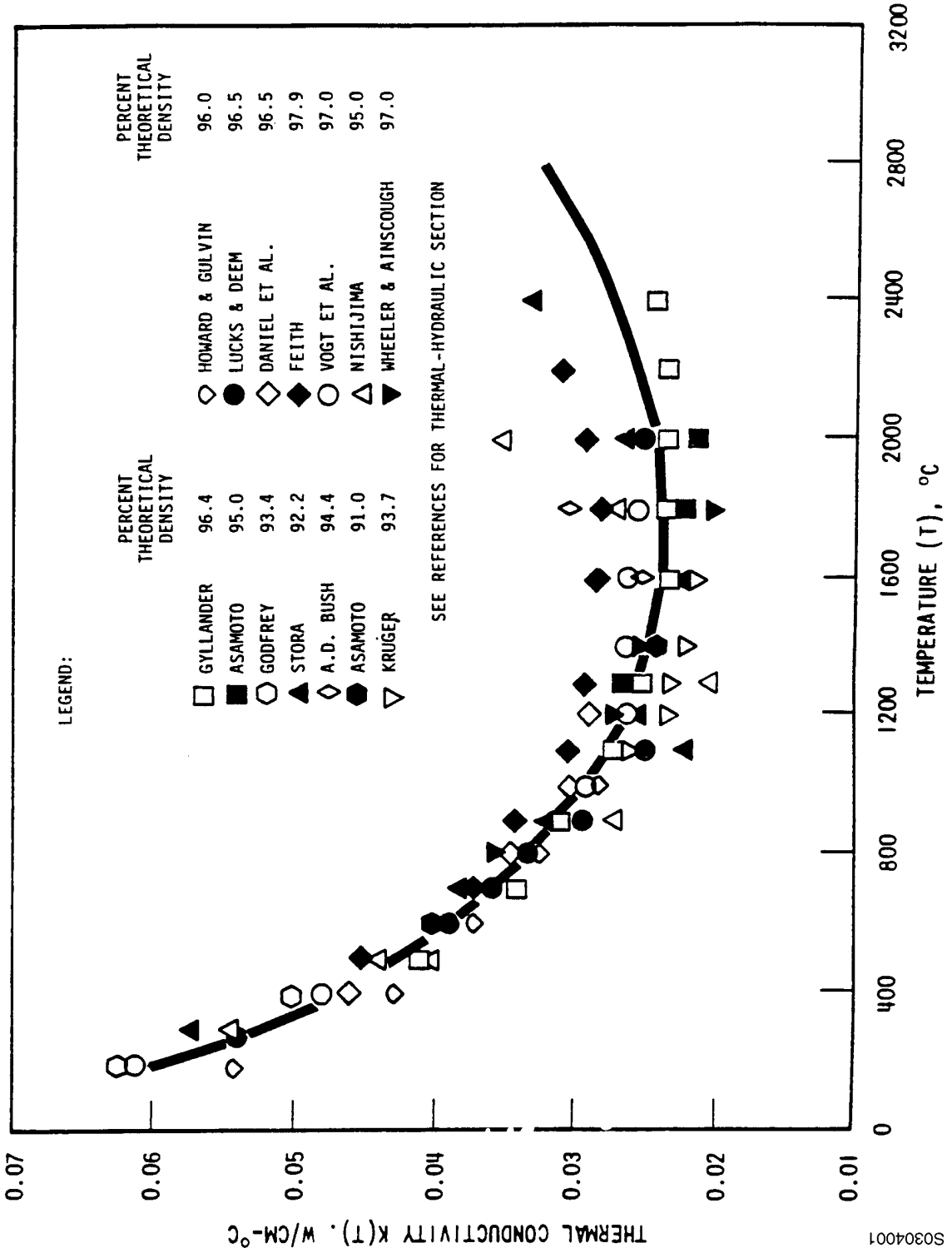

Figure 3.4-1
THERMAL CONDUCTIVITY OF URANIUM DIOXIDE

Figure 3.4-2
HIGH-POWER FUEL ROD EXPERIMENTAL PROGRAM

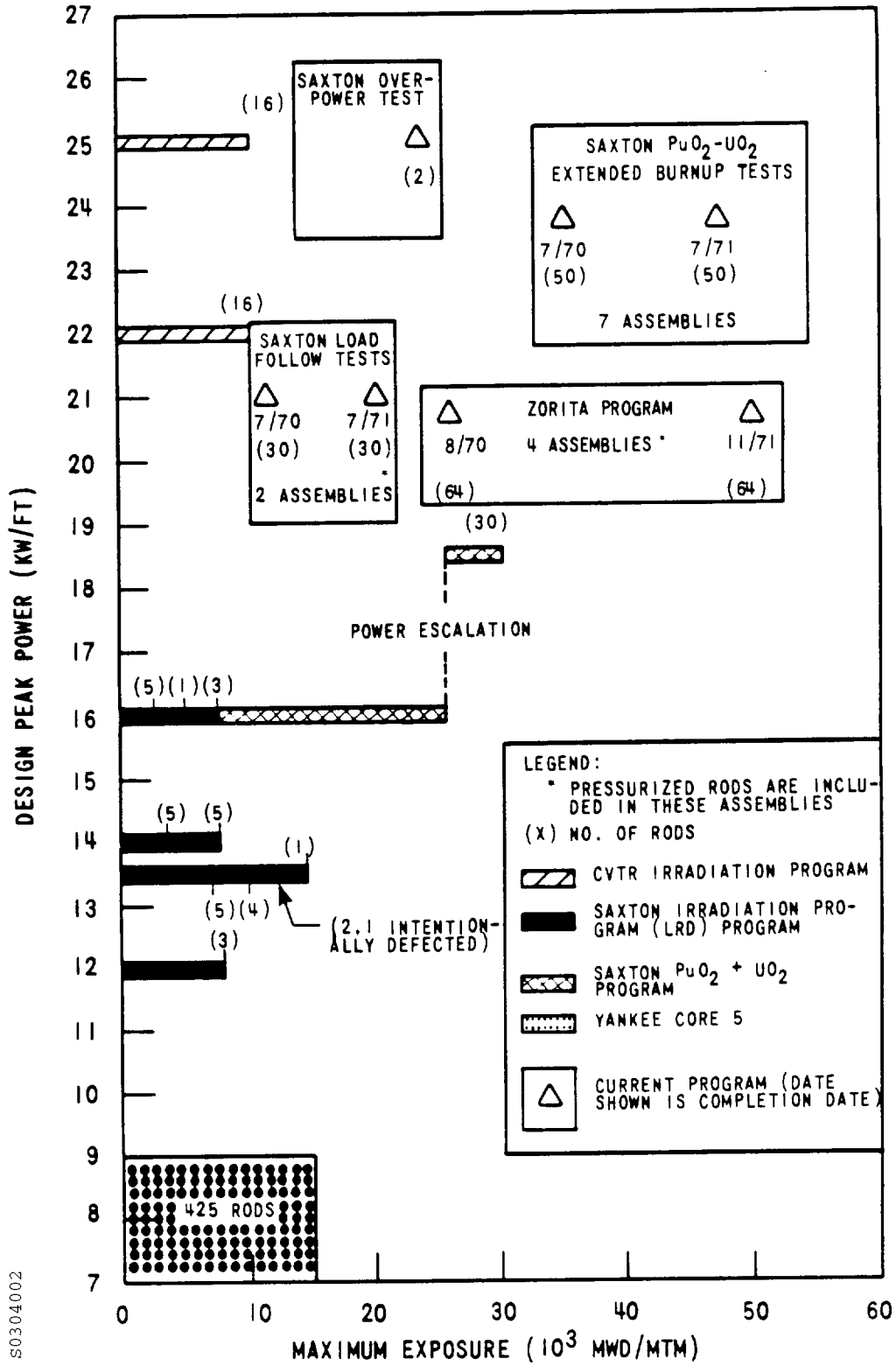

Figure 3.4-3
COMPARISON OF W-3 PREDICTION AND UNIFORM FLUX DATA

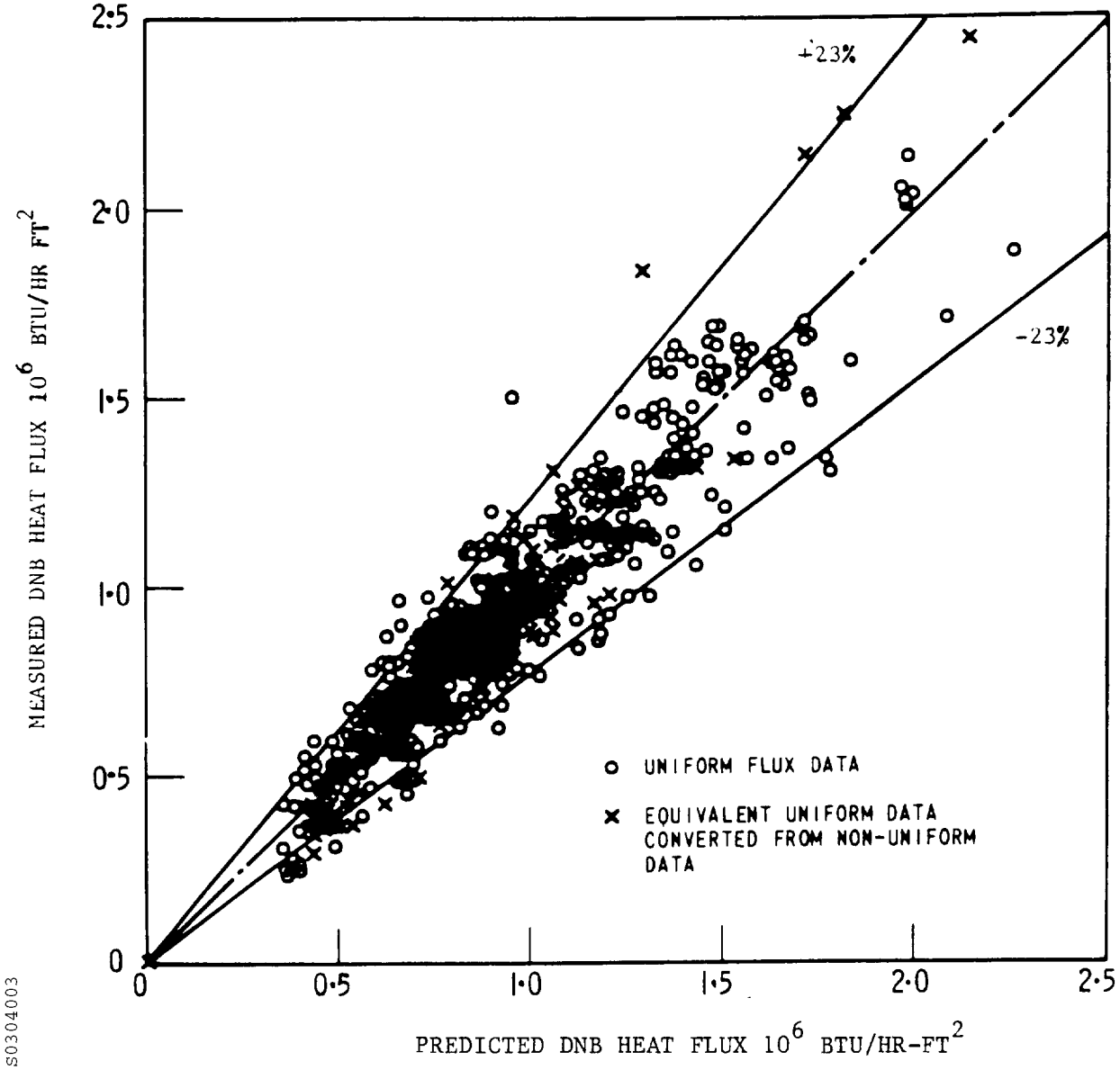

Figure 3.4-4
W-3 CORRELATION PROBABILITY DISTRIBUTION CURVE

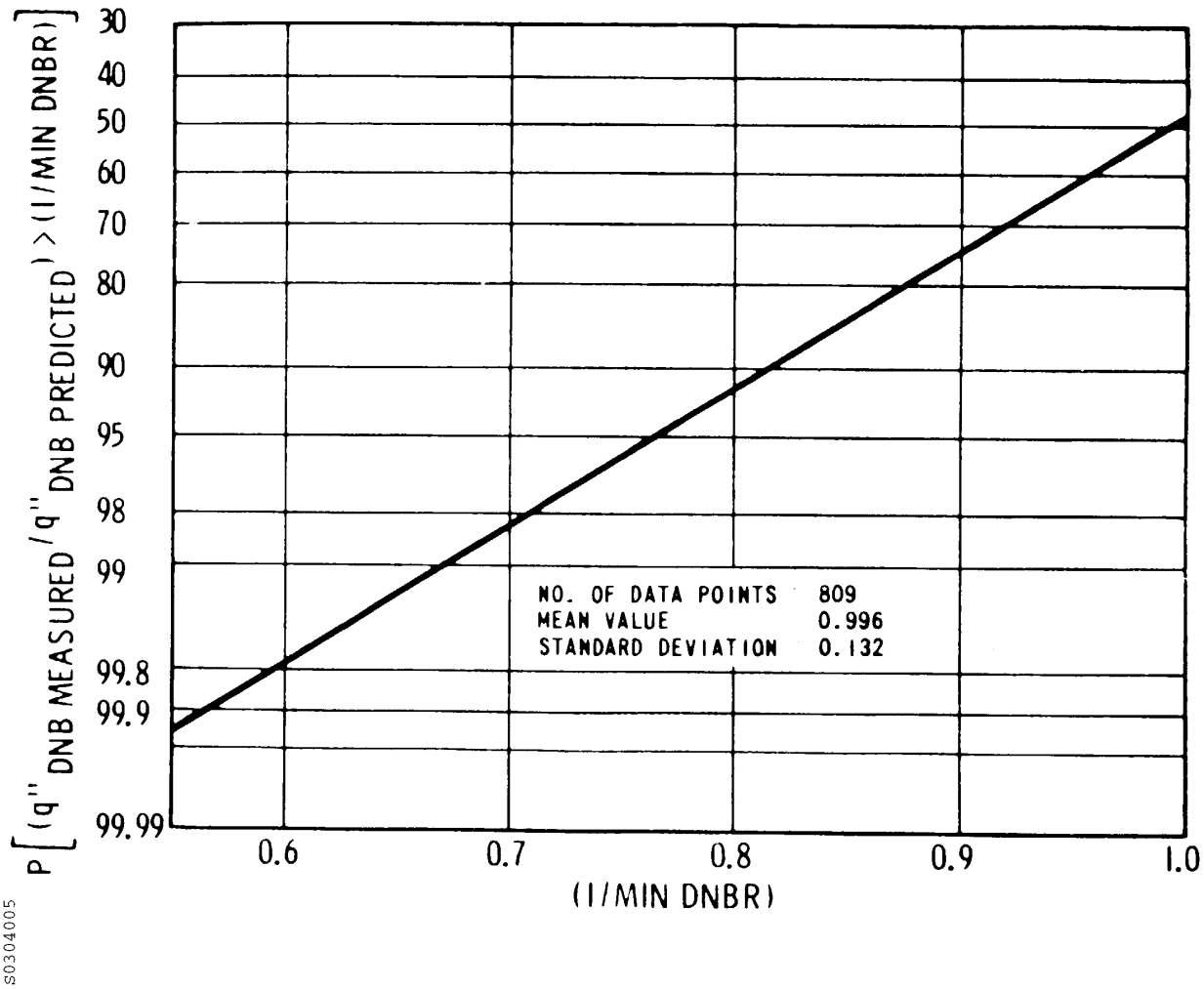

Figure 3.4-5
COMPARISON OF W-3 CORRELATION WITH ROD BUNDLE DNB DATA
(SIMPLE GRID WITHOUT MIXING VANE)

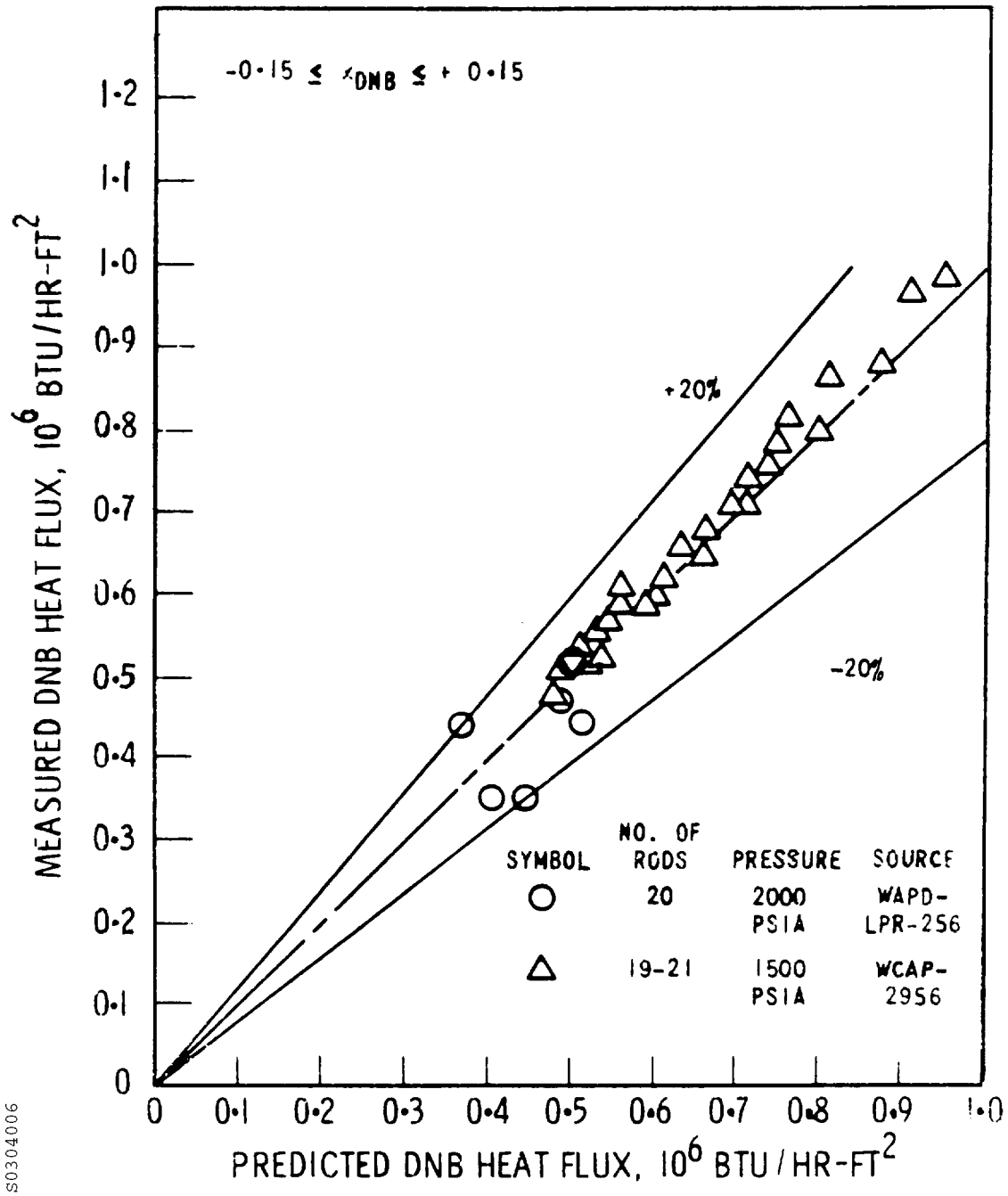

Figure 3.4-6
COMPARISON OF W-3 CORRELATION WITH ROD BUNDLE DNB DATA
(SIMPLE GRID WITH MIXING VANE)

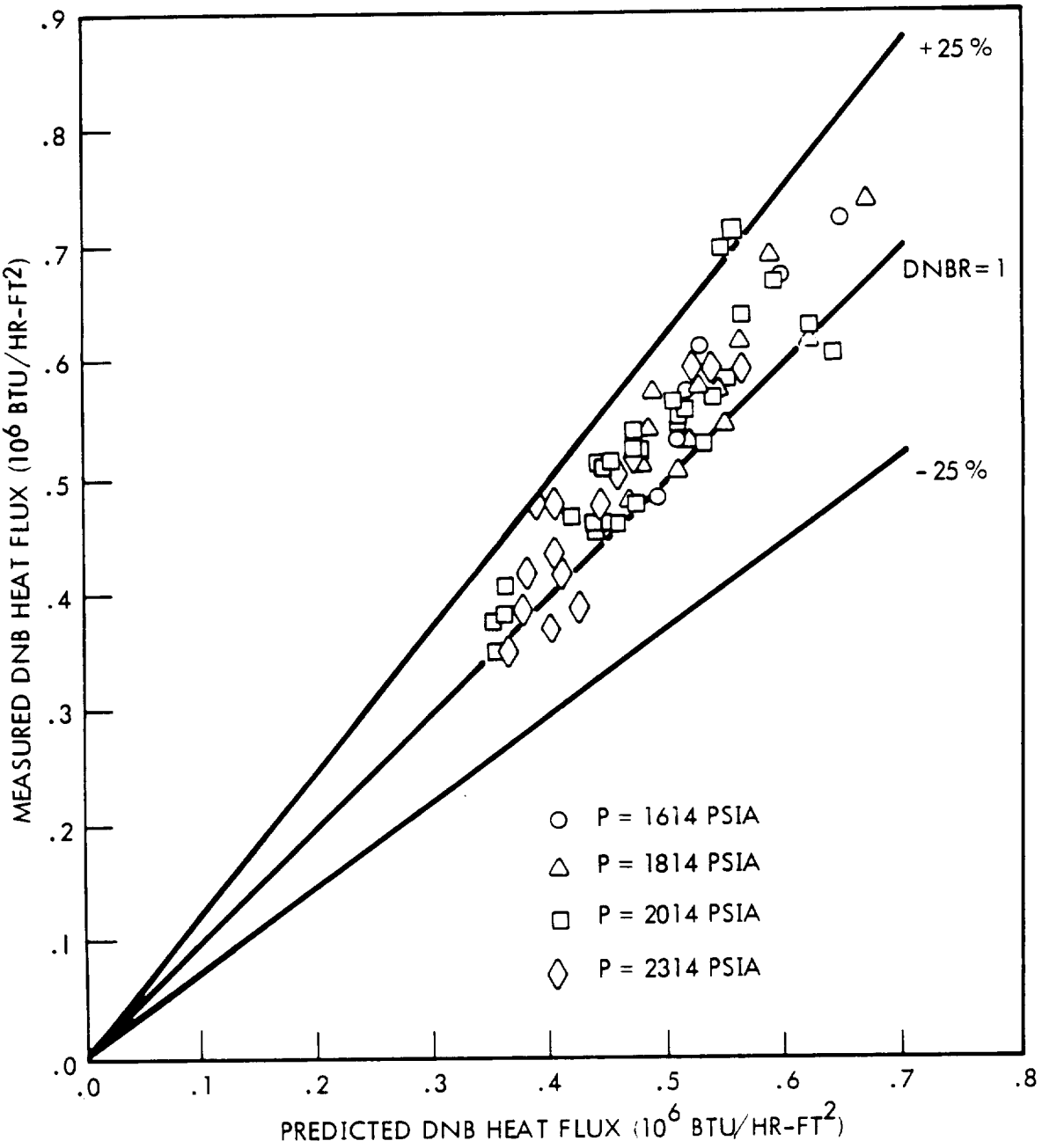

S0304007

Figure 3.4-7
MEASURED VERSUS PREDICTED CRITICAL HEAT FLUX WRB-1 CORRELATION

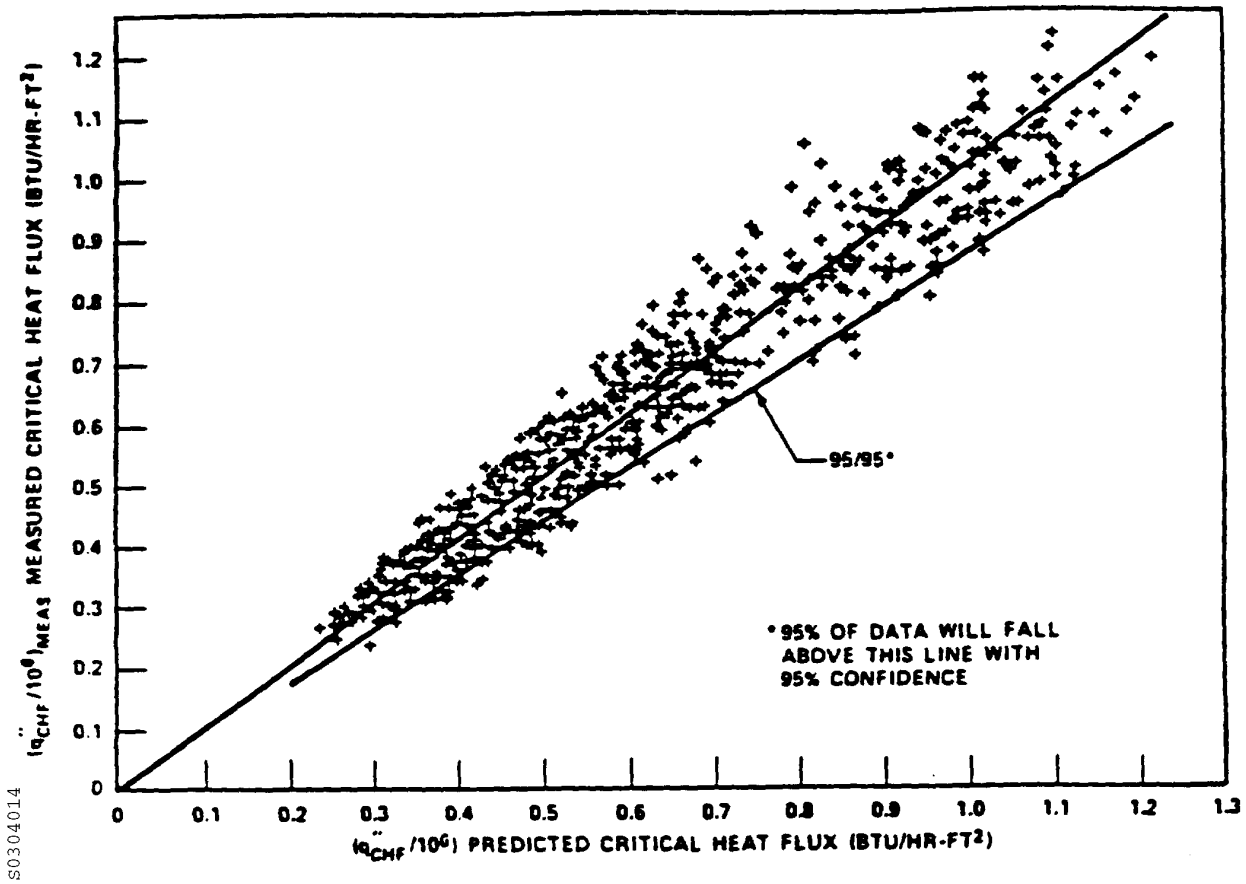

Figure 3.4-8
COMPARISON OF NON-UNIFORM DNB DATA WITH W-3 PREDICTIONS

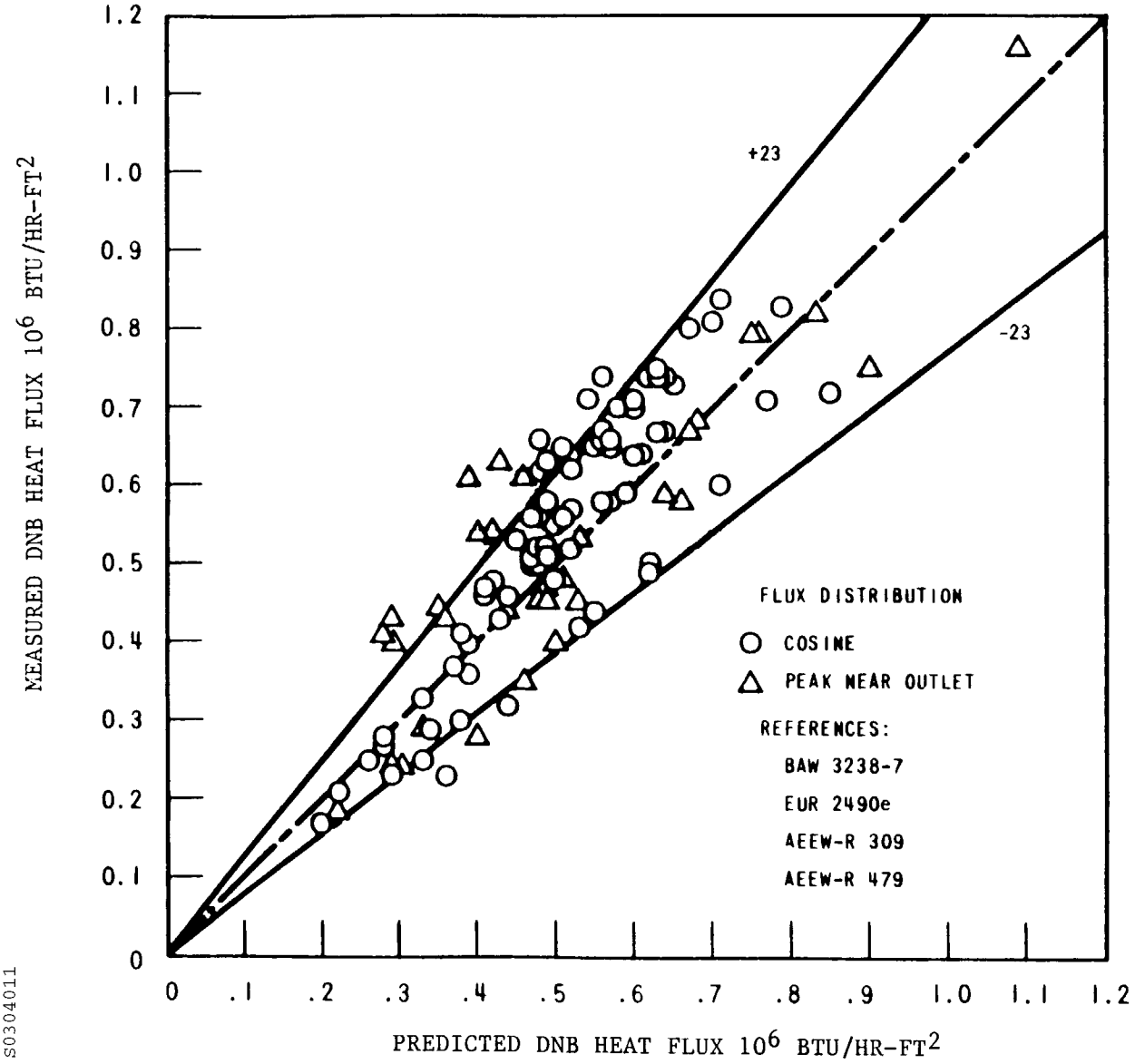

Figure 3.4-9
COMPARISON OF W-3 PREDICTION WITH MEASURED DNB LOCATION

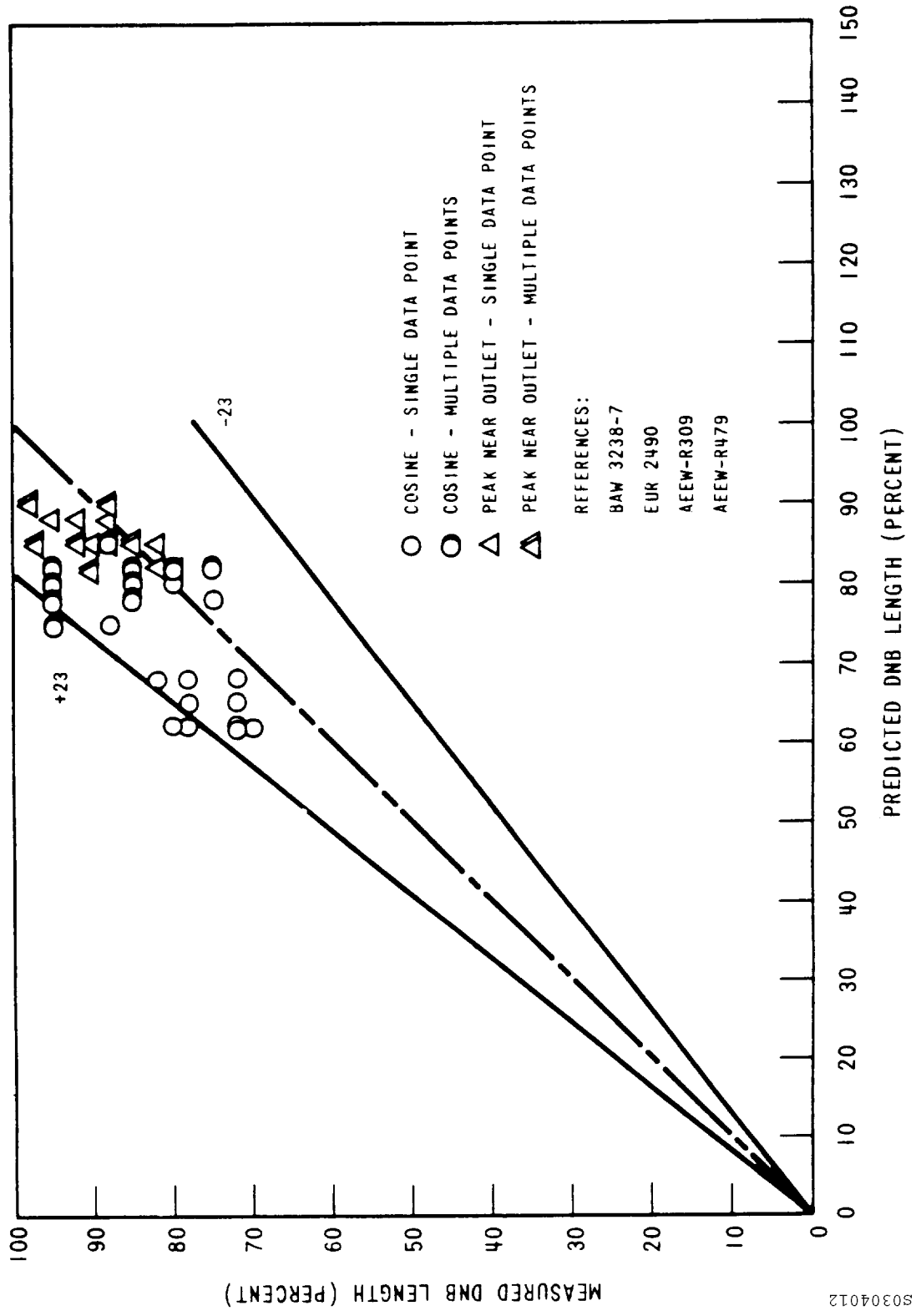

Intentionally Blank

3.5 MECHANICAL DESIGN

The reactor core cross section and reactor vessel internals are shown in Figures 3.5-1 and 3.5-2, respectively. The core, consisting of the fuel assemblies, control rods, source rods, and guide thimble plugging devices, provides and controls the heat source for reactor operation. The internals, consisting of the upper and lower core support structure, are designed to support and orient the fuel assemblies and control rod assemblies, direct the coolant flow to and from the core components, and support and guide the incore instrumentation. A listing of the mechanical design parameters of the initial cores is given in Table 3.5-1.

The fuel assemblies are arranged in a roughly circular cross-sectional pattern. The assemblies within a region are identical in configuration, but contain fuel of different enrichments depending on the location of the assembly within the core. Small differences may exist between different regions of fuel, as new design features are incorporated into reload fuel assemblies. The fuel is in the form of slightly enriched uranium dioxide ceramic pellets. The pellets are stacked to an active height of 144 inches within Zircaloy-4 or ZIRLO tubular cladding, which is then plugged and seal-welded at the ends to encapsulate the fuel.

The core is divided into regions of several different enrichments. The loading arrangement for the initial cycle is indicated on Figure 3.5-3. Refueling generally takes place in accordance with an in-out movement schedule. The enrichments of the fuel for the three fuel regions in the first core cycle are given in Table 3.5-1. Limitations on the enrichment of reload fuel are provided in the Technical Specifications.

The fuel rods of all regions are internally pressurized with helium during fabrication. Heat generated by the fuel is removed by demineralized borated light water, which flows upward through the fuel assemblies and acts as both moderator and coolant.

The control rod assemblies consist of groups of individual control rods supported by a spider at the top end and thereby actuated as a group. In the inserted position, the control rods fit within hollow guide thimbles in the fuel assemblies. The guide thimbles are an integral part of the fuel assemblies and occupy locations within the regular fuel assembly pattern where fuel rods have been deleted. In the withdrawn position, the control rods are guided and supported laterally by guide tubes forming an integral part of the upper core support structure. Figure 3.5-4 shows the typical fuel assembly structural components and a control rod assembly. The relative positions of the control rods in a fuel assembly are shown in Figure 3.5-5.

As shown in Figure 3.5-2, the fuel assemblies are positioned and supported vertically in the core between the upper and lower core plates. The core plates are provided with pins that index into closely fitting mating holes in the fuel assembly top and bottom nozzles. The pins maintain the fuel assembly alignment, permitting free movement of the control rods.

Operational or seismic loads imposed on the fuel assemblies are transmitted through the core plates to the upper and lower core support structures. Vertical loads are transmitted to the

internals support ledge at the pressure vessel flange. Horizontal loads are transmitted to the lower radial support and internals support ledge. The internals also provide a form-fitting baffle surrounding the fuel assemblies, confining the upward flow of most of the coolant in the core area to the fuel-bearing region.

3.5.1 Reactor Internals

The reactor internals are designed to support and orient the fuel assemblies and control rod assemblies. The internals also absorb the control rod assembly dynamic loads and transmit these and other loads to the reactor vessel flange, provide a passageway for the reactor coolant, and support incore instrumentation. The reactor internals are shown in Figure 3.5-2. The internals are designed to withstand the combination of forces due to weight, preload of fuel assemblies, differential hydraulic pressure, control rod assembly dynamic loading, vibration, and earthquake acceleration. The internals were analyzed similarly to those of Connecticut Yankee (Haddam Neck), San Onofre, Jose Cabrera (Spain), Saxton, and Yankee (Rowe). The structure satisfies stress values prescribed in the ASME Code, Section III, Nuclear Vessels. The dynamic criteria for design and the stress levels of the internals in each unit are similar to those used for Connecticut Yankee.

The internals are designed to the criteria stated in Chapter 15, including Appendix 15A.

The reactor internals are equipped with bottom-mounted incore instrumentation supports. These supports are designed to sustain the applicable loads outlined above.

In a hypothesized downward vertical displacement of the internals, energy-absorbing devices would limit the displacement by contacting the vessel bottom head. The load is transferred through the energy-absorbing devices to the vessel. The cylindrically shaped energy absorbers are contoured on their bottom surface to the reactor vessel bottom head geometry. Their number (four) and design are determined so as to limit the forces imposed to a safe fraction of yield strength. Assuming a downward vertical displacement, the potential energy of the system is absorbed mostly by the strain energy of the energy-absorbing devices.

In the unlikely event that the normal core support structure fails, the energy-absorbing devices would limit the fall of the core as well as absorb the energy of the drop which would otherwise be imparted to the vessel. The energy of fall was calculated assuming a complete and instantaneous failure of the primary core support and would be absorbed during the plastic deformation of a controlled volume of stainless steel, loaded in tension, in each device. The maximum deformation of this austenitic stainless piece would be limited to approximately 15%, after which a positive stop is provided to ensure support. Standard textbook calculations were used to derive the amount of strain.

The displacement in the hot condition is on the order of 0.5 inch, and there is an additional strain displacement in the energy-absorbing devices of approximately 0.75 inch. Alignment features in the internals prevent cocking of the internals structure during this postulated

displacement so that the control rod assemblies are able to be inserted upon trip. The displacement distance of about 1.25 inches is not enough to cause the tip of any of the control rods to come out of the guide thimbles.

The components of the reactor internals are divided into three parts, consisting of the lower core support structure, including the entire core barrel and thermal shield, the upper core support structure, and the incore instrumentation support structure.

3.5.1.1 Lower Core Support Structure

The major containment and support member of the reactor internals is the lower core support structure, shown in Figure 3.5-6. This support structure assembly consists of the core barrel, the core baffle, the lower core plate and support columns, the thermal shield, the intermediate diffuser plate, and the bottom support plate, which are welded to the core barrel. All the major material for this structure is type 304 stainless steel. The core support structure is supported at its upper flange from a ledge in the reactor vessel head flange, and its lower end is restrained in the transverse direction by a radial support system attached to the vessel wall. Within the core barrel are axial baffle and former plates, which are attached to the core barrel wall and form the enclosure of the assembled core. The lower core plate is positioned at the bottom level of the core below the baffle plates, and provides support and orientation for the fuel assemblies.

The lower core plate is perforated for flow purposes, and contains the lower locating pins for the fuel assemblies. Columns are placed between this plate and the bottom support plate of the core barrel in order to stiffen this plate and transmit the core load to the bottom support plate.

An intermediate perforated diffuser plate is placed between the bottom support plate and the lower core plate to uniformly diffuse coolant flowing into the core.

The one-piece thermal shield is fixed to the core barrel at the top with rigid bolted connections. The bottom of the thermal shield is connected to the core barrel by means of six axial flexures. This number is consistent with the number of flexures used on other three-loop plants. This bottom support allows for differential axial growth of the shield with respect to the core barrel, but restricts radial or horizontal movement of the bottom of the shield.

The adequacy of the flexures has been evaluated and verified utilizing the information gained from the instrumentation of the thermal shield during the hot-functional test of the three-loop H. B. Robinson Unit 2 reactor. This study was performed by correlating the hot-functional data with tests performed on thermal shields in the manufacturing facilities (determination of normal modes, natural frequency and flexure stresses). The result of these analyses indicates an adequate margin based on the criteria of Section III of the ASME Code.

In the event of a failure of the flexures, the thermal shield will remain fixed at the top and will become free at the bottom. Mechanical shaker tests performed on actual thermal shields indicate that the vibration effects will not affect the structural adequacy of the thermal shield support, with stress levels remaining within the limits of Section III of the ASME Code.

Irradiation baskets in which encapsulated materials samples can be inserted and irradiated during reactor operation are attached to the outer side of the thermal shield (Section 4.1.7).

The lower core support structure, consisting principally of the core barrel, serves to provide passageways and control for the coolant flow. Inlet coolant flow from the vessel inlet nozzles proceeds down the annulus between the core barrel and the vessel wall, on both sides of the thermal shield, and into a plenum at the bottom of the vessel. It then turns and flows up through the bottom support plate, passes through the intermediate diffuser plate and then through the lower core plate. The flow holes in the diffuser plate are arranged to prevent gross inlet flow maldistribution to the core. After passing through the core, the coolant enters the area of the upper support structure and then generally flows radially to the core barrel outlet nozzles and directly through the vessel outlet nozzles.

A small amount of water also flows between the baffle plates and core barrel to provide additional cooling of the barrel. Similarly, a small amount of the entering flow is directed into the vessel head plenum and exits through the vessel outlet nozzles.

Downward-directed loads from weight, fuel assembly preload, control rod assembly dynamic loading, and earthquake acceleration are carried by the lower core plate partially into the lower core plate support flange on the core barrel and partially through the lower support columns into the bottom support plate. Finally, the load enters through the core barrel and ends in the core barrel flange supported by the vessel head flange. Transverse loads are carried by the core barrel to be shared by the lower radial support and the vessel head flange. Loads resulting from transverse acceleration of the fuel assemblies are transmitted to the core barrel by connections of the lower core support plate and a radial support-type connection of the upper core plate, as shown in Figure 3.5-7.

The main radial support system for the lower end of the core barrel is accomplished by “key” and “keyway” joints to the reactor vessel wall. At four equally spaced points around the circumference, Inconel blocks are welded to the vessel inside wall. Each of these blocks has a “keyway” geometry. Opposite each of these is a “key” that is attached to the barrel. During assembly, as the internals are lowered into the vessel, the keys engage the keyways in the axial direction. With this design, the internals are provided with a support at their extremities, and may be viewed as a beam fixed at the top and simply supported at the bottom.

Radial and axial expansions of the core barrel are accommodated, but transverse movement of the core barrel is restricted by this design. Cycle stresses in the internal structures are within the limits of ASME Code Section III, thus eliminating any possibility of failure of the core support.

3.5.1.2 **Upper Core Support Assembly**

The upper core support assembly, shown in Figure 3.5-7, consists of the top support plate, deep beam sections, upper core plate, support columns, and guide tube assemblies. The support columns establish the spacing between the top support plate, deep beam sections, and the upper

core plate, and are fastened at top and bottom to these plates and beams. The support columns transmit the mechanical loadings between the two plates. The guide tube assemblies, shown on Figure 3.5-8, sheath and guide the control rod assembly drive shafts and control rod assembly, and provide no other mechanical functions. They are fastened to the top support plate and are guided by pins in the upper core plate for proper orientation and support. Additional guidance for the control rod assembly drive shafts is provided by the control rod assembly shroud tube, which is attached to the upper support plate and guide tube.

The upper core support assembly, which is removed as a unit during the refueling operation, is positioned in its proper orientation with respect to the lower support structure by flat-sided pins pressed into the core barrel, which in turn engage in slots in the upper core plate. At an elevation in the core barrel where the upper core plate is positioned, the flat-sided pins are located at equal angular positions. Slots are milled into the core plate at the same positions. As the upper support structure is lowered into the main internals, the slots in the plate engage the flat-sided pins in the axial direction. Lateral displacement of the plate and of the upper support assembly is restricted by this design.

Fuel assembly locating pins protrude from the bottom of the upper core plate and engage the fuel assemblies as the upper core support assembly is lowered into place. Proper alignment of the lower core support structure, the upper core support assembly, and the fuel and control rod assemblies is ensured by this guidance arrangement. The upper core support assembly is restrained from any axial movements by a large circumferential spring located between the upper barrel flange and the upper core support assembly. This spring is compressed by the reactor vessel head flange when the closure bolts are tightened.

Vertical loads from hydraulic loads, earthquake acceleration, and fuel assembly preload are transmitted through the upper core plate via the support columns to the deep beams and top support plate to the reactor vessel head. Transverse loads from coolant cross flow, earthquake acceleration, and possible vibrations are distributed by the support columns to the top support plate and upper core plate. The top support plate is particularly stiffened to minimize deflection.

3.5.1.3 **Incore Instrumentation Support Structures**

The incore instrumentation support structure consists of bottom mounted instrumentation thimble guides that carry the retractable flux thimble thermocouples through the bottom of the vessel. The flux thimble thermocouples consist of a detector path to allow measurement of neutron flux and thermocouples to measure core exit temperature.

Conduits extend from the bottom of the reactor vessel down through the primary concrete shield area and up to a thimble seal table. The trailing ends of the thimbles at the seal table are extracted approximately 15 feet during refueling of the reactor in order to avoid interference within the core. The thimbles are closed at the leading ends and serve as the pressure barrier between the reactor pressurized water and the containment atmosphere.

Mechanical seals between the retractable thimbles and the conduits are provided at the seal table. During normal operation, the retractable thimbles are stationary and are retracted only during refueling or for maintenance. Chapter 7 contains more information on the layout of the incore instrumentation system.

The incore instrumentation support structure is designed for adequate support of instrumentation during reactor operation, and for resisting damage or distortion during refueling.

3.5.1.4 **Evaluation of Core Barrel and Thermal Shield**

The core internals design is based on the experience gained from previous analyses, tests, and operational results. Data from previous Westinghouse pressurized water reactors was evaluated, and information derived was considered in the Surry design. For example, Westinghouse used a one-piece thermal shield that is attached rigidly to the core barrel at one end and permitted to flex at the other. The earlier designs were multi-piece thermal shields that rested on vessel lugs and were not rigidly attached to the top.

Early core barrel designs employed threaded connections, such as tie rods, that joined the bottom support to the bottom of the core barrel, and a bolted connection that attached the core barrel to the upper barrel. Such designs were associated with thermal shield oscillation, which created forces on the core barrel. Other forces were induced by unbalanced flow in the lower plenum of the reactor. In subsequent control rod assembly designs, fuel followers and a large bottom plenum in the reactor have not been required.

The reactor core barrel incorporates improvements based on the Connecticut Yankee (Haddam Neck) and the Jose Cabrera (Spain) reactor core barrels. Deflection-measuring devices employed in the Connecticut Yankee and the Jose Cabrera reactors during hot-functional testing, and strain gauges employed in the Jose Cabrera reactor, provided important information for use in the design of the internals. Careful inspections of Connecticut Yankee and Jose Cabrera reactor internals such as structural welds, nozzle interfaces, upper core plate supports, and thermal shield attachments uncovered no defects.

Substantial scale model testing was performed by Westinghouse. These tests included a complete full-scale fuel assembly operating at reactor flow, temperature, and pressure conditions. Tests were also run on a one-seventh scale model of the Indian Point Unit 2 reactor. Results of these tests indicated movement of only a few mils at full scale. Strain gauge measurements taken on the core barrel also indicated very low stresses. Testing to determine thermal shield excitation due to inlet flow disturbances was also performed. Information gathered from these tests was then used in the design of the thermal shield and core barrel.

3.5.2 Core Components

3.5.2.1 Fuel Assembly

All of the fuel assemblies, from regions prior to Region 12 of both Surry units were of the 15 x 15 LOPAR design. Fuel assemblies from Region 1 and subsequent regions are of the 15 x 15 SIF design. Both the SIF and LOPAR assemblies are of similar design, and their overall configurations are shown in Figure 3.5-9. A comparison of nominal design features of the 15 x 15 LOPAR assembly with the 15 x 15 SIF assembly is found in Table 3.5-3. The assemblies are square in cross section, nominally 8.426 inches on a side, and have a fuel column height of 144 inches. The overall height of the 15 x 15 LOPAR assembly is 159.71 inches while the overall height of the Zircaloy SIF assembly is 159.975 inches.

Beginning with Batch 16 at both units, the Surry fuel assemblies include fuel rod cladding, guide thimbles, instrumentation tubes and mixing vane grids fabricated from ZIRLO (Reference 14). This advanced zirconium alloy is being incorporated to improve the corrosion resistance of the fuel. ZIRLO is also dimensionally more stable than Zircaloy under irradiation, but most other properties (e.g., yield strength) are very similar to Zircaloy-4. Minor changes to some as-built dimensions (e.g., fuel rod length) were made to reflect the different behavior of the ZIRLO alloy. The as-built fuel assembly length was decreased slightly (to approximately 159.8 inches, between the LOPAR and Zircaloy-4 SIF assembly lengths) to allow for assembly growth to higher burnups. The fuel assembly envelope dimensions remained unchanged.

The fuel rods in both a SIF and LOPAR fuel assembly are arranged in a square array with 15 rod locations per side and a nominal centerline-to-centerline pitch of 0.563 inch between rods. Of the total possible 225 rod locations per assembly, 20 are occupied by guide thimbles for the control rods and burnable poison rods, and one central thimble is reserved for incore instrumentation. The remaining 204 locations contain fuel rods. In addition to fuel rods, a fuel assembly also includes a top nozzle, a bottom nozzle, and seven grid assemblies. The five intermediate (mixing vane) grids on the SIF assemblies are Zircaloy or ZIRLO, while the two end grids are Inconel. All seven grids on the LOPAR assembly are made of Inconel.

Beginning with Region 15, a protective Inconel grid was added directly above the bottom nozzle to enhance debris resistance. Some minor changes to the fuel rod were also made in conjunction with use of the protective grid.

These include: use of a slightly longer bottom end plug which, together with repositioning the rods to directly above the bottom nozzle, ensures a solid metal interface between the protective grid and the fuel rod; and use of an external grip top end plug to facilitate rod positioning during manufacturing of assemblies with protective grids.

Further small dimensional changes were made to the fuel starting with Surry 2 Batch 20. The fuel assembly length was increased to match the Zircaloy-4 SIF design (159.975 inches) and the fuel rod length was increased by a comparable amount, as indicated in Table 3.5-3, to take

advantage of the low growth rate of ZIRLO. The external grip feature was also removed from the fuel rod top end plug, slightly decreasing its length. These changes allowed use of a slightly longer bottom end plug on the fuel rods, to enhance debris resistance, as well as a minor increase in the fuel rod plenum volume, providing a small benefit for rod internal pressure analyses.

The 21 guide thimbles, in conjunction with the grid assemblies and the top and bottom nozzles, comprise the basic structure of the fuel assembly. The top and bottom ends of the guide thimbles are fastened to the top and bottom nozzles, respectively. The grid assemblies are fastened to the guide thimbles at each location along the height of the fuel assembly at which lateral support for the fuel rods is required. The fuel rods are contained and supported, and the rod-to-rod centerline spacing is maintained along the assembly within this skeletal framework.

Demonstration assemblies with 17 rod locations per side in a square array have been used in the past in the Surry reactors. The assemblies were used to demonstrate the feasibility of extended discharge burn-ups. WCAP 8362 (Reference 1) concludes that the presence of 17 x 17 demonstration assemblies does not adversely affect reactor performance relative to an all 15 x 15 assembly core.

Reconstituted fuel assemblies, which contain small numbers of non-fueled solid zircaloy or stainless steel rods in the place of failed fuel rods, may be used in Surry reload cores. Assemblies which have low burnup and have been determined to contain failed rods may be reconstituted to allow for the continued utilization of the energy remaining in the fuel assembly. The non-fueled rods are manufactured from solid zircaloy or stainless steel, may be slightly oversize in diameter to compensate for grid spring relaxation and any grid degradation that may occur during failed rod removal, and have a tapered end to ease insertion and prevent grid damage. In Reference 10, NRC concurred that the presence of reconstituted assemblies does not adversely affect reactor performance or safety relative to a core containing no reconstituted assemblies.

3.5.2.1.1 Bottom Nozzle

The bottom nozzle is a square pedestal structure which controls the coolant flow distribution to the fuel assembly and functions as the bottom structural element of the fuel assembly. The nozzle is fabricated from stainless steel similar to type 304, and it consists of a perforated plate joined to four angle legs with pads or feet. The angle legs and plate form a plenum space for the inlet coolant flow into the fuel assembly. The perforated plate serves as the bottom end support for the fuel rods. The bottom support surface for the fuel assembly is formed under the plenum space by the four pads at the bottom of the angle legs.

The guide thimbles, which carry axial loads imposed on the assembly, are fastened to the bottom nozzle plate. These loads, as well as the weight of the assembly, are distributed through the nozzle to the lower core support plate. Indexing and positioning of the fuel assembly in the core is fixed by two holes in diagonally opposite pads, which mate with two locating pins in the lower core plate. Lateral loads imposed on the fuel assembly are also transferred to the core support structures through the locating pins.

3.5.2.1.2 Top Nozzle

The top nozzle is a square box-like structure that functions as the fuel assembly upper structural element and forms a plenum space where the heated reactor coolant mixes and is directed toward the flow holes in the upper core plate. The nozzle is comprised of an adaptor plate, nozzle enclosure, top plate, two clamps, holddown springs, and assorted hardware. The LOPAR assemblies had single- or double-leaf holddown springs, while the SIF assembly has a three-leaf spring. All parts with the exception of the springs and their holddown bolts are constructed of stainless steel similar to type 304. The springs are made from age-hardenable Inconel 718, and the bolts from Inconel 600 or Inconel 718.

The adaptor plate is square in cross-section, and is perforated by machined slots to provide for coolant flow through the plate. On LOPAR fuel assemblies, the top ends of the guide thimble adaptors are welded to the adaptor plate. In the SIF assembly removable top nozzle design, the guide thimble adaptors are mechanically attached to the adaptor plate as described in Reference 11. Thus, the adaptor plate, which acts as the fuel assembly top end plate, provides a means of distributing evenly among the guide thimbles any axial loads imposed on the fuel assemblies, and limits any excessive axial movement of fuel rods.

The nozzle enclosure is a square thin-walled shell that forms the plenum section of the top nozzle. The bottom end of the enclosure is welded to the periphery of the adaptor plate, and the top end joins the periphery of the top plate.

The top plate is square in cross-section, with a large central opening. The opening allows clearance for the control rods to pass into the guide thimbles in the fuel assembly, and provides for coolant exit from the fuel assembly into the upper internals area. Two pads containing axial through-holes, located on diametrically opposite corners of the top plate, provide a means of positioning and aligning the top of the fuel assembly. Like the bottom nozzle, alignment pins in the upper core plate mate with the holes in the top nozzle plate.

Holddown forces of sufficient magnitude to oppose the hydraulic lifting forces on the fuel assembly are obtained by means of the leaf springs, which are mounted on the top plate. The springs are fastened in pairs to the top plate at the two corners where alignment holes are not located, and extend out from the corners parallel to the sides of the plate. On LOPAR fuel assemblies, each pair of springs is fastened with a clamp that fits over the ends of the springs. Each clamp is secured with two bolts, which pass through the clamp and springs and thread into the top plate. At assembly, the spring-mounting bolts are torqued sufficiently to preload against the maximum spring load, and then are lock-welded to the clamp, which is counter-bored to receive the bolt head. On the SIF fuel assemblies, attachment of the holddown springs was modified. The counterbore was eliminated from the clamp design, allowing the holddown spring screws to bear directly on the springs. The clamp, which is tack welded to the top nozzle, continues to fit over the end of the springs, and acts as a cover for the screw heads. A lock wire that is welded to the clamp ensures that the spring screws remain in position during operation.

The spring load is obtained through deflection of the spring by the upper core plate. The spring projects above the fuel assembly and is depressed by the core plate when the internals are loaded into the reactor. The free end of the spring is bent downward and is captured in a slot in the top plate. This is done to guard against release of loose parts in the reactor in the event (however remote) of spring fracture.

In addition, the fit between the upper spring and slot and between the spring set and the mating slot in the clamp is sized to prevent rotation of either end of the spring set into the control rod path in the event of spring fracture.

In addition to its plenum and structural functions, the nozzle provides a protective housing for components that mate with the fuel assembly. In handling a fuel assembly with a control rod assembly inserted, the control rod assembly spider is protected by the nozzle. During operation in the reactor, the top nozzle protects the control rods from coolant cross flows in the unsupported span between the top nozzle adaptor plate and the end of the guide tube in the upper internals package. Other fuel insert components that mate with the fuel assembly thimble tubes, such as plugging devices, source assemblies, flux suppression inserts and burnable poison assemblies, are similarly protected by the top nozzle of the fuel assembly.

3.5.2.1.3 Guide Thimbles

The control rod guide thimbles in the fuel assembly provide guide channels for the control rods during insertion and withdrawal. The guide thimbles are fabricated from a single piece of Zircaloy-4 or ZIRLO tubing, which is drawn to two different diameters. The larger inside diameter at the top provides a relatively large annular area for rapid insertion during a reactor trip. It also accommodates a small amount of upward cooling flow during normal operations. The bottom portion of the guide thimble has a smaller diameter to cause a dashpot action when the control rods approach the end of travel in the guide thimbles. The transition zone at the dashpot section is conical in shape so that there are no rapid changes in diameter in the tube.

Flow holes are provided just above the transition of the two diameters to permit the entrance of cooling water during normal operation, and to accommodate the outflow of water from the dashpot action during reactor trip.

The control rod guide thimbles are closed at the bottom by means of a welded end plug. The end plugs are subsequently fastened to the bottom nozzle during fuel assembly fabrication. Flow holes are provided in the end plugs to permit entrance of cooling water during normal operation and to regulate dashpot action during control rod trip. The instrumentation thimble is left open at the bottom to receive the incore instrumentation.

3.5.2.1.4 Grids

The grid assemblies consist of individual slotted straps that are interlocked in an “egg-crate” arrangement. The Inconel grids (all grids in LOPAR fuel assemblies and end grids in SIF assemblies) are furnace-brazed to permanently join the straps at their points of intersection. The

SIF Zircaloy or ZIRLO grid straps (all mid-grids) and the Inconel protective grids are permanently joined by welding. Details such as springs, support dimples, mixing vanes, and tabs are punched and formed in the individual straps prior to assembly.

Two types of grid assemblies are used in the 15 x 15 LOPAR fuel assembly. Grids with mixing vanes that project from the upper edges of the straps into the coolant stream are used in the high-heat region of the fuel assemblies to promote mixing of the coolant. A grid of this type is shown in Figure 3.5-11. The grids located at the bottom and top ends of the assembly are of the non-mixing type. They are similar to the mixing type but do not have mixing vanes on the internal straps. Inconel 718 is used for the grid material because of its corrosion resistance and high strength properties. After the combined brazing and solution annealing temperature cycle, the grid material is age-hardened to obtain the material strength necessary to develop the required grid spring forces.

Two types of structural grid assemblies are used in the 15 x 15 SIF assembly. The top and bottom grids are the same non-mixing vane grids used in the LOPAR assemblies. The middle mixing vane grids are similar to the mixing vane grids used on the LOPAR assemblies with the exception that they are made of Zircaloy or ZIRLO. There are also some dimensional differences between the Inconel and zirconium alloy grid straps to compensate for differences in material strength properties. The Inconel is used for the end grids primarily for its high strength and corrosion resistance. Zirconium-based alloys are now used for the mid-grids primarily for their low neutron absorption properties.

The outside straps on all structural grids contain mixing vanes on their upper edges that also aid in guiding the grids and fuel assemblies past projecting surfaces during handling or core loading and unloading. In addition, there are small tabs projecting downward from the lower edge of the outside straps; the irregular contour of the straps is also for guiding.

On the Batch 15 fuel only (fresh feed to Cycle 13), the orientation of the mixing vane grids was slightly modified (Reference 13), with every other mixing vane grid being rotated 90 degrees in the clockwise direction. The purpose for the rotation was to minimize the susceptibility of the fuel assembly to flow induced vibration. There were no physical or material changes to the grids or their axial positions, and this change did not impact the pressure drops, DNB performance, or other thermal-hydraulic performance of the Surry fuel assembly. However, subsequent testing showed that this change could affect the DNB performance of some (other) fuel designs, so grid rotation was not applied to later batches of Surry fuel.

Starting with Batch 15 of the Surry Units 1 and 2, the fuel assemblies incorporate an additional protective bottom Inconel grid (P-grid), located directly above the bottom nozzle (Reference 13). The straps of the P-grid subdivide the flow holes in the bottom nozzle, reducing the amount and size of debris that can enter the fuel assembly. The P-grid inner grid straps contain paired horizontal dimples that provide coplanar four-point contact within each grid cell. (To accommodate the coplanar dimples, alternating cells have the dimples at alternating elevations.)

The P-grid is designed to have its dimples on the full diameter of the fuel rod's solid bottom end plug throughout the design life of the fuel assembly.

The protective grid is fabricated from Inconel-718. The straps are welded at the intersects and to the outer grid strap, similar to the Zircaloy and ZIRLO grids. The top of the P-grid outer grid strap retains the anti-snag features used in the top and bottom Inconel grids. The bottom portion of the outer grid strap is bent inward toward the top of the bottom nozzle to minimize potential for hang-up. In addition, the protective grid has a slightly smaller envelope than the bottom non-mixing vane grid and the bottom nozzle to minimize the potential for interaction with other fuel assemblies during handling. The interface between the P-grid, the bottom nozzle, and the fuel rod is illustrated in Figure 3.5-10.

Hydraulic tests showed that the impact of incorporating the protective grids into the fuel assemblies was effectively offset by positioning the fuel rods on the bottom nozzle. The magnitude of the effect on the pressure drop loss coefficients was negligible, so there is no change to the DNB performance of the fuel.

3.5.2.1.5 Fuel Rods

The fuel rods consist of uranium dioxide ceramic pellets contained in slightly cold-worked and partially annealed Zircaloy-4 or ZIRLO tubing, which is plugged and seal-welded at the ends to encapsulate the fuel. Sufficient void volume and clearances are provided within the rod to accommodate fission gases released from the fuel, differential thermal expansion between the cladding and the fuel, and fuel swelling due to accumulated fission products without overstressing of the cladding or seal welds. Shifting of the fuel within the cladding is prevented during handling or shipping prior to core loading by a carbon steel or stainless steel helical compression spring that bears on the top of the fuel pellet column. The holddown force to prevent fuel shifting is obtained by compression of the spring between the top end plug and the top of the fuel pellet stack.

Beginning in Cycle 21, each fuel assembly may contain from 0 to 148 integral fuel burnable absorber (IFBA) rods. The IFBA fuel rod design includes a thin layer of boride coating on the outer surface of the majority of the fuel pellets in the fuel rod, as well as axial blankets. The axial blanket is a six-inch (approximate) stack of slightly enriched annular fuel pellets without boride coating located at the top and bottom of the fuel stack in each IFBA rod. Cores may continue to use discrete (fixed) burnable poison rod assemblies in conjunction with IFBA fuel assemblies.

All fuel rods are internally pressurized with helium during fabrication. The fuel rod void space is sized to ensure adherence to the pressure criteria. The rod internal pressure is evaluated for the limiting fuel rod, assuming a conservative operating history. The evaluation is based on expected operating conditions at the peak steady-state power, and also considers the fission gas release from normal operating transients. The model used to predict the quantity of fission gas in the gap is based on an extensive comparison with both published and proprietary data covering a variety of conditions. The internal pressure of the lead rod in the reactor is limited to a value that

does not cause the diametral gap to increase due to outward cladding creep during steady state operation, and does not cause extensive DNB propagation to occur.

Additional information on the rod internal pressure design basis can be found in WCAP-8964-A (Reference 2).

The fuel pellets are right circular cylinders consisting of slightly enriched uranium dioxide powder, which is compacted by cold pressing and sintering to the required density. The ends of each pellet are dished slightly to allow the greater axial expansion at the center of the pellets to be taken up within the pellets themselves and not in the overall fuel length. Some pellets may have a thin coating of boride material applied to the circumferential surface as discussed in Section 3.5.2.1.5.

A lower pellet density was used in the outer fuel regions of the first core to compensate for the anticipated effects of the higher burn-up experienced in these regions. Reload cores have a uniform nominal pellet density that is slightly higher than those used in the initial core.

The fuel enrichments listed in Table 3.5-1 were used for the three regions in the first core loading. Enrichments used in reload fuel regions are discussed in the reload safety evaluation prepared for each subsequent core cycle.

Each fuel assembly is identified by a serial number engraved on the top nozzle. The fuel pellets are fabricated by a batch process so that only one enrichment region is processed at any given time. The serial numbers of the assemblies and corresponding enrichment are documented and verified by the manufacturer prior to shipment.

Each assembly is assigned a specific core loading position prior to insertion. A record is then made of the core loading position, serial number, and enrichment. Before core loading, two independent reviews are made to ensure that the loading assignment is correct. The serial number is checked before an assembly is loaded into the core. After the core is completely loaded, each serial number is checked again for agreement with the core loading drawing.

Any error in enrichment, beyond the normal manufacturing tolerances, can cause power shapes which are more peaked than those calculated with the correct enrichments. There is an 8% uncertainty margin between the calculated worst value and the design value of $F\Delta h$ assumed for the analysis of normal steady-state operation and anticipated transients. The incore system of movable flux detectors, which is used to verify power distribution limits, is capable of detecting anomalies (such as fuel enrichment errors, core loading errors, or misaligned control rods) that cause peaking factors or core tilts in excess of design values. Power distribution measurements are taken at low power when extremely adverse power distribution can be tolerated. The analysis described below shows that the power increase due to any combination of misplaced fuel assemblies would significantly raise peaking factors and would be readily observable with the incore flux monitors. In addition, thermocouples located in the flux thimbles monitor the outlet of

about one-third of the fuel assemblies in the core. There is a high probability that the thermocouples would also indicate any abnormally high coolant temperature rise.

An analysis of the effect of misplacing a fuel assembly was performed on a core very similar to the initial Surry core. The power distribution in the X-Y plane of the core was calculated using a "full core" description with the PDQ-07 code. A discrete representation was used wherein each individual fuel rod was described by a mesh point. The radial power-peaking factor for the reference case (Case 1) was 1.370.

In Case 2, the central fuel assembly which would normally be of 2.15 weight percent enrichment, was assumed to be interchanged with an outer fuel assembly of 3.3 weight percent enrichment. The radial power-peaking factor for this case was 2.538 and occurred in the central fuel assembly. The power distribution was badly skewed with a tilt of approximately 15% across the core. Incore instrumentation would easily detect a misplacement of this nature.

In Case 3, the central 2.15 weight percent enrichment fuel assembly in the core was assumed to be interchanged with a neighboring 2.70 weight percent enrichment fuel assembly. The radial power-peaking factor for this case was 1.625. A power distribution tilt of approximately 10% results in the two rows of fuel adjacent to the interchanged fuel assemblies, which would be detected by the incore instrumentation. The interchange of 2.15 and 2.70 weight percent enrichment fuel assemblies not at the core center would introduce more pronounced power distribution tilts than Case 3.

The possibility of having an assembly in which all the fuel is of the wrong enrichment was also considered. In this case there was no interchange of assemblies, but there was one assembly in the core that departed from the nominal enrichment.

An analysis of the effect of an inadvertent loading of an assembly with an enrichment increased by 20% over the nominal value showed that the error was detectable at many of the detector locations in the core. In the case of a centrally placed assembly with this enrichment error, five flux detectors would show a signal more than 5% above the expected value. If the assembly bearing the enrichment error was placed off-center and as far from a flux detector as possible, the tilt caused by a 20% error in enrichment would be detectable in more than half of the detector locations in the core, either as a flux increase over expected symmetric values or as a flux decrease on the opposite side of the core.

If the movable detector system failed to detect an assembly enrichment error, the peaking factors would still show margin to the design conditions through the inclusion of measurement uncertainties, and normal plant operation could be safely continued. It is not credible that any positive indication of power distribution anomalies that are sufficiently large to cause a significant departure from design conditions would be ignored. These measurements are an integral part of the physics start-up tests where considerable emphasis is placed on obtaining good power distribution measurements.

In the event that a single fuel pin or a single fuel pellet had a higher enrichment than the nominal value, then the local power generation would be increased approximately by the percentage of the enrichment error. In the case of an enrichment error greater than 8% there exists a possibility, depending on location, that design limits on fuel rating would be violated for that pin or pellet. The consequences of such a local reduction of DNBR and increase in clad and fuel temperatures would be limited to the incorrectly loaded pin or pins.

During initial core loading and subsequent refueling operations, detailed written handling and checkoff procedures are utilized throughout the loading sequence. The initial cores were loaded in accordance with a core loading plan similar to that illustrated in Figure 3.5-3, which shows the locations of the different enrichment fuel assemblies typically used in initial cores. The actual core loading plans for both initial and reload cores show the identification number for the fuel assembly used in each core location.

During subsequent refueling operations, reconstituted fuel assemblies (see Section 3.5.2.1) may be included among the fuel assemblies used for reloading the core.

3.5.2.2 **Control Rod Assemblies**

The control rod assemblies each consist of a group of individual control rods fastened at the top end to a common spider assembly. These assemblies, one of which is shown in Figures 3.5-4 and 3.5-12, are provided to control the reactivity of the core under operating conditions. These assemblies contain absorber material for 142 inches of their length. The number of control rod assemblies for the initial cores is specified in Table 3.5-1. Part length rods have since been removed.

The absorber material used in the control rods is silver-indium-cadmium alloy, which is essentially “black” to thermal neutrons and has sufficient additional resonance absorption to significantly increase its worth. The alloy is in the form of rods, which are sealed in stainless steel tubes to prevent the rods from coming in direct contact with the coolant.

When the control rod assembly has been fully withdrawn, the tip of the control rods remains engaged in the guide thimbles so that alignment between control rods and thimbles is maintained. Since the control rods are long and slender, they are relatively free to conform to any small misalignments encountered with the guide thimble.

The spider assembly is in the form of a center hub with radial vanes containing cylindrical fingers from which the control rods are suspended. Handling detents and detents for connection to the drive shaft are machined into the upper end of the hub. A spring pack is assembled into a skirt integral to the bottom of the hub to stop the control rod assembly and absorb the impact energy at the end of an insertion. The radial vanes are joined to the hub and the fingers joined to the vanes by furnace brazing. A centerpost that holds the spring pack and its retainer is threaded into the hub within the skirt and welded to prevent loosening in service. All components of the spider

assembly are made from type 304 stainless steel except for the springs, which are Inconel X-750 alloy, and the retainer, which is 17-4 PH stainless in the H 1100 condition.

The control rods are fastened securely to the spider. The rods are first threaded into the spider fingers, pinned to maintain joint tightness, and the pins are then welded in place. The end plug below the pin position is designed with a reduced section to permit flexing of the rods to correct for small operating or assembly misalignments.

In construction, the silver-indium-cadmium rods are inserted into cold-worked stainless steel tubing which is then sealed at the bottom and the top by welded end plugs. Sufficient diametral and end clearance is provided to accommodate relative thermal expansions and to limit the internal pressure to acceptable levels.

The bottom plugs are made bullet-nosed to reduce the hydraulic drag during a reactor trip and to guide smoothly into the dashpot section of the fuel assembly guide thimbles. The upper plug is threaded for assembly to the spider and has a reduced end section to make the joint more flexible.

The original control rod assembly design was replaced prior to Surry 1 & 2 Cycle 11 with an “enhanced performance” control rod assembly design. The enhanced design is essentially the same as the original with the exception of the cladding tubes which are hard chrome plated to increase both wear resistance and the life of the control rods. The ends of the cladding tubes are not plated, however, to preclude weld contamination of the end plug. Trace element impurities in the cladding were also restricted to lower values than previously allowed to reduce corrosion in the cladding. In addition, the absorber rodlet diameter in the lower twelve inches of the absorber rods was reduced to decrease cladding strain due to swelling induced by irradiation of the absorber.

The chrome plated stainless steel clad silver-indium-cadmium alloy absorber rods are resistant to radiation and thermal damage. thereby ensuring their effectiveness under all operating conditions.

3.5.2.3 **Neutron Source Assemblies**

Two neutron source assemblies were utilized in the initial cores. These assemblies consisted of three secondary source rods and one primary source rod, twelve burnable poison rods and four thimble plugs each. The primary source rods contained capsules of Plutonium-Beryllium source material 24 inches long. The secondary source rods contained Antimony-Beryllium pellets stacked to a height of 121.754 inches. The primary source, secondary source and burnable poison rods utilized 304 SS cladding materials. The rods were fastened to a spider at the top end similar to the control rod spiders. The neutron source rods were inserted, as part of two burnable poison rod assemblies, into the control rod guide thimbles in fuel assemblies at unrodded locations in the core.

For the initial Unit 1 and Unit 2 cores following the steam generator replacement outages (Unit 1 Cycle 6 and Unit 2 Cycle 5), each core contained two new primary source assemblies containing one primary source rod and 12 burnable poison rods each. Each core also contained three secondary source assemblies containing four secondary source rods and sixteen thimble plugs each. The primary source rods contained a 1.5-inch length of Californium-252. Aluminum oxide spacers were used to maintain the source material position in the rod. The secondary source rods contained Sb-Be pellets stacked to a height of 67.87 inches. The primary source, secondary source and burnable poison rods all utilized 304 SS cladding material. The rods on the primary source assemblies were attached to a base plate similar to the standard burnable poison assemblies. The secondary source rods were fastened to a spider at the top end similar to the control rod spiders. The rods in the neutron source assemblies were inserted into the control rod guide thimbles in fuel assemblies at unrodded locations in the core.

The primary sources were used in the initial cycles (and in the first cycles following steam generator replacement) to ensure adequate count rate for the source range detectors at the beginning of cycle. No primary sources are currently placed in reload cycles. Secondary sources were loaded in reload cores through Cycle 14 at each unit. However, the source detector minimum count rate can be provided by the fuel assemblies on the periphery of the core, and secondary sources are not normally required. The option remains to load secondary sources into reload cores to charge them for possible future use.

Design criteria similar to those for the fuel rods were used for the design of the source rods. The requirements for the source rods included that the cladding be free-standing, internal pressures remain less than reactor operating pressure, and sufficient internal gaps and clearances be provided to allow for differential expansions between the source material and cladding.

3.5.2.4 **Plugging Devices**

It is permissible to limit bypass flow through the guide thimbles in fuel assemblies that do not contain insert components such as control rod assemblies, source assemblies, or burnable poison rods, by fitting the fuel assemblies at those locations with plugging devices. The plugging devices consist of a flat retaining plate with short rods suspended from the bottom surface of the plate and a spring pack assembly attached to the top surface. During installation in the core, the plugging devices fit within the fuel assembly top nozzles and rest on the top nozzle adaptor plate. The short rods project into the upper ends of the guide thimbles to reduce the bypass flow area. The spring pack is compressed by the upper core support assembly when it is lowered into place.

All components in the plugging devices, except for the springs, are constructed from type 304 stainless steel. The springs used in each plugging device are wound from an age-hardenable Inconel X-750 to obtain higher strength.

Beginning with Cycle 10 of each unit, all plugging devices were removed from the core (Reference 12).

3.5.2.5 **Burnable Poison Rod Assemblies**

Burnable poison rod assemblies (BPRA) may be incorporated into the core design to reduce the soluble boron requirement for control of excess reactivity, and to shape the core power distribution. The number of BPRA or BPRA poison rods may vary from one operating cycle to the next, and may be used in any fuel assembly not under a control rod bank location. BPRA burnable poison rods are commonly referred to as fixed, discrete, and/or removable burnable poison rods. This type of burnable poison is “fixed” and “discrete” in the sense that the neutron absorber is contained in solid form (not soluble) in discrete rods (separate from the fuel). BPRA burnable poison is removable because the BPRA itself may be removed from the fuel assembly.

The BPRA burnable poison rods consist of $A1_20_3$-B_4C pellets contained within Zircaloy-4 tubular cladding that is plugged and seal-welded at the ends to encapsulate the pellets. The pellets are supported by the bottom end plug and, depending on pellet stack length, spacers may also be employed. A typical BPRA burnable poison rod is shown in Figure 3.5-13.

The BPRA burnable poison rods in each fuel assembly are grouped and attached together at the top end of the rods by a flat retaining plate that fits inside the fuel assembly top nozzle and rests on the top nozzle adaptor plate. The retaining plate and the poison rods are held down and restrained against vertical motion through a spring pack attached to the plate. This spring is compressed by the upper core plate when the reactor upper internals package is lowered into the reactor, and this ensures that the poison rods cannot be lifted out of the core by flow forces. Each rod is attached to the retaining plate.

The clad in the poison rod assemblies is cold-worked Zircaloy-4 seamless tubing. The upper and lower end plugs, nuts and solid spacers are fabricated from Zircaloy-4. The spring spacers are 302 or 304 stainless steel. The hold-down assembly is fabricated from stainless steel similar to type 304, except for the hold-down springs which are wound from Inconel 718 wire.

3.5.2.6 **Evaluation of Core Components**

3.5.2.6.1 Fuel Evaluation

The fission gas release and associated buildup of internal gas pressure in the fuel rods is calculated by the PAD code, based on experimentally determined release rates. The increase of internal pressure in the fuel rod due to this phenomenon is included in the determination of the maximum cladding stresses.

The total allowable plastic tensile creep strain in the cladding, considering the combined effects of internal fission gas pressure, external coolant pressure, fuel pellet swelling, and clad creep, is limited to less than 1% from the unirradiated condition throughout the operating life of the fuel. The cladding stresses also remain below the design limit under normal operating conditions throughout the operating life of the fuel.

In the event of cladding defects, the high resistance of uranium dioxide fuel pellets to attack by water protects against substantial fuel deterioration. Thermal stress in the pellets, while causing some fracture of the bulk material during temperature cycling, does not result in pulverization or gross void formation in the fuel matrix. As shown by operating experience and extensive experimental work in the industry, the thermal design parameters conservatively account for any changes in the thermal performance of the fuel element due to pellet fracture.

The consequences of a breach of cladding are greatly reduced by the inherent ability of uranium dioxide to retain fission products, including those that are gaseous or volatile. This retentiveness decreases with increasing fuel temperature and fuel burn-up, but remains a significant factor even at full-power operating temperature in the maximum burn-up element.

A survey (Reference 4) of high-burn-up uranium dioxide fuel element behavior indicated that for a given initial uranium dioxide void volume, which is a function of the fuel density, it is possible to conservatively define the fuel swelling as a function of burn-up. The fuel densification and swelling model is a semi-empirical model that considers the effects of the initial density and burnup. The model was developed using data from fuel that operated to a range of burnups in several commercial reactors (References 15 & 16).

The Region 1 fuel was initially expected to be irradiated for only the first cycle of reactor operation, so an initial density of 94% was used for this fuel. Since the Region 2 and 3 fuel was expected to be retained through two and three cycles of operation, respectively, lower fuel pellet densities were specified for these regions to accommodate the anticipated effects of the higher burnups this fuel would reach. The specified initial density was 93% for Region 2, and 92% for Region 3. Reload cores have utilized a slightly higher nominal pellet density. The operation of this fuel to approved burnup levels is supported by the current fuel densification and swelling model, and by operating experience with higher density fuel.

The integrity of fuel rod cladding so as to retain fission products or fuel material is directly related to cladding stress and strain under normal operating and overpower conditions. Design limits and damage limits (cladding perforation) in terms of stress and strain are as follows:

	Damage Limit	Design Limit
Stress	Ultimate strength	0.2% offset yield strength
	57,000 psi minimum	45,000 psi minimum
Strain	1.7%	1.0%

The damage limits given above are minimum values. Actual damage limits depend upon neutron exposure and normal variation of material properties, and would generally be greater than the minimum damage limits indicated. Throughout the fuel rod life, the actual stresses and strains are below the design limits. Thus, significant margins exist between actual operating conditions and the damage limits.

Other parameters having an influence on cladding stress and strain and the relationship of these parameters to the damage limits are as follows:

1. Internal gas pressure: The internal gas pressure required to produce cladding stresses equal to the damage limit under normal operating conditions is well in excess of the maximum design pressure. The maximum rod internal pressure experienced during operation depends upon the initial pressure, void volume, and fuel rod power history.

2. Cladding temperature: The strength of the fuel cladding is temperature dependent. The minimum ultimate strength reduces to the design yield strength at an average cladding temperature of approximately 850°F. The maximum average cladding temperature during normal operating conditions is expected to remain below this value.

3. Burn-up: Fuel burn-up produces fuel swelling, which produces cladding strain. The strain damage limit is not expected to be reached until the peak pellet burn-up is well in excess of that reached with currently approved fuel burn-up limits. The peak pellet burn-up for fuel in equilibrium annual cycling was projected to be approximately 49,000 MWD/MTU based on a design equilibrium batch average burn-up of approximately 31,500 MWD/MTU. With the 18-month cycles currently in effect and planned, typical batch average burn-ups of about 45,000 to 50,000 MWD/MTU can be achieved. A 60,000 MWD/MTU lead rod burn-up is the NRC approved limit (Reference 5). As part of the reload design process (Reference 6), each reload core is evaluated to ensure compliance with the vendor's fuel design criteria. Compliance with the design limits ensures that the clad strain damage limits are not exceeded during the cycle.

4. Fuel temperature and kW/ft: At zero burn-up, cladding damage is calculated to occur at 31 kW/ft based on clad strain reaching the damage limit. At this power rating, 17% of the pellet central region is expected to be in the molten condition. For reload cores, the overpower concerns are addressed by ensuring that a fuel centerline temperature limit of 4700°F is not exceeded at any point in the cycle for any Condition I or Condition II event (Reference 6). This limit precludes centerline melting for approved burn-up limits.

There are no Technical Specification restrictions on fuel residence time. The high-density prepressurized fuel is typically used for two to four cycles of operation. Current Westinghouse fuel is stable with respect to densification, so significant axial pellet column gaps and clad flattening do not occur (Reference 7).

The design bases and functional requirements for the fuel assembly structural components are discussed in References 11, 14, and 17.

3.5.2.6.2 Evaluation of Control Rods

Time of control rod assembly trip and control rod cooling were evaluated as follows:

1. Analytical techniques were used to predict the trip behavior of a control rod assembly. Tests were also performed under an experimental program conducted in the Westinghouse Reactor Evaluation Center, and the results verified these analytical techniques.

   The calculated control rod insertion trip to the dashpot entry at full flow rate and operating temperature is less than the design value.

2. Control rod guide thimble and dashpot flow analyses have been performed to determine the adequacy of thimble design to meet cooling requirements. Results indicated that adequate cooling flow is provided in the dashpot and the thimble to prevent boiling.

3.5.2.6.3 Evaluation of Burnable Poison Rods

The BPRA burnable poison rods are positively positioned in the core inside fuel assembly guide thimbles, and held in place by attachments to an upper structure assembly compressed beneath the upper core plate. In order to maintain encapsulation of the absorber material throughout the design lifetime, the BPRA burnable poison rod design incorporates sufficient margin to accommodate the anticipated effects of gas release, absorber material swelling, clad growth and creep, stress, strain, and corrosion.

The BPRA burnable poison rods consist mainly of a column of poison pellets encapsulated within cold-worked, Zircaloy-4 seamless tubing. The individual pellets are a sintered ceramic of relatively low density $A1_20_3$-B_4C and are in the form of a solid, right circular cylinder with flat ends. Rod fabrication is initiated by loading a spring spacer into the tubing, followed by the poison pellets. The spring spacer is loaded into the plenum gap region of the rod to support the pellet stack for shipping, handling and operation. For operation, the spring preload ensures a bearing load on the pellet stack and individual pellets, such that no axial gaps are available in he rod to allow clad creep collapse. A solid spacer may also be employed depending on the length of the pellet stack.

The assembled BPRA burnable poison rods are prepressurized with dry, high purity helium gas. During operation, the pressurized helium gas provides good heat transfer across the pellet-to-clad diametral gap and reduces the pressure differential across the clad wall thickness which contributes to clad creep ovality. Sufficient volume is provided in the rod plenum gap region, accounting for the reduction in available volume due to the spring spacer, to accommodate the prepressurization gas plus the gas released from the poison due to the neutronic reaction between the B^{10} isotope and thermal neutrons.

Fuel rods containing integral burnable absorber (IFBA) are evaluated as described in Section 3.5.2.6.1. The evaluation also considers the effects of gas that accumulates inside the rod as a result of neutron absorption by the boride burnable absorber material. The same design limits apply to all fuel rods, whether or not the rod contains integral poison.

3.5.2.6.4 Effects of Vibration and Thermal Cycling on Fuel Assemblies

Reactor coolant flow can induce fuel rod vibration. The effect of the vibration on the fuel assembly and individual fuel rods is minimal. The cyclic stress range associated with deflections of such small magnitude is insignificant and has no effect on the structural integrity of the fuel rod.

The fuel assembly grids provide sufficient fuel rod support to limit fuel rod vibration and to maintain cladding wear to within acceptable limits. Significant operating experience exists with Westinghouse fuel using the grid designs found in the LOPAR and SIF assemblies. Significant wear of the cladding or grid supports is not expected during the life of the assembly, nor have grid or fuel rod abnormalities been observed on this fuel.

The effect of thermal cycling of the fuel on the grid to rod support is a slight relative movement between the grid contact surfaces and the clad. This movement is gradual during heatup and cooldown, and the grid assemblies allow thermal expansion of the rods without imposing restraint sufficient to develop buckling or distortion of the fuel rods. The number of such thermal cycles is small over the life of a fuel assembly, so this motion is a negligible contribution to wear of the contacting parts.

The deflection of the control rods, or rods of fuel insert components such as burnable poison rods, flux suppression inserts (Unit 1 only, Cycles 13 through 20), thimble plugs or source rods, is limited by the fit within the fuel assembly guide thimbles. Analyses performed for the original core insert components indicate that cyclic deflections within the limited range allowed by the guide thimbles results in an insignificantly low stress in either the insert rodlets or in the joint of the rodlet to a spider or retainer plate.

3.5.3 Control Rod Drive Mechanism

3.5.3.1 Control Rod Assembly Design Description

The control rod drive mechanisms are used for withdrawal and insertion of the control rod assemblies in the reactor core, and to provide sufficient holding power for stationary support.

Fast total insertion, or reactor trip, is obtained by simply removing the electrical power to allow the control rod assemblies to fall by gravity.

The complete drive mechanism, shown in Figure 3.5-14, consists of the internal latch assembly, the pressure vessel, the operating coil stack, and the drive shaft assembly.

Each assembly is an independent unit that can be dismantled, removed, or installed separately. Each drive mechanism is threaded and seal-welded onto an adaptor located on top of the reactor pressure vessel, and is connected to the control rod assembly directly below by means of a grooved drive shaft. The upper section of the drive shaft is suspended from the working components of the drive mechanism. The drive shaft and control rod assembly remain connected during all reactor operations, including trip of the control rod assemblies.

Reactor coolant fills the pressure-containing parts of the drive mechanism. All working components and the shaft are immersed in the reactor coolant, and utilize it for cooling and lubrication of sliding parts.

Three magnetic coils, which form a removable electrical unit and surround the control rod drive mechanism pressure housing, induce magnetic flux through the housing wall to operate the working components. They move two sets of latches that lift or lower the grooved drive shaft.

The three magnets are turned on and off in a fixed sequence by solid-state switches. The sequencing of the magnets produces step motion over the 144 inches of normal control rod travel.

The mechanism is capable of handling a 360-lb load, including the drive rod weight, at a rate of 45 inches per minute. Lift capacity is available for overcoming mechanical friction between the moving and the stationary parts. Gravity provides the drive force for control rod assembly insertion and the weight of the whole control rod assembly is available to overcome any resistance.

The mechanisms are designed to operate in water at 650°F and 2485 psig. The temperature at the mechanism head adaptor is much less than 650°F because it is located in a region of limited water flow from the reactor core.

A multiconductor cable connects the mechanism operating coils to the dc power supply through the power programmer. The power supply is described in Section 7.3.

All part-length control rod assemblies have been removed. On Unit 1, the part-length control rod drive mechanisms have been removed from all core locations except H04. The mechanism housing at location H04 is used for the reactor vessel head vent system. On Unit 2 all the part-length control rod drive mechanisms have been removed and a direct penetration in the reactor vessel head is used for the reactor vessel head vent system. To maintain the pressure boundary function, adapter plugs were threaded on the part-length locations and then seal welded with a canopy weld. To maintain cooling airflow characteristics, dummy cans were attached to the adapter plugs to occupy the volume of the removed part-length control rod drive mechanisms.

3.5.3.1.1 Latch Assembly

The latch assembly contains the working components that withdraw and insert the drive shaft and attached control rod assembly. It is located within the pressure housing and consists of the pole pieces of three electromagnets. They actuate two sets of latches that engage the grooved section of the drive shaft.

The upper set of latches move up or down to raise or lower the drive rod by 0.625 inch. The lower set of latches have a 0.047-inch axial movement to shift the weight of the control rod assembly from the upper to the lower latches.

3.5.3.1.2 Pressure Vessel

The pressure vessel consists of the latch housing and the rod travel housing. The latch housing is the lower portion of the vessel, and contains the latch assembly. The rod travel housing is the upper portion of the vessel. It provides spaces for the drive shaft during its movement.

The housings are designed in accordance with the requirements for Class A vessels of ASME Code Section III, Nuclear Vessels.

3.5.3.1.3 Operating Coil Stack

The operating coil stack is an independent unit that is installed on the drive mechanism by sliding it over the outside of the pressure housing. It rests on a pressure housing flange without any mechanical attachment, and may be removed and installed while the reactor is pressurized.

The three operating coils (A, B, and C) are made of round copper wire insulated with a double layer of filament-type glass yarn.

The design operating temperature of the coils is 450°F. Coil temperature can be determined by resistance measurement. Forced air cooling along the outside of the coil stack maintains a coil temperature of approximately 390°F.

3.5.3.1.4 Drive Shaft Assembly

The main function of the drive shaft is to connect the control rod assembly to the mechanism latches. Grooves for engagement and lifting by the latches are located throughout the 144 inches of control rod travel. The grooves are spaced 0.625 inch apart to coincide with the mechanism step length, and have a 45-degree slot angle.

The drive shaft is attached to the control rod assembly by a coupling. The coupling has two flexible arms that engage the grooves in the spider assembly.

A 0.25-inch-diameter disconnect rod runs down the inside of the drive shaft. It utilizes a locking button at its lower end to lock the coupling and control rod assembly. At its upper end, there is a disconnect assembly for remote disconnection of the drive shaft assembly from the control rod assembly.

During unit operation, the drive shaft assembly remains connected to the control rod assembly at all times.

3.5.3.1.5 Position Indicator Coil Stack

The position indicator coil stack slides over the rod travel housing section of the pressure vessel. It detects drive shaft position by means of a cylindrically wound differential transformer that spans the normal length of control rod travel (144 inches).

3.5.3.1.6 Drive Mechanism Materials

All parts exposed to reactor coolant, such as the pressure vessel, latch assembly, and drive rod, are made of metals that resist the corrosive action of the water.

Three types of metals are used exclusively: stainless steel, Inconel X, and cobalt-based alloys. Wherever magnetic flux is carried by parts exposed to the main coolant, stainless steel is used. Cobalt-based alloys are used for the pins, latch arm tips, and pin shoe facing in the latch arms.

Inconel X is used for the springs of both latch assemblies, and type 304 (Unit 1) and type 316 (Unit 2) stainless steel is used for all pressure containment. Hard chrome plating provides wear-resistant surfaces on the sliding parts, and prevents galling between mating parts during assembly.

Outside of the pressure vessel, where the metals are exposed only to the reactor containment environment and cannot contaminate the reactor coolant, carbon and stainless steels are used. Carbon steel, because of its high permeability, is used for magnetic flux return paths around the operating coils, and is zinc-plated 0.001-inch thick to prevent corrosion.

3.5.3.2 **Principles of Operation**

The drive mechanism shown schematically in Figure 3.5-14 withdraws and inserts its control rod assembly as electrical pulses are received by the operator coils.

An ON and OFF sequence that is repeated by a silicon-controlled rectifier in the power programmer causes either withdrawal or insertion of the control rod assembly. Position of the control rod assembly is indicated by the differential transformer action of the position indicator coil stack surrounding the rod travel housing. The differential transformer output changes as the top of the ferromagnetic drive shaft assembly moves up within the rod travel housing.

In normal operation, the stationary gripper coil of the drive mechanism holds the control rod assembly withdrawn from the core in a static position until the movable gripper coil is energized.

3.5.3.2.1 Control Rod Assembly Withdrawal

The control rod assembly is withdrawn by repetition of the following sequence of events:

1. Movable Gripper - ON

   The movable gripper armature raises and swings the movable gripper latches into the drive shaft groove.

2. Stationary Gripper Coil - OFF

   Gravity causes the stationary gripper latches and armature to move downward until the load of the drive shaft is transferred to the movable gripper latches. Simultaneously, the stationary gripper latches swing out of the shaft groove.

3. Lift Coil - ON

   The 0.625-inch gap between the lift armature and the lift magnet pole closes, and the drive rod raises one step length.

4. Stationary Gripper Coil - ON

   The stationary gripper raises and closes the gap below the stationary gripper magnetic pole, and swings the stationary gripper latches into a drive shaft groove. The latches contact the shaft and lift it 0.047 inch. The load is thus transferred from the movable to the stationary gripper latches.

5. Movable Gripper Coil - OFF

   The movable gripper armature separates from the lift armature under the force of one spring and gravity. Three links, pinned to the movable gripper armature, swing the three movable gripper latches out of the groove.

6. Lift Coil - OFF

   The gap between the lift armature and the lift magnet pole opens. The movable gripper latches drop 0.625 inch to a position adjacent to the next groove.

3.5.3.2.2 Control Rod Assembly Insertion

The sequence for control rod assembly insertion is similar to that for control rod assembly withdrawal:

1. Lift Coil - ON

   The movable gripper latches are raised to a position adjacent to a shaft groove.

2. Movable Gripper Coil - ON

   The movable gripper armature raises and swings the movable gripper latches into a groove.

3. Stationary Gripper Coil - OFF

   The stationary gripper armature moves downward and swings the stationary gripper latches out of the groove.

4. Lift Coil - OFF

   Gravity separates the lift armature from the lift magnet pole, and the control rod assembly drops down 0.625 inch.

5. Stationary Gripper Coil - ON

   See Section 3.5.3.2.1, event number 4.

6. Movable Gripper Coil - OFF

See Section 3.5.3.2.1, event number 5.

The sequences described above are considered to be one step or one cycle, and the control rod moves 0.625 inch for each cycle. Each sequence can be repeated at a rate of up to 72 steps per minute, and the control rods can therefore be withdrawn or inserted at a rate of up to 45 in/min. Tripping by gravity is not subject to the rate limit of 45 in/min.

3.5.3.2.3 Control Rod Assembly Tripping

If power to the stationary gripper coil is cut off, as it is for tripping, the combined weight of the drive shaft and the control rod assembly is sufficient to move the latches out of the shaft groove. The control rod assembly falls by gravity into the core. The tripping occurs as the magnetic field, holding the stationary gripper armature against the stationary magnet, collapses, and the stationary gripper armature is forced down by the weight acting upon the latches.

3.5.4 Fuel Assembly and Control Rod Assembly Mechanical Tests

To prove the mechanical adequacy of the fuel assembly and control rod assembly, functional test programs were conducted on three test assemblies representative of the Surry LOPAR design. One test was run on a full-scale San Onofre (Reference 9) mock-up version of the fuel assembly and control rod assembly, and the other two on two full-scale assemblies for a 12-foot active core. One of the 12-foot assemblies incorporated stainless steel guide tubes, and the other incorporated Zircaloy-4 guide tubes. These tests were performed with silver-indium-cadmium control rods.

The test assemblies were tested under simulated reactor operating conditions at 1800 psig, 575°F, and flow velocities up to 16.5 ft/sec in the Westinghouse Reactor Evaluation Center for a total of more than 6400 hours.

Each test assembly was subjected to trip cycling equivalent to one or more station lifetimes. The test history for each prototype is summarized in Table 3.5-2.

Each of three test fuel assemblies remained in excellent mechanical condition. No measurable signs of wear on the fuel tubes or control rod guide thimbles were found.

The control rods were also found to be in excellent condition, with maximum wear on absorber cladding measuring approximately 0.001 inch.

3.5.4.1 Loading and Handling Tests

Tests simulating the loading of the test fuel assemblies into a core location were conducted to determine that proper provisions were made for guidance of a fuel assembly during refueling operations. A dummy fuel assembly is still used to test operability of fuel movement equipment.

3.5.4.2 **Lateral and Axial Bending Tests**

3.5.4.2.1 Lateral Bending Tests

A prototype fuel assembly was subjected to lateral bending tests in order to determine the mechanical characteristics of the assembly, and to verify that it was capable of withstanding the loads and deflections that would be encountered during shipping, handling, and core operation. The lateral bending tests showed than an assembly is capable of withstanding lateral deflections in excess of 0.25 inch at mid-height when supported as in the core, and in excess of 0.5 inch at the top nozzle when standing free, without evidence of damage. Deflections encountered during shipment and core operation, and specified allowable (and normally expected) deflections during handling and storage, do not exceed these limits.

3.5.4.2.2 Axial Load Test

In axial tests, the prototype assembly was successfully loaded to 2200 lb or more with no resulting damage. The maximum column load expected to be experienced in service is 1000 lb. The test results have been used as a reference in the design of fuel-handling equipment to establish the limits for inadvertent axial loads during refueling.

3.5 REFERENCES

1. Westinghouse Electric Corporation, *Irradiation of 17 x 17 Demonstration Assemblies in Surry Units No. 1 and 2*, *Cycle 2*, WCAP-8362, July 1974.
2. D. H. Risher et al, *Safety Analysis for the Revised Fuel Rod Internal Pressure Design Basis*, WCAP-8964-A, August 1978.
3. *Use of Burnable Poison Rods in Westinghouse Pressurized Water Reactors*, WCAP 7113, October 1967.
4. R. C. Daniel et. al., *Effects of High Burnup of Zircaloy-Clad Bulk UO_2, Plate Fuel Element Samples*, WAPD-263, September 1965.
5. B. C. Buckley and L.B. Engle (NRC) to W.L. Stewart (Virginia Electric and Power Company), *Surry, Units 1 and 2, and North Anna, Units 1 and 2—Removal of 45,000 MWD/MTU Batch Average Burnup Restriction (TAC Nos. M87767, M87768, M87812, and M87813)*, letters dated December 14, 1993 and April 20, 1994.
6. Nuclear Engineering Staff, *Reload Nuclear Design Methodology,* VEP-FRD-42 Rev. 2.1-A, August 2003.
7. S. L. Davidson, R. L. Oelrich, and P. J. Kersting, *Assessment of Clad Flattening and Densification Power Spike Factor Elimination in Westinghouse Nuclear Fuel,* WCAP-13589-A, March 1995.

8. *Nuclear Design of Westinghouse Pressurized Water Reactor with Burnable Poison Rods,* WCAP-9000 (proprietary), 1968.

9. *Large Closed Cycle Water Reactor Research and Development Program,* Quarterly Progress Reports for the period January 1963 through June 1965, WCAP-3738, 3739, 3743, 3750, 3269-2, 3269-3, 3269-5, 3269-6, 3269-12, and 3269-13.

10. J. D. Neighbors (NRC) to W. L. Stewart (Virginia Electric and Power Company), Transmittal of Amendment 102 with Safety Evaluation, Serial No. 85-649, dated August 1985.

11. Davidson, *Reference Core Report—Vantage 5 Fuel Assembly,* Westinghouse Report WCAP-10444-P-A, dated September 1985.

12. W. L. Stewart (Virginia Power) to U. S. Nuclear Regulatory Commission, Subject; *Proposed Technical Specifications Change Surry Improved Fuel Assembly,* Serial No. 87-188, May 26, 1987.

13. T. A. Brookmire (Ed.), *Reload Transition Safety Report for Implementation of Performance and Debris Resistance Features at Surry Units 1 and 2,* Technical Report NE-965, Rev. 0, December 1993.

14. S. L. Davidson and D. L. Nuhfer (Eds.), *VANTAGE+ Fuel Assembly Reference Core Report,* WCAP-12610 (Proprietary), June 1990, including Appendices A through G and Addenda 1 through 4.

15. R. A. Weiner et al., *Improved Fuel Performance Models for Westinghouse Fuel Rod Design and Safety Evaluations,* WCAP-10851-P-A (Proprietary), August 1988.

16. J. P. Foster et al., *Westinghouse Improved Performance Analysis and Design Model (PAD 4.0),* WCAP-15063-P-A, Revision 1, with Errata, (Proprietary), July 2000.

17. *Addendum 1 to WCAP-12488-A, Revision to Design Criteria,* WCAP-12488-A, Addendum 1-A, Revision 1 (Proprietary), January 2002.

The following information is HISTORICAL and is not intended or expected to be updated for the life of the plant.

Table 3.5-1

CORE MECHANICAL DESIGN PARAMETERS[a]

(INITIAL CORE)

Parameter	Value
Active portion of the core	
Equivalent diameter	119.7 in.
Active fuel height	144 in.
Length-to-diameter ratio	1.202
Total cross-section area	78.3 ft^2
Fuel assemblies	
Number	157
Rod array	15 x 15
Rods per assembly	204[b]
Rod pitch	0.563 in.
Overall dimensions	8.426 × 8.426 in.
Fuel weight (as UO_2)	175,600 lb
Total weight	226,200 lb
Number of grids per assembly	7
Fuel rods	
Number	32,028
Outside diameter	0.422 in.
Diameter, gap: Regions 1 and 2	0.0075 in.
Region 3	0.0085 in.
Clad thickness	0.0243 in.
Clad material	Zircaloy-4
Fuel pellets	
Material	UO_2 sintered
Density of the first core loading	
Region 1 (inner)	94 (% theoretical)
Region 2 (inner)	93 (% theoretical)
Region 3 (outer)	92 (% theoretical)
Fuel enrichments of first core loading	
Region 1 (inner)	1.85 (wt.%)
Region 2 (inner)	2.55 (wt.%)
Region 3 (outer)	3.10 (wt.%)

a. All dimensions are for cold conditions.

b. Twenty-one fuel rods are omitted: 20 guide thimbles are provided to provide passage for control rods, and one is provided to contain incore instrumentation.

The following information is HISTORICAL and is not intended or expected to be updated for the life of the plant.

Table 3.5-1 (continued)

CORE MECHANICAL DESIGN PARAMETERS[a]

(INITIAL CORE)

Parameter	Value
Fuel pellets (continued)	
Fuel enrichments of first core loading (continued)	
Equilibrium regions	3.20 (wt.%)
Diameter: Regions 1 and 2	0.3659 in.
Region 3	0.3649 in.
Length	0.600 in.
Control rod assemblies	
Neutron absorber	Ag-In-Cd
Cladding material	SS 304, cold-worked
Clad thickness	0.024 in.
Number of assemblies	53
Full length	48
Part length	5
Number of control rods per assembly	20
Core structure	
Core barrel	
i.d.	133.9 in.
o.d.	137.9 in.
Thermal shield	
i.d.	142.6 in.
o.d.	148.0 in.
Burnable poison rods	
Number	816
Number of rods per assembly	12
Number of assemblies	68
Material	Borosilicate glass
Outside diameter	0.4395 in.
Inner tube, o.d.	0.2365 in.
Clad material	SS 304
Inner tube material	SS 304
Boron loading (natural)	0.0429 gm/cm of glass rod

a. All dimensions are for cold conditions

Table 3.5-2
FUEL ASSEMBLY AND CONTROL ROD ASSEMBLY TEST HISTORY

Test	Test Time, hr	Number of Trips	Total Linear Travel, ft	Total Driven Travel, ft	Total Trip Travel, ft
San Onofre, 10-foot assembly, stainless steel guide thimbles	4132	1461	38,927	27,217	11,710
12-foot assembly, stainless steel guide thimbles	1000	600	45,000	38,500	6500
12-foot assembly, Zircaloy-4 guide thimbles	1277	600	124,200	117,700	6500

Table 3.5-3
COMPARISON OF LOPAR AND SIF ASSEMBLY NOMINAL DESIGN PARAMETERS

Parameter	15 x 15 LOPAR Design	15 x 15 SIF Design
Fuel Assembly Length	159.710 in.	159.975 in. (Zircaloy) 159.775 to 159.975 in. (ZIRLO) [a]
Fuel Rod Length	151.85 in.	152.17 to 152.185 in. (Zircaloy) [b] 152.680 152.880 in. (ZIRLO) [a]
Assembly Envelope	8.424 in.	8.424 in.
Compatible with Core Internals	Yes	Yes
Fuel Rod Pitch	0.563 in.	0.563 in.
Number of Fuel Rods/Assembly [c]	204	204
Number of Guide Thimbles/Assembly	20	20
Number of Instrumentation Tubes/Assembly	1	1
Compatible w/Movable In-core Detector System	Yes	Yes
Fuel Tube Material	Zircaloy-4	Zircaloy-4 or ZIRLO [a]
Fuel Rod Clad o.d.	0.422 in.	0.422 in.
Fuel Rod Clad Thickness	0.0243 in.	0.0243 in.
Fuel/Clad Gap	7.5 mil	7.5 mil
Fuel Pellet Diameter	0.3659 in.	0.3659 in. [e]
Guide Thimble Material	Zircaloy-4	Zircaloy-4 or ZIRLO [a]
Guide Thimble o.d. above dashpot	0.546 in.	0.533 in.
Guide Thimble Wall Thickness	0.017 in.	0.017 in.
Structural Material - Five Inner Grids	Inconel	Zircaloy-4 or ZIRLO [a]
Structural Material - Two End Grids	Inconel	Inconel
Grid Inner Strap Thickness	13.5 mil (Inconel Grid)	26 mil (Zircaloy-4 or ZIRLO Grid) [a] 13.5 mil (Inconel) 10.5 mil (P-grid) [d]

a. ZIRLO was introduced on Batch 16 fuel (Cycle 14). The increased ZIRLO fuel assembly and fuel rod lengths were introduced with Surry 2 Batch 20 fuel.
b. Original SIF fuel rods (Batch 12, introduced in Cycle 10) were 152.185 inches long. Length was decreased slightly starting with Batch 13 (Cycle 11) as part of Westinghouse standardization of 15 x 15 fuel products.
c. Reconstituted fuel assemblies may contain some solid metal filler rods in place of fuel rods.
d. Debris filter bottom nozzles were introduced on Batch 13 fuel. P-grids were introduced on Batch 15 fuel (Cycle 13).
e. Starting with Batch 23 (Cycle 21) annular pellets may be used in the top and bottom of fuel rods containing IFBA. The specified diameter does not include the thickness of any IFBA coating that may be used.

Table 3.5-3 (continued)
COMPARISON OF LOPAR AND SIF ASSEMBLY NOMINAL DESIGN PARAMETERS

Parameter	15 x 15 LOPAR Design	15 x 15 SIF Design
Grid Outer Strap Thickness	20.5 mil (Inconel Grid)	32 mil (Zircaloy-4 or ZIRLO Grid) [a] 20.5 mil (Inconel, P-grid) [d]
Grid Support for Fuel Rods (Structural Grids) (P-grid)[d]	6 points 2 springs, 4 dimples	6 points: 2 springs, 4 dimples 4 points: 4 dimples
Grid Inner Strap Height, less vanes		
(Inner Grids)	1.50 in.	2.25 in.
(End Grids)	1.50 in.	1.522 in.
(P-grid) [d]		0.690 in.
Grid Fabrication Method	Brazed joining of interlocking straps	Welded joining of interlocking straps (Inner Grids, P-grid) [d] Brazed joining of interlocking straps (End Grids)
Grid/Guide Thimble Attachment	Thimbles bulged together with sleeves prebrazed onto grid straps	Thimbles bulged together with sleeves prewelded to grid straps
Top Nozzle	Non-removable	Removable
Top Nozzle Holddown Springs	1- or 2-leaf	3-leaf
Compatible with Fuel Handling Equipment	Yes	Yes
Bottom Nozzle	Reconstitutable	Reconstitutable, Debris Filter [d]

a. ZIRLO was introduced on Batch 16 fuel (Cycle 14). The increased ZIRLO fuel assembly and fuel rod lengths were introduced with Surry 2 Batch 20 fuel.
d. Debris filter bottom nozzles were introduced on Batch 13 fuel. P-grids were introduced on Batch 15 fuel (Cycle 13).

Figure 3.5-1
CORE CROSS SECTION

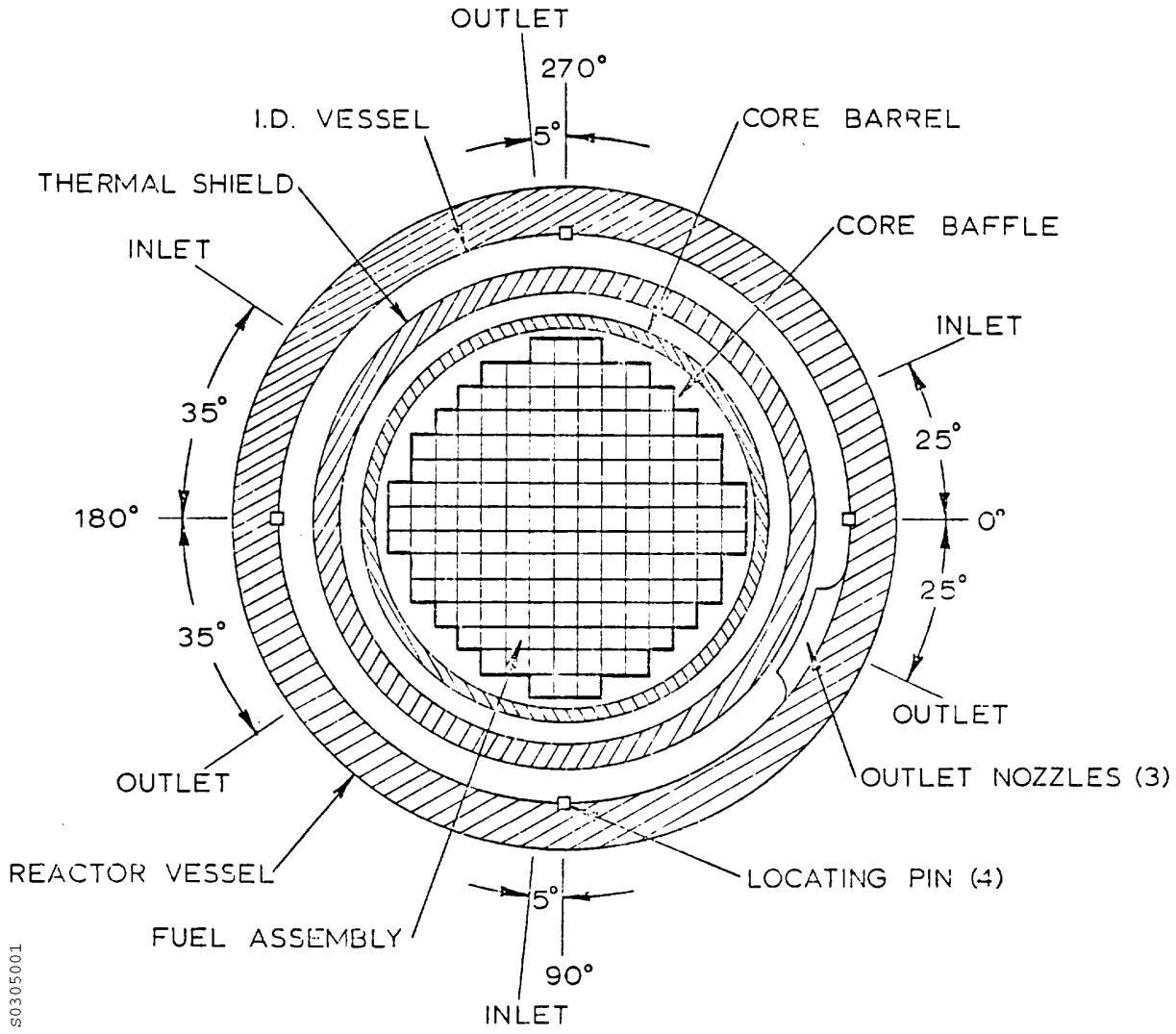

Figure 3.5-2
TYPICAL REACTOR VESSEL AND INTERNALS

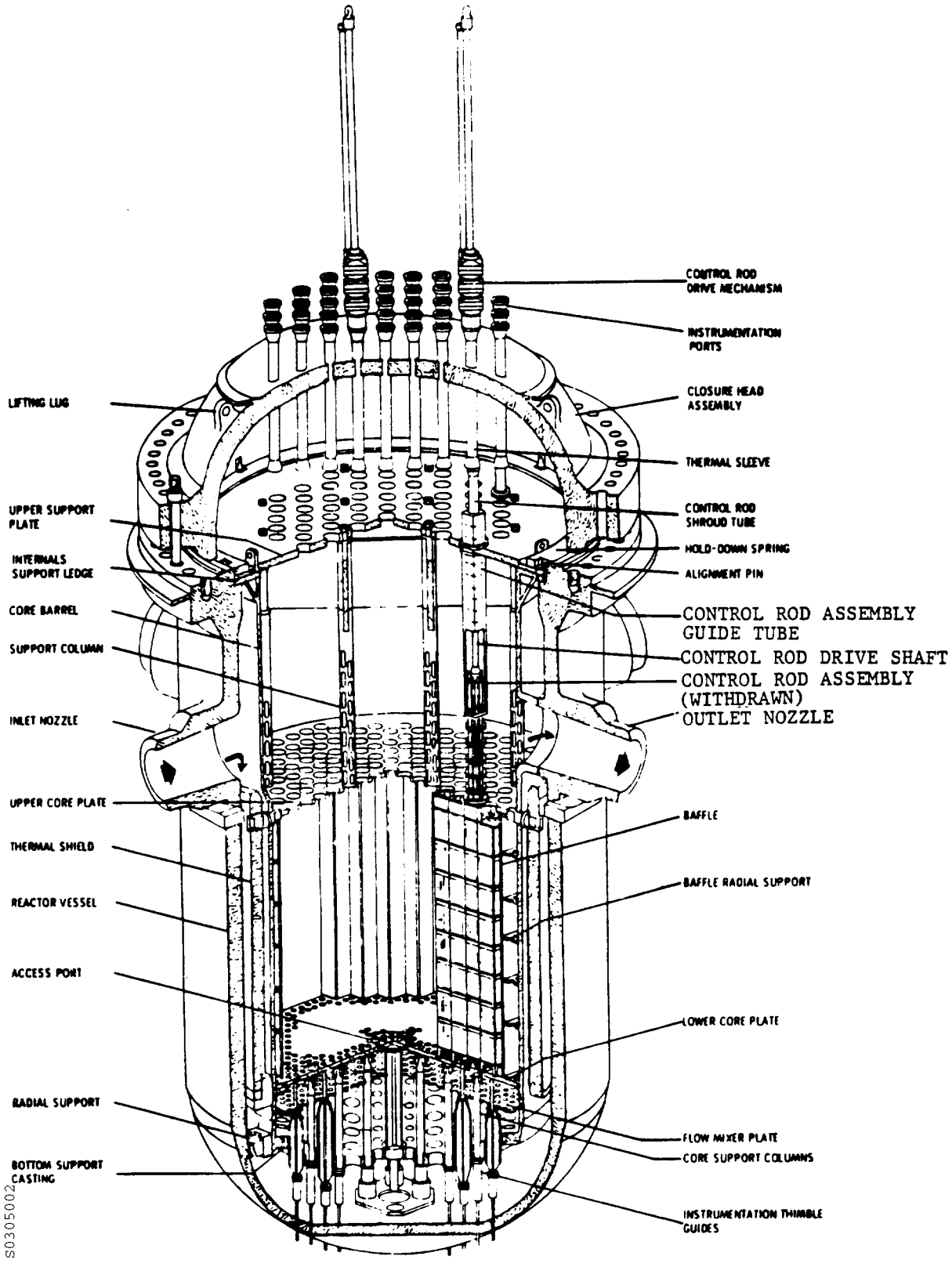

The following information is HISTORICAL and is not intended or expected to be updated for the life of the plant.

Figure 3.5-3
INITIAL CORE LOADING ARRANGEMENT

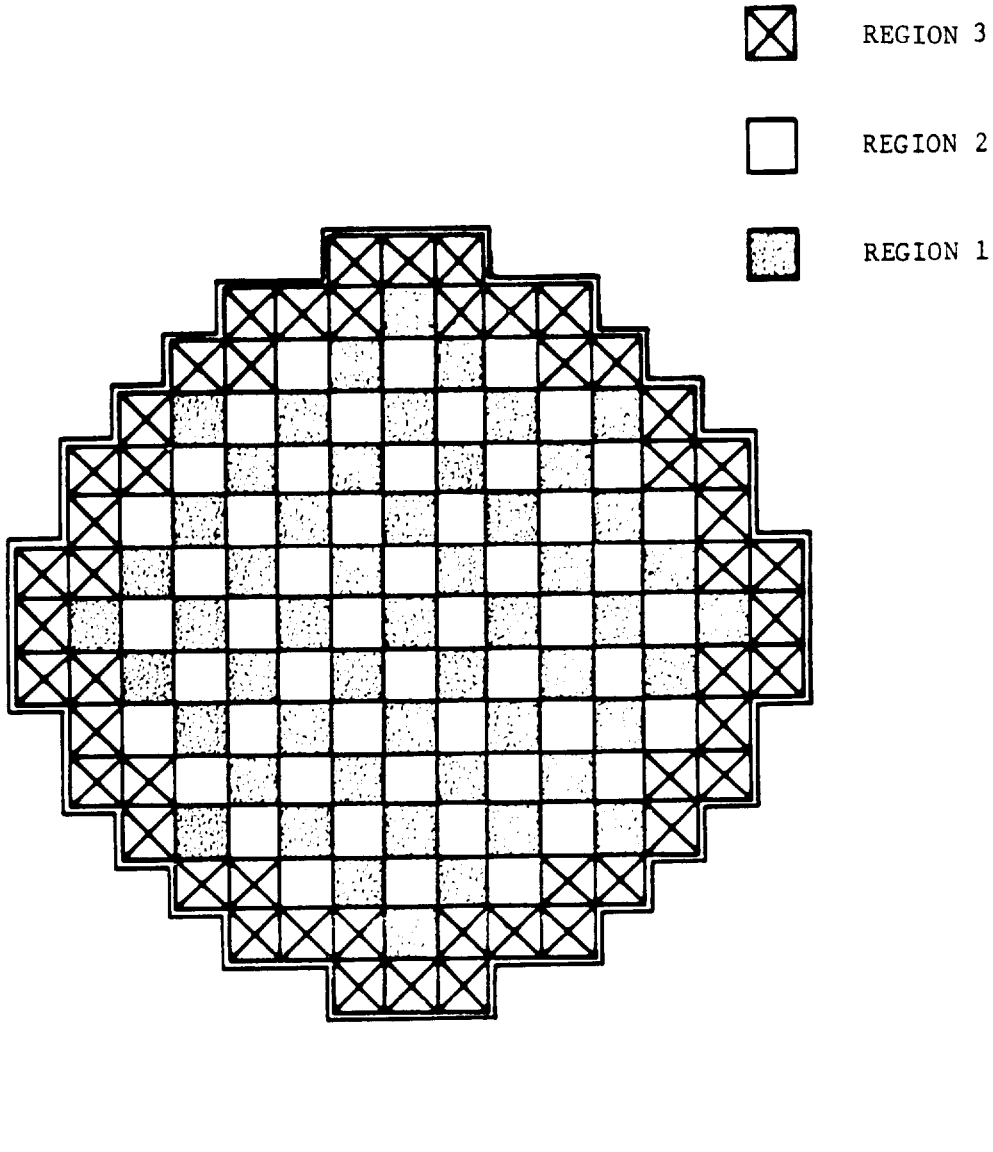

Figure 3.5-4
TYPICAL LOPAR FUEL ASSEMBLY WITH CONTROL ROD

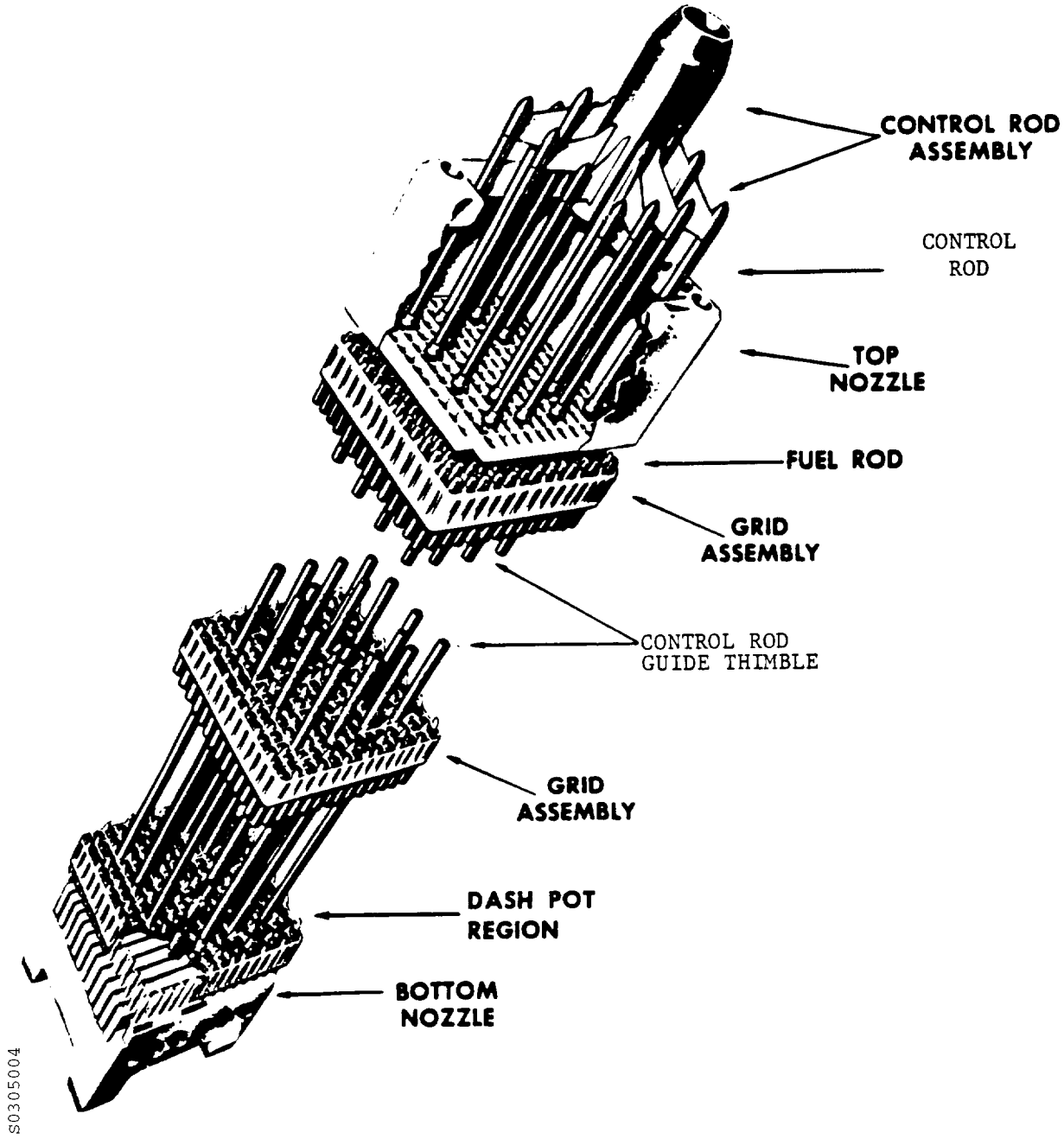

Figure 3.5-5
FUEL ASSEMBLY AND CONTROL ROD ASSEMBLY CROSS SECTION

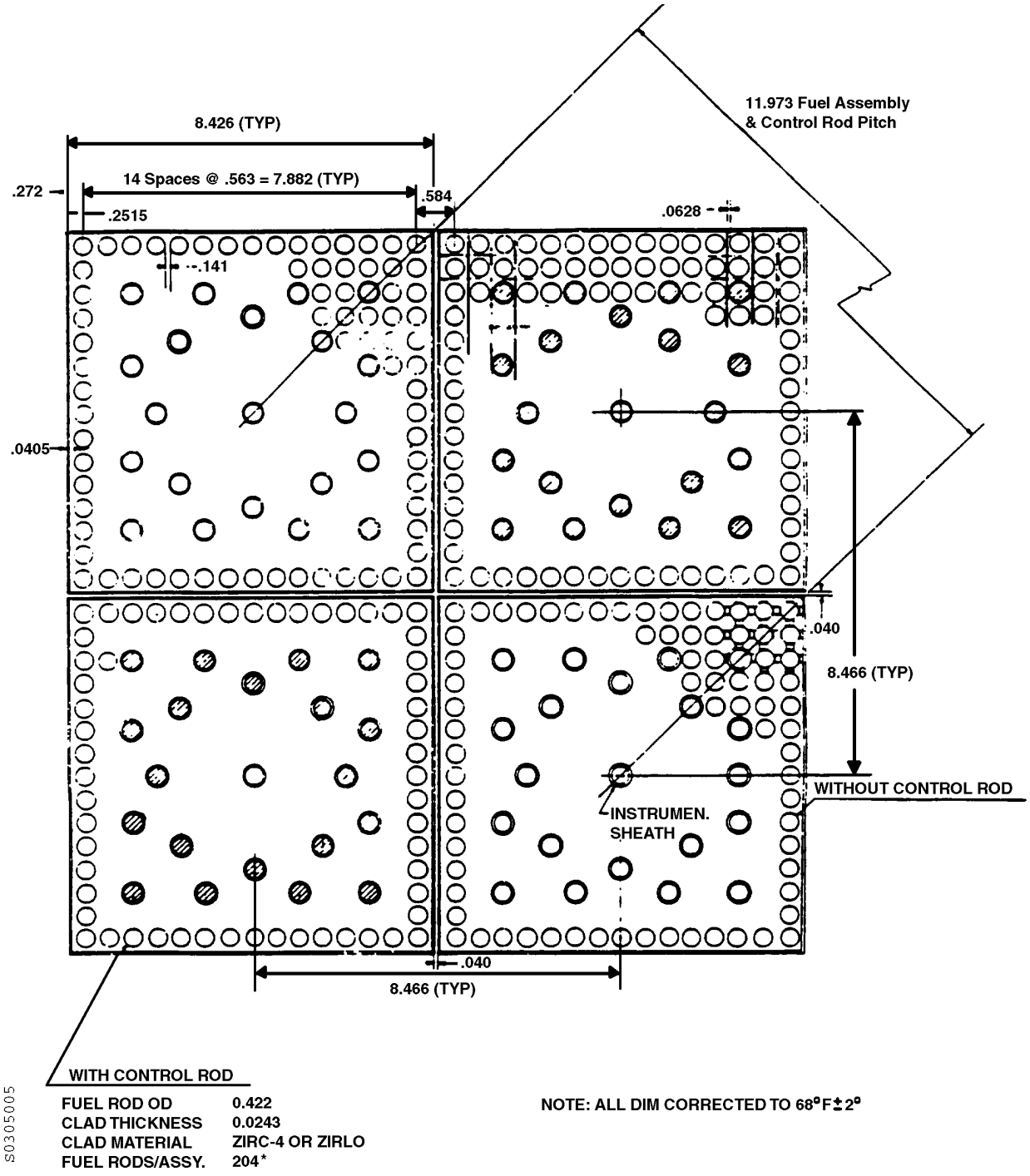

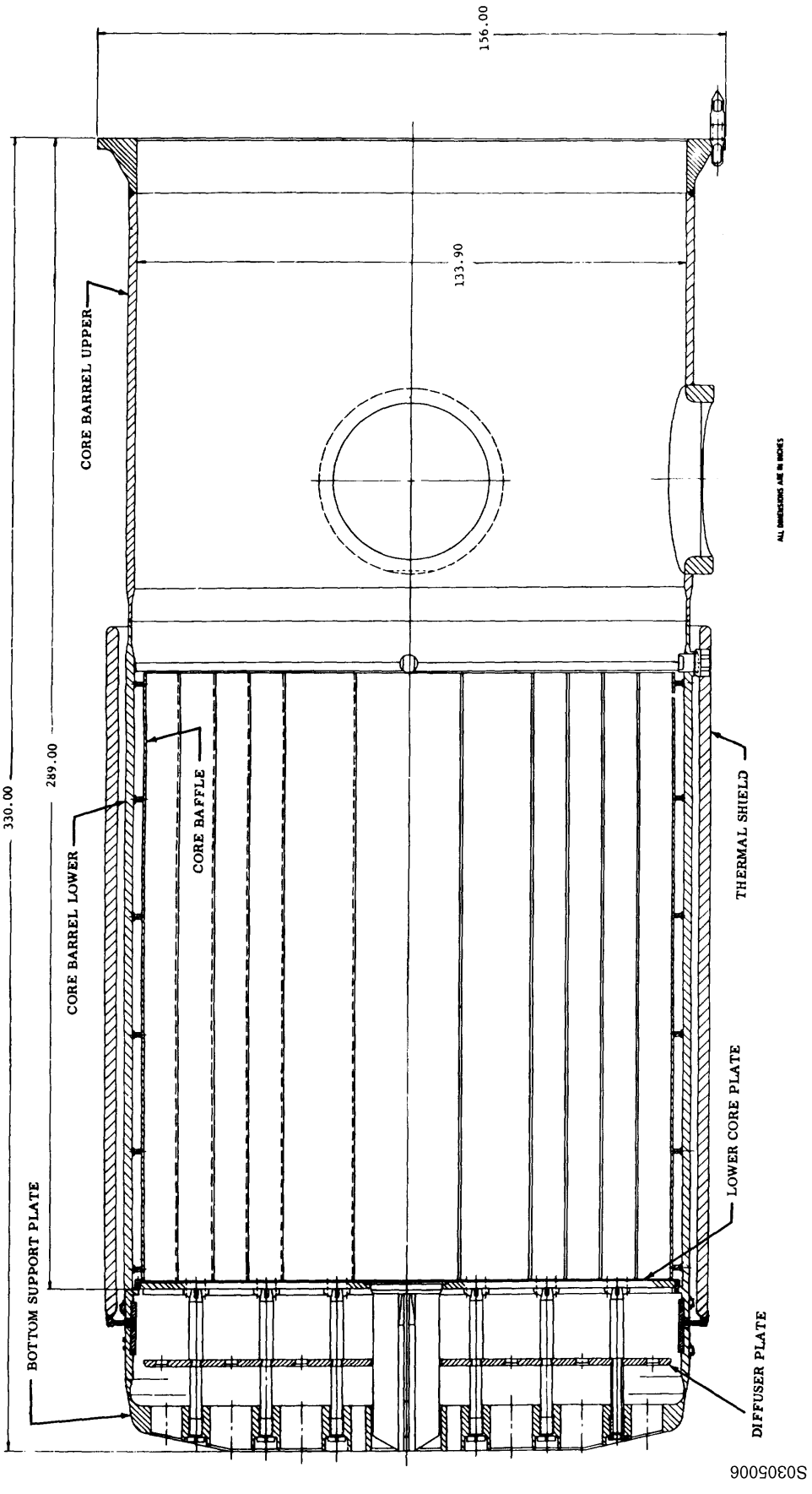

Figure 3.5-6
LOWER CORE SUPPORT STRUCTURE

Figure 3.5-7
UPPER CORE SUPPORT ASSEMBLY

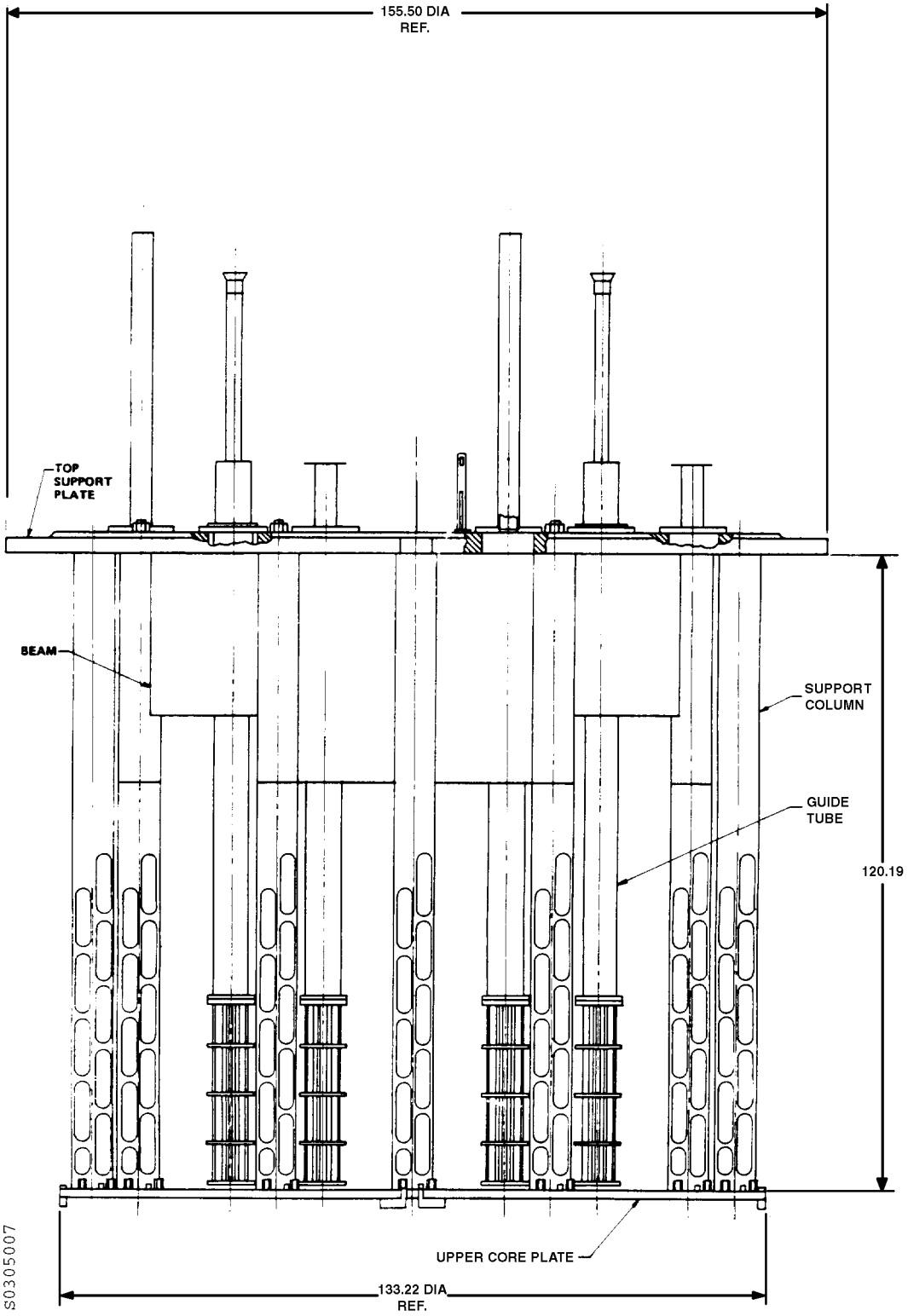

Figure 3.5-8
GUIDE TUBE ASSEMBLY

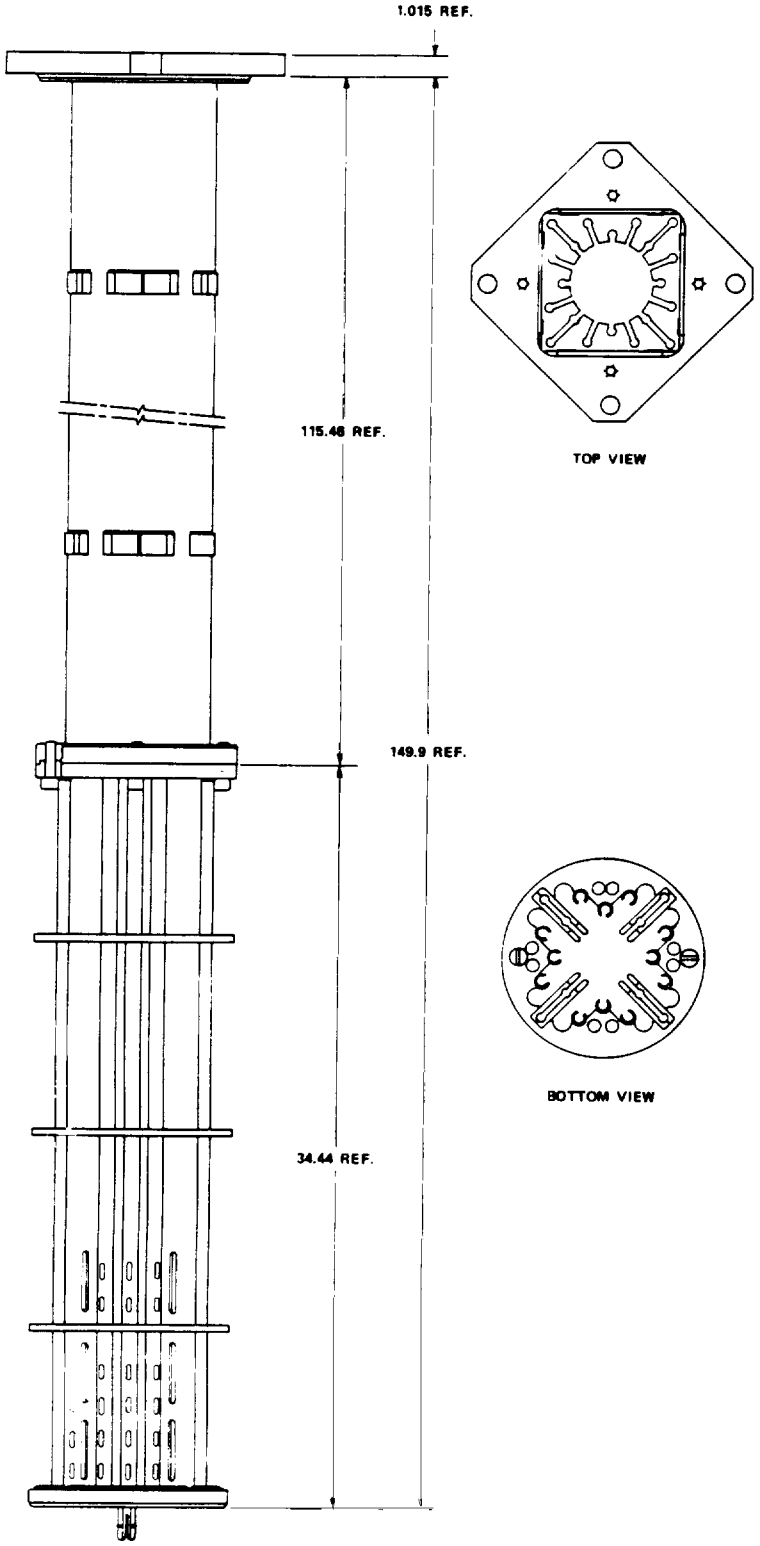

Figure 3.5-9
OUTLINE FOR TYPICAL SIF AND 15 X 15 LOPAR FUEL ASSEMBLIES

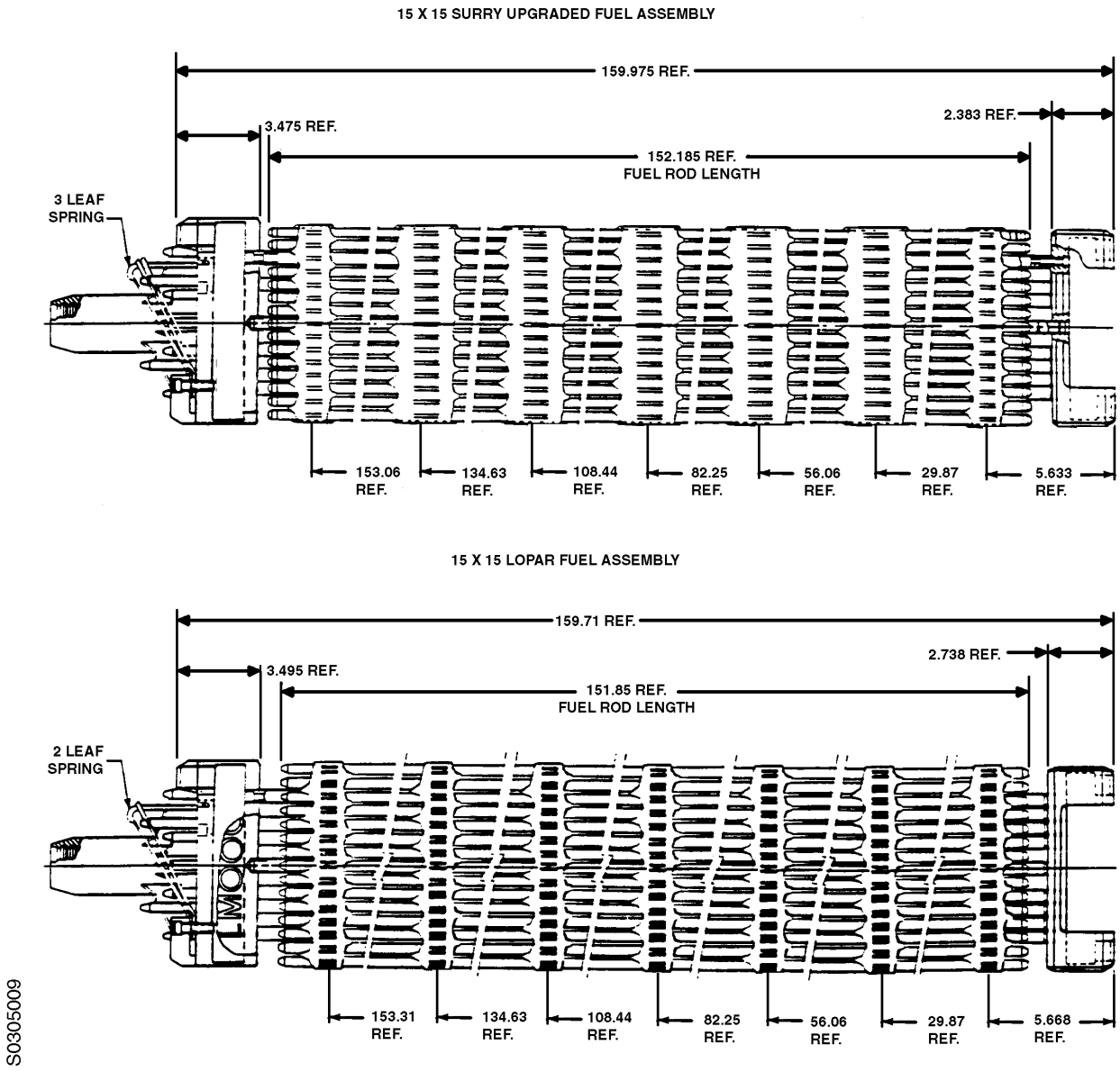

Figure 3.5-10
BOTTOM NOZZLE/PROTECTIVE GRID/FUEL ROD INTERFACE

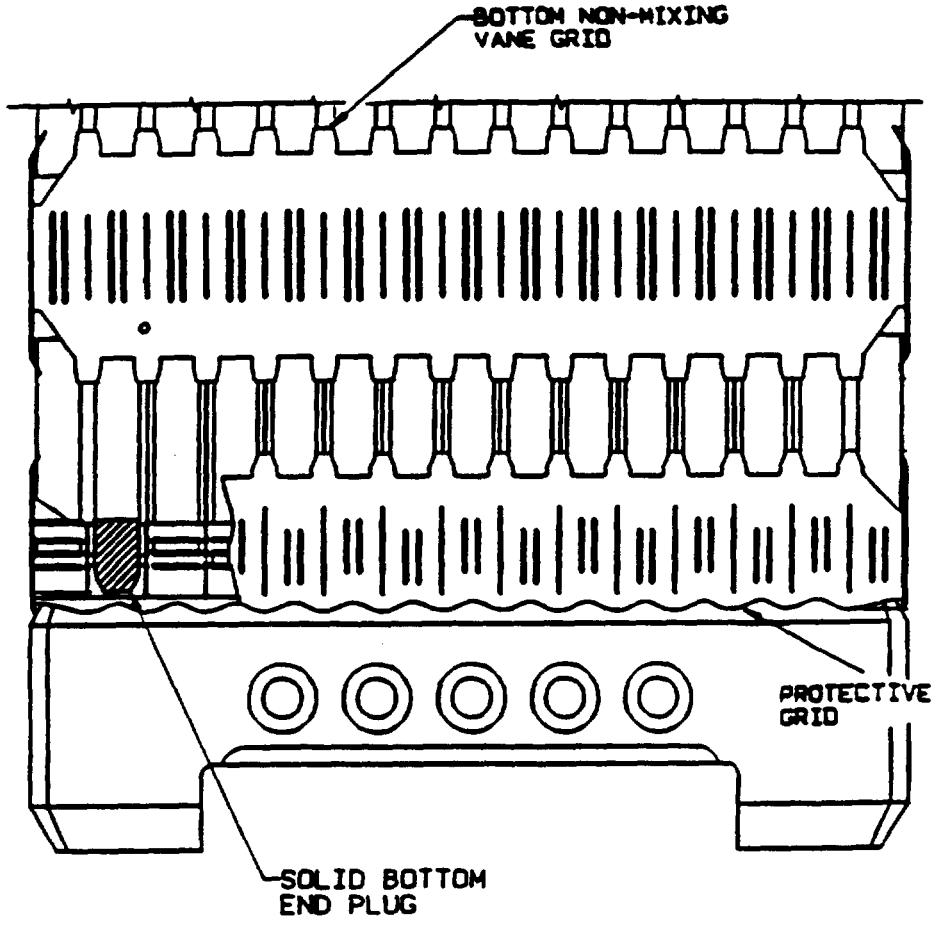

Figure 3.5-11
REPRESENTATIVE GRID ASSEMBLY
(INCONEL MIXING VANE GRID SHOWN)

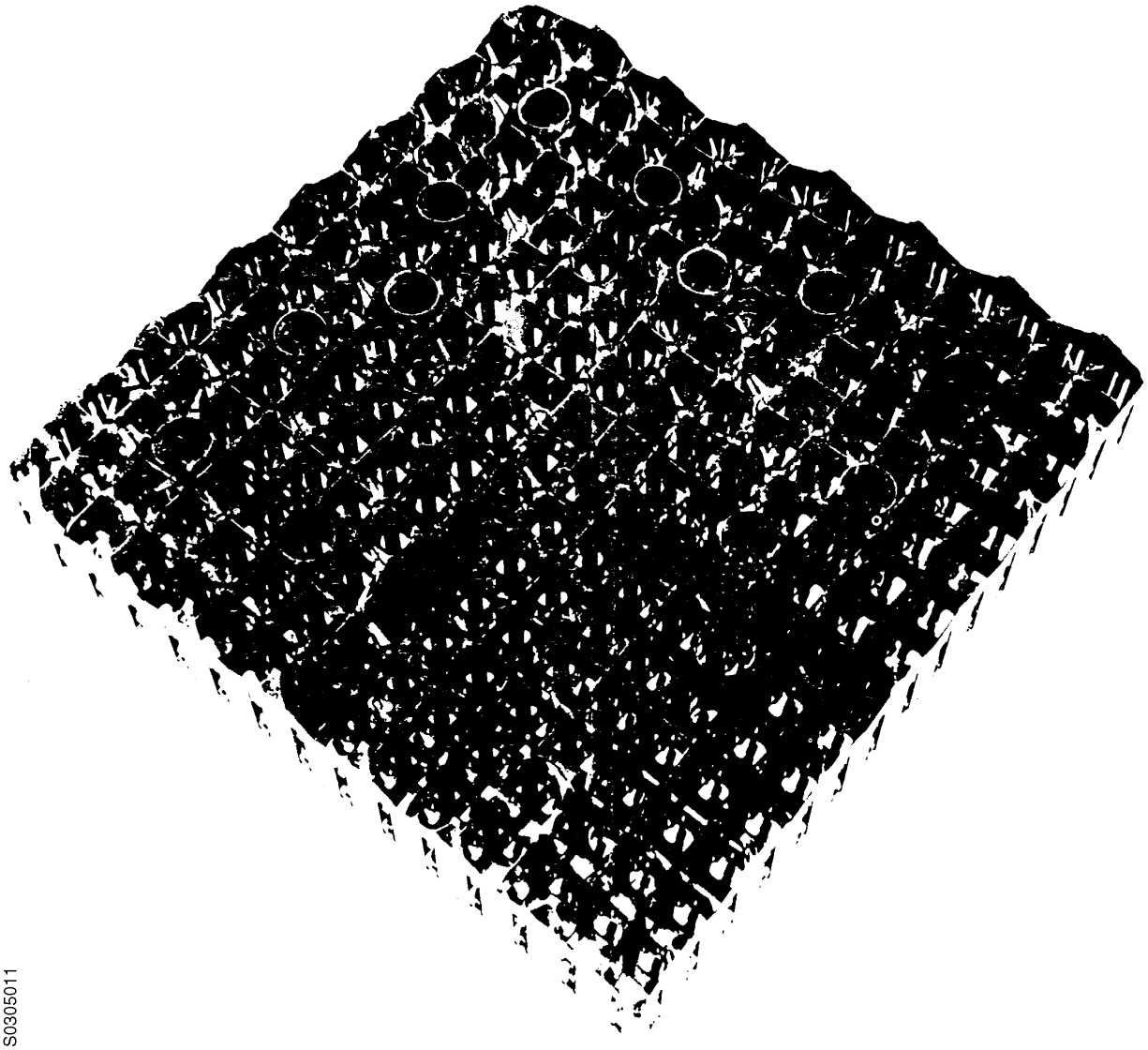

S0305011

Figure 3.5-12
CONTROL ROD ASSEMBLY OUTLINE

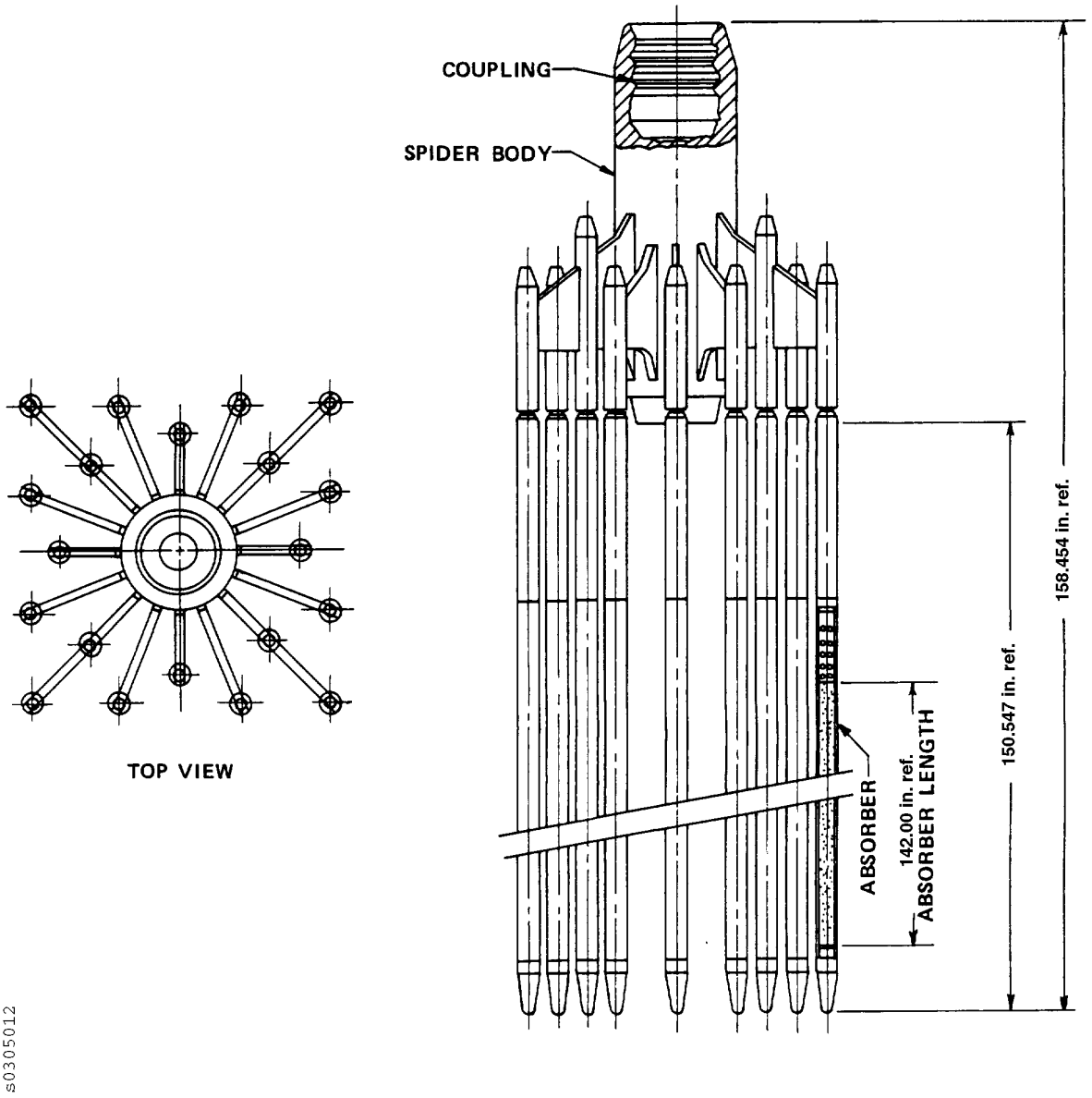

Figure 3.5-13
DETAIL OF BURNABLE POISON ROD

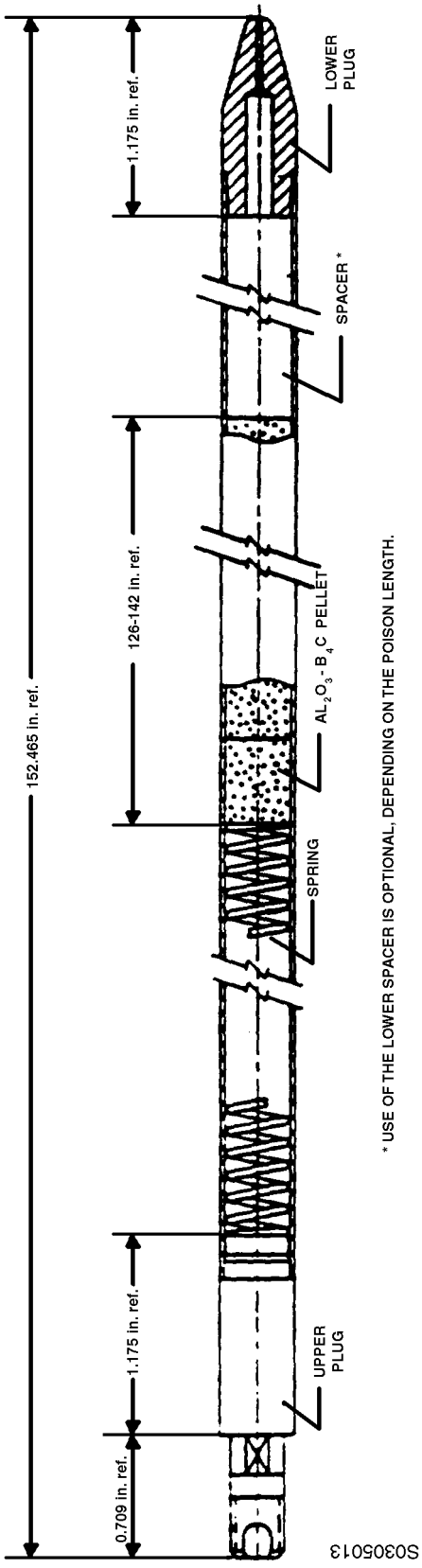

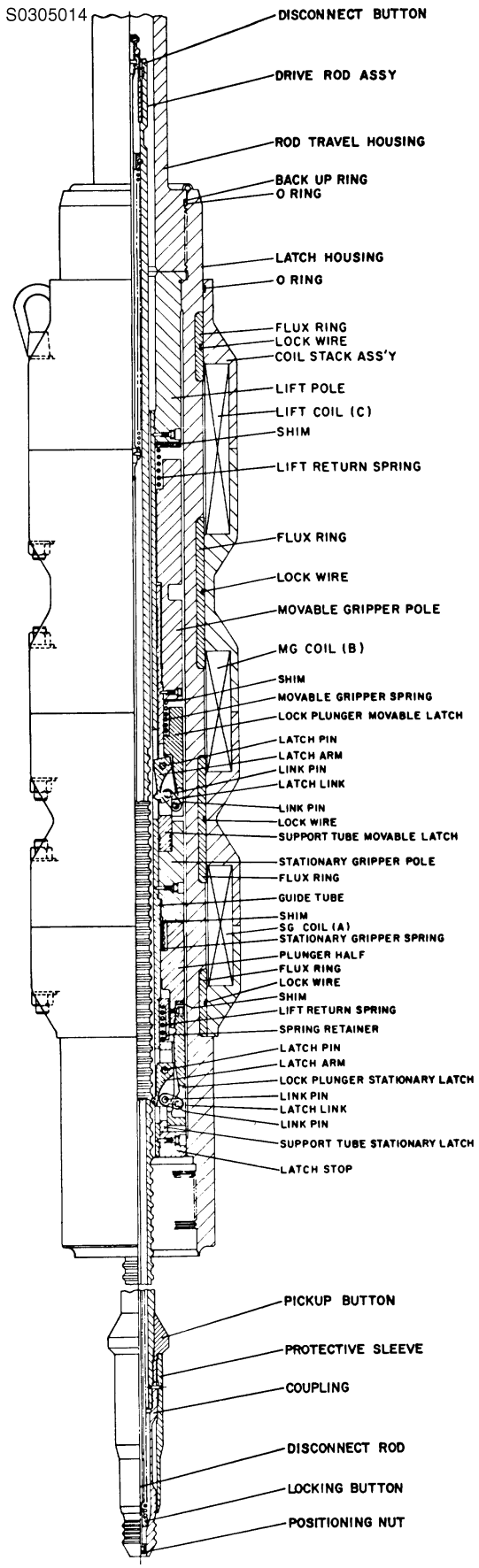

Figure 3.5-14
CONTROL ROD DRIVE MECHANISM ASSEMBLY

Figure 3.5-15
SURRY UNIT 1
FSI AND EXCORE DETECTOR LOCATIONS

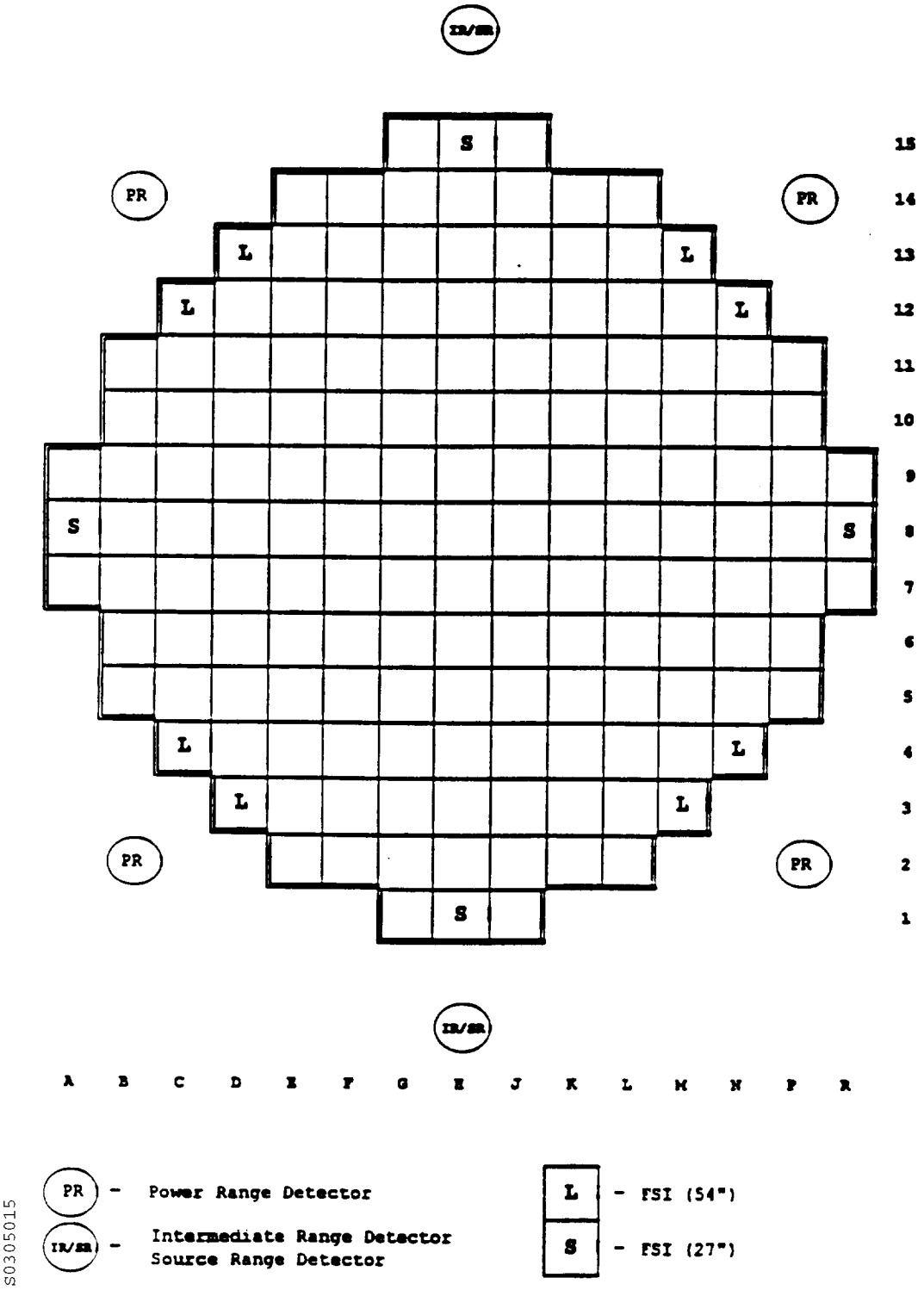

Note that FSIs were removed after Cycle 20 of Unit 1.

Figure 3.5-16
SURRY UNIT 1
FLUX SUPPRESSION INSERT (FSI) ASSEMBLY

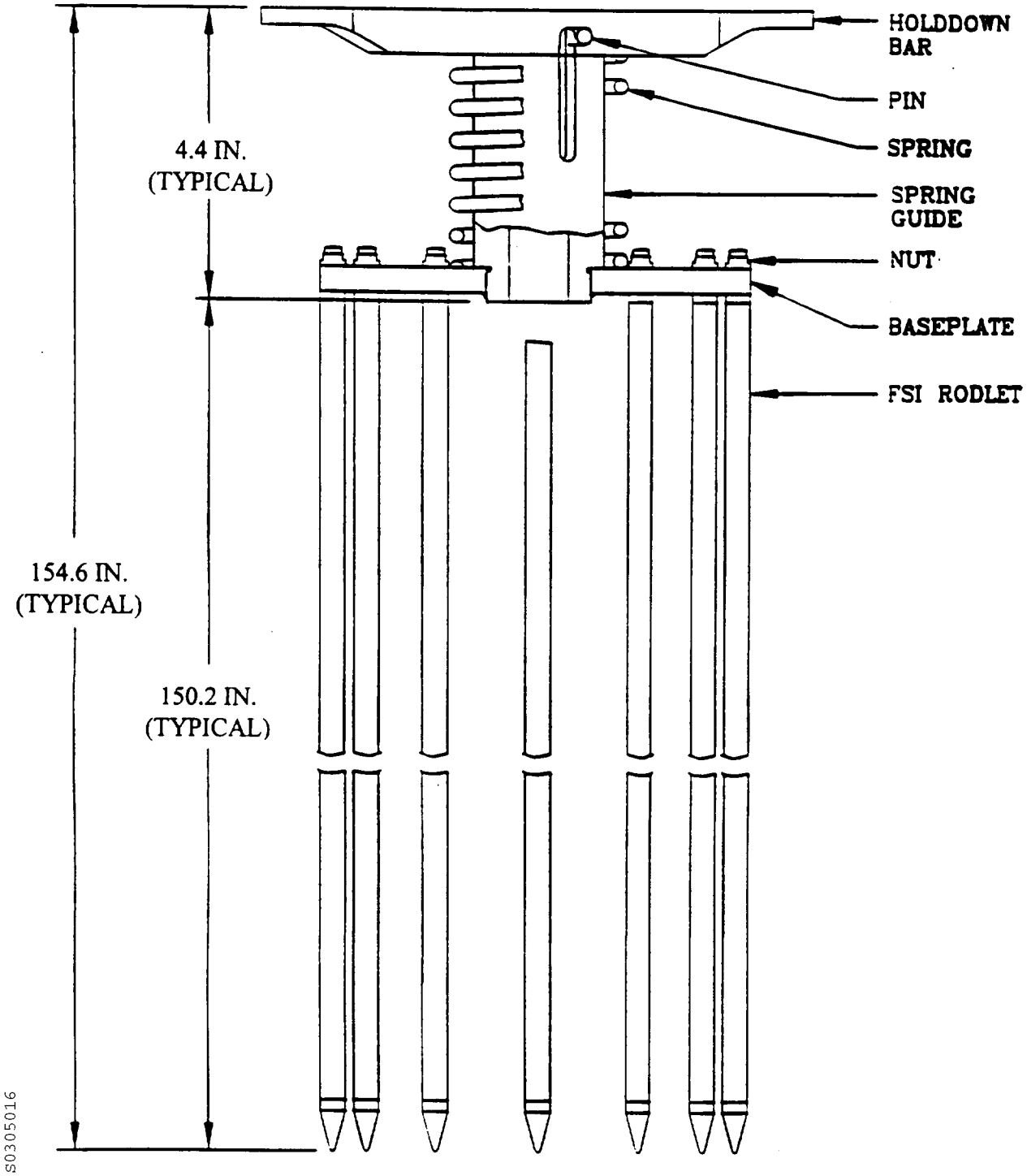

3.6 TESTS AND INSPECTIONS

3.6.1 Physics Tests

3.6.1.1 Tests to Confirm Reactor Core Characteristics

A detailed series of start-up physics tests are performed each cycle from zero power up to and including 100% power. As part of these tests, a series of core power distribution measurements are made from at or below 30% power to 100% power by means of the core movable detector system. These measurements are analyzed and the results compared with the analytical predictions upon which safety analyses were based.

3.6.1.2 Tests Performed During Operation

To detect and eliminate possible errors in the calculations of the initial reactivity of the core and the reactivity depletion rate, the predicted relation between fuel burnup and the boron concentration necessary to maintain adequate control characteristics is normalized to accurately reflect actual core conditions. When full power is reached initially during each cycle, and with the control groups in the desired positions, the boron concentration is measured and the predicted curve is adjusted to this point. As power operation continues, the measured boron concentration is compared with the predicted concentration, and the slope of the curve relating burnup and reactivity is compared with that predicted. This normalization should be completed after about 10% of the cycle burnup has occurred. Thereafter, actual boron concentration can be compared with the predicted concentration, and the reactivity prediction of the core can be continuously evaluated.

Any reactivity anomaly greater than 1% would be unexpected, and its occurrence would be thoroughly investigated and evaluated.

3.6.2 Thermal/Hydraulic Tests and Inspections

General hydraulic tests on models have been used to confirm the design flow distributions and pressure drops (References 1 & 2). Fuel assemblies and control and drive mechanisms are also tested in this manner. Appropriate onsite measurements are made to confirm the design flow rates.

Vessel and internals inspections were reviewed prior to initial startup to confirm such thermal and hydraulic design values as bypass flow. A reactor coolant flow test, as noted in Table 13.3-1, was performed following fuel loading but before initial criticality to verify that proper coolant flow rates had been used in the core thermal and hydraulic analysis. Periodic testing is performed to verify the RCS flow rates used in design calculations are met.

3.6.3 Core Component Tests and Inspections

To ensure that all materials, components, and assemblies conformed to the design requirements, a release point program was established with the manufacturer. This program

required surveillance of all raw materials, special processes (i.e., welding, heat treating, non-destructive testing, etc.), and those characteristics of parts that directly affected the assembly and alignment of the reactor internals. The surveillance was accomplished by the issuance of an Inspection Release by the quality control organization after conformance had been verified.

A resident quality control representative performed a surveillance/audit program at the manufacturer's facility, witnessed the required tests and inspections, and issued the inspection releases. An example would be the radiographic examination of the welds joining core barrel shell courses.

Components and materials supplied by Westinghouse to the assembly manufacturer were subjected to a similar program. Quality control engineers developed inspection plans for all raw materials, components, and assemblies. Each level of manufacturing was evaluated by a qualified inspection for conformance, e.g., witnessing the ultrasonic testing of core plate raw material. Upon completion of specified events, all documentation was audited prior to releasing the material or component for further manufacturing. All documentation and inspection releases are maintained in the quality control central records section. All materials are traceable to the mill heat number.

In conclusion, a set of "as built" dimensions were taken to verify conformance to the design requirements and ensure proper fitup between the reactor internals and the reactor pressure vessel.

3.6.3.1 **Fuel Product Assurance**

Fuel product assurance philosophy is generally based on the performance of inspections by the supplier to a 95% confidence that at least 95% of the product meets specification, unless otherwise noted. This confidence level is based on past experience gained during the manufacturing of over 10,000 metric tons of uranium cores. The following inspections are included:

1. Component parts - Parts received are generally inspected to a 95 x 95 confidence level. The characteristics inspected depend upon the component parts, and include dimensional and visual inspections, and check audits of test reports, material certifications, and non-destructive examinations such as X-ray and ultrasonic tests. Supplier material processes and component specifications specify in detail the inspections to be performed. All material used in the manufacture of the core is accepted and released by Quality Control.
2. Pellets - Inspection is performed to a 95 x 95 confidence level for the dimensional characteristics such as diameter, length, and squareness of ends. Additional visual inspections are performed for cracks, chips, and pores according to standards established at the beginning of production. These standards are based upon standards used in previous cores that have in turn served as standards for millions of pellets manufactured and used in operating cores. Density is determined in terms of weight per unit length. Chemical analyses are performed on each blend of pellets throughout pellet production. The hydrogen content of pellets loaded into fuel tubing is also tested and controlled.

Pellets that are coated with a boride material for use in integral fuel burnable absorber (IFBA) rods undergo additional inspections to determine the linear boron concentration on the pellet and the adherence of the coating.

3. Rod Inspection - Fuel rod inspection consists of the following non-destructive examination techniques and methods associated with the parameters or characteristics identified:

   a. *Leak testing* - Each rod is tested, using a calibrated mass spectrometer, with helium being the detectable gas.

   b. *Enclosure welds* - Rod welds are inspected by ultrasonic test or x-ray as an alternative method in accordance with a qualified technique and the applicable specification.

   c. *Dimensional* - All rods are dimensionally inspected prior to final release. The requirements include such items as camber and visual appearance. A sample of rods is evaluated for length.

   d. *Plenum dimensions* - All fuel rods are inspected by gamma scanning radiography or other approved methods to ensure proper plenum dimensions.

   e. *Pellet-to-pellet-gaps* - All fuel rods are inspected by gamma scanning or other approved methods to ensure that no significant gaps exist between pellets.

   f. *Gamma scanning* - Non-IFBA fuel rods are active gamma scanned to verify enrichment control prior to acceptance for assembly loading. IFBA fuel rods are passive gamma scanned to verify enrichment control and zone lengths prior to acceptance for assembly loading.

   Traceability of rods and associated rod components is maintained throughout manufacture and Quality Control release.

4. Final QC Release - The rods, upon final inspection, are released and available for fuel assembly loading.

5. Assembly - Inspection consists of 100% inspection for drawing and specification requirements.

6. Other inspections - The following inspections are performed as part of the routine inspection operation:

   a. Measurements, other than those specified above, that are critical to thermal/hydraulic analyses are obtained to enable evaluation of manufacturing variations to a 99.5% confidence level.

   b. Tool and gauge inspection and control is performed, including standardization to primary and secondary working standards. Tool inspection is performed at prescribed intervals on all serialized tools. Complete records are kept of the calibration and condition of tools.

c. Check audit inspection of all inspection activities and records to ensure that prescribed methods are followed and that all records are correct and properly maintained.

d. Surveillance of outside contractors, including approval of standards and methods, is performed where necessary.

To prevent the possibility of mixing enrichments during fuel manufacture and assembly, meticulous process control is exercised.

The UF_6 gas is normally received from the enrichment plant in sealed containers, the contents of which are fully identified.

Upon receipt by the supplier, an additional identification tag completely describing the contents is affixed to the containers before transfer to UF_6 storage.

The UF_6 is converted to UO_2. After conversion the UO_2 is normally milled and then blended. The blended powder is inspected by Quality Control and released for pelleting based on a chemical analysis.

Pellet production lines are physically separated from each other, and pellets of only a single enrichment and design are produced in a given production line or a segregated part of the line.

Finished pellets are placed on trays which are identified as to enrichment and transferred to closed storage carts.

If the storage carts are moved out of the established control area, the carts are locked and sealed to prevent mixing of pellets of different designs and enrichments. Unused powder and substandard pellets are returned to storage.

Loading of the pellets into the cladding is again accomplished in separated production lines, and again only one design and enrichment at a time is loaded on a line.

A bar code that provides traceability information is laser etched on each fuel tube. The bar code provides a reference of the fuel pellets contained in the fuel rods. Other approved methods of identification may be used.

At the time of installation into an assembly, an inspector verifies that all fuel rods in an assembly have the same contract identification, and that the top nozzle to be used on the assembly carries the correct identification information. The top nozzle identification is then used by manufacturing and station fuel handling personnel to maintain fuel assembly traceability. All fabrication plant personnel handling fuel materials should have thorough medical examinations and should be checked for color blindness.

3.6.3.2 **Control Rod, Burnable Poison Rod and Source Rod Tests and Inspections**

All clad/end plug and/or seal welds in control rods, burnable poison rods, flux suppression insert rods, and source rods are checked for integrity by visual inspection; ultrasonic test or,

alternatively, may also be inspected by x-ray; and helium leakage in accordance with qualified techniques and supplier specifications. Beginning with Cycle 20 at both units, the feed burnable poison rods are fabricated with a new end plug welding process, and the vendor no longer performs ultrasonic testing or x-ray on these components.

3.6 REFERENCES

1. G. Hetsroni, *Hydraulic Tests of the San Onofre Reactor Model*, WCAP-3269-8, 1964.
2. G. Hetsroni, *Studies of the Connecticut-Yankee Hydraulic Model*, WCAP-2761, 1965.
3. Westinghouse Product Specification NFP 31038, Revision 28, *Fuel Rod Assemblies*.
4. Westinghouse Product Specification NFP 31032, Revision 20, *Uranium Oxide Powder.*
5. Westinghouse Product Specification NFP 31029, Revision 41, *Uranium Dioxide Pellets*.
6. Westinghouse Process Specification NPS 80030 UM, Revision 22, *Manufacturing Uranium Oxide Powder.*
7. Westinghouse Process Specification NPS 80030 XL, Revision 42, *Manufacturing of Uranium Dioxide Pellets*.

Intentionally Blank